modeling metal and dust enrichment in the first galaxies

Raffaella Schneider
Sapienza Università di Roma

raffaella.schneider@uniroma1.it

Outline of the lecture

- introduction: constraints on the first Gyr
- first star formation
- the formation of second-generation stars
- stellar metal and dust yields
- chemical evolution with dust
- dust enrichment in z > 6 galaxies
- summary and take-home messages

Terra Incognita: the Universe @ cosmic dawn

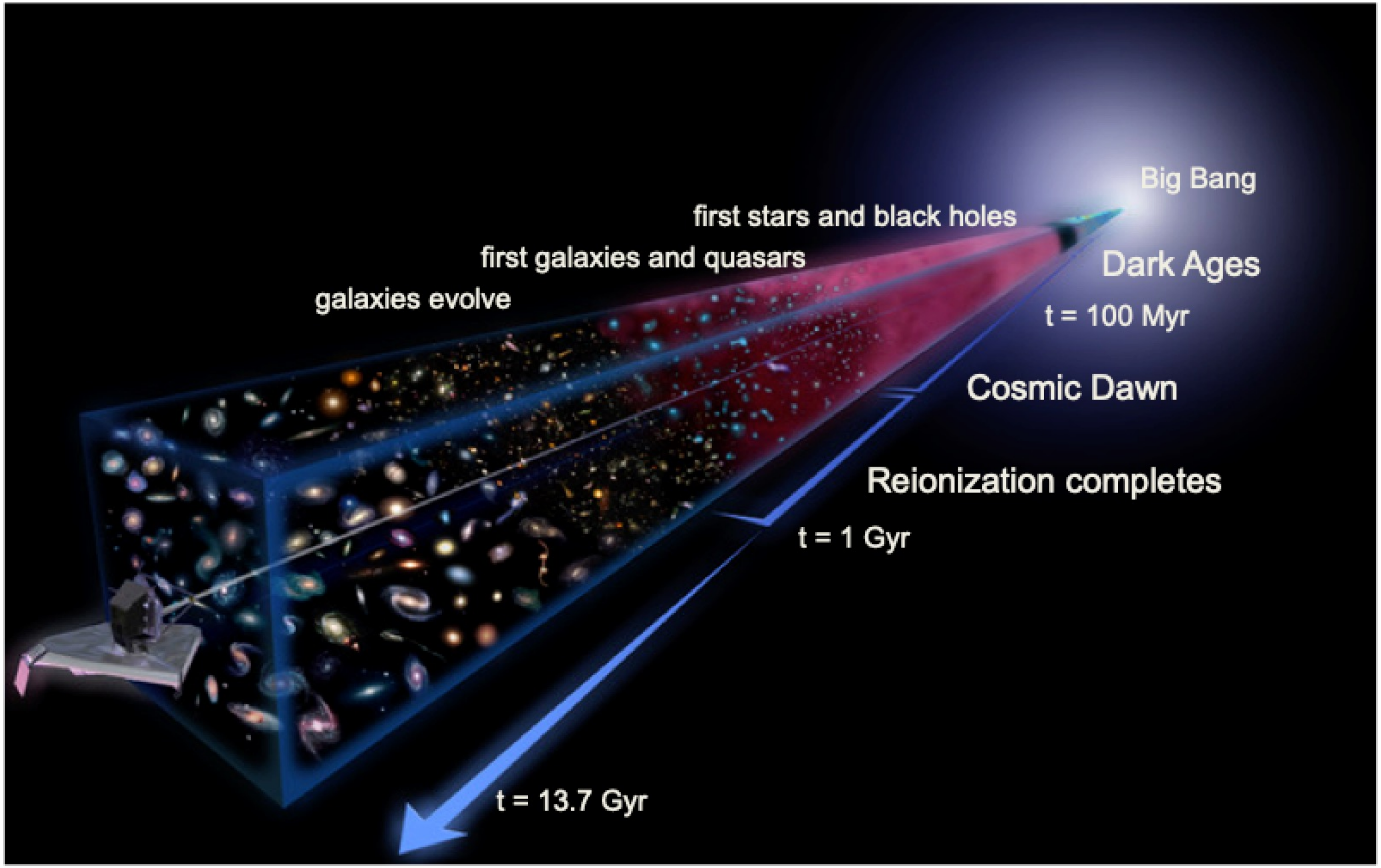

global constraint: CMB measurement of τ_e

Planck 2015 CMB temperature map and power spectrum

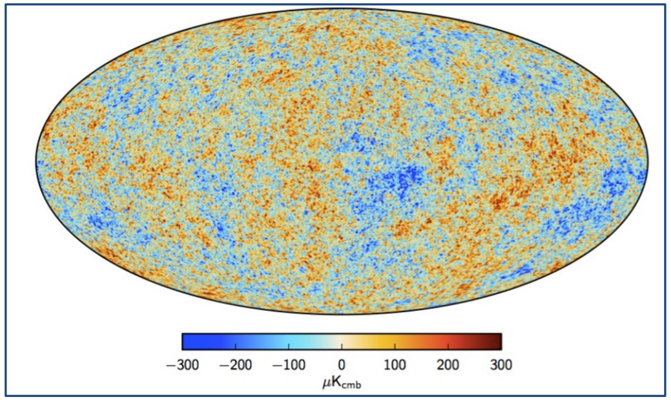

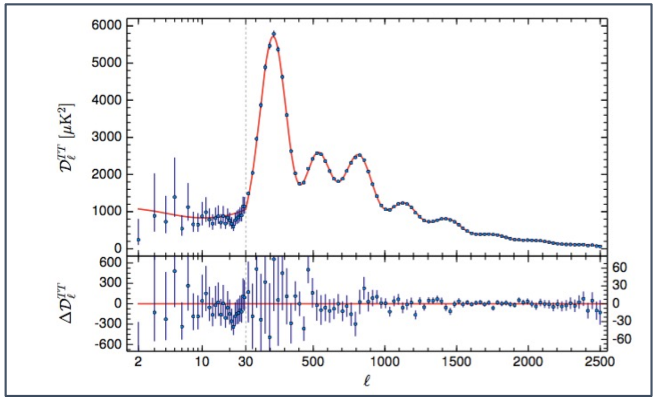

optical depth to Thomson scattering

$\tau = 0.066 \pm 0.012$

instantaneous reionization redshift

$z_{rei} = 8.8 \; (7.4 – 10.5)$

evolution of the cosmic SFR and Thomson scattering τ

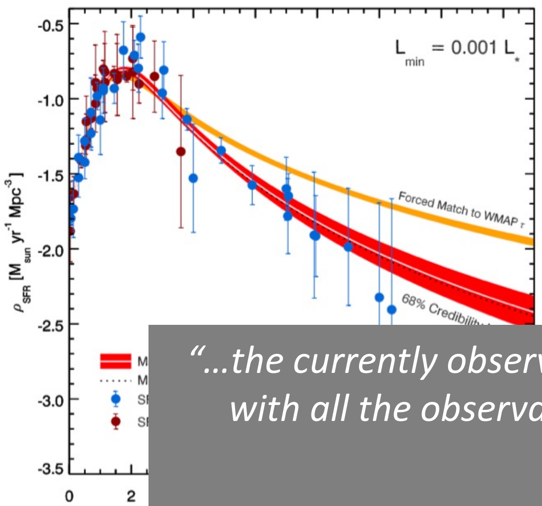

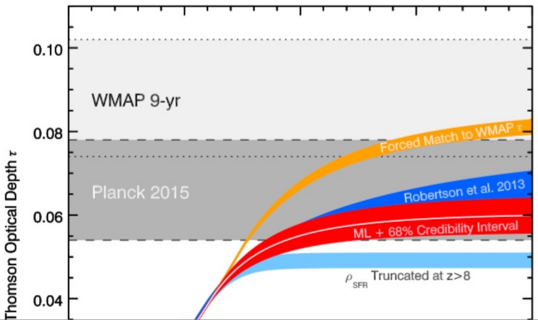

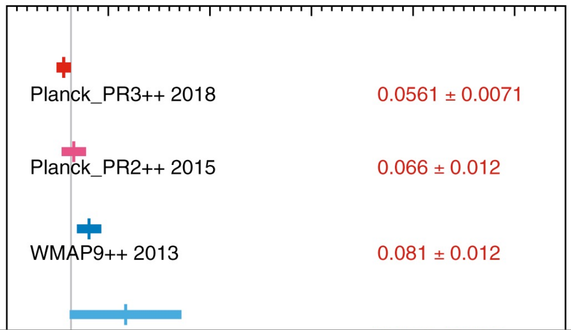

"…the currently observed galaxy population at z < 9 and M_{UV} < - 17 seems to be sufficient to comply with all the observational constraints without the need for high-redshift (z = 10–15) galaxies."

Planck collaboration, 2016

"…the latest results from the final full mission Planck measurements…are consistent with models in which reionization happened relatively fast and late."

Planck collaboration, 2018

global constraint: EDGES measurement of 21cm absorption at 78 MHz

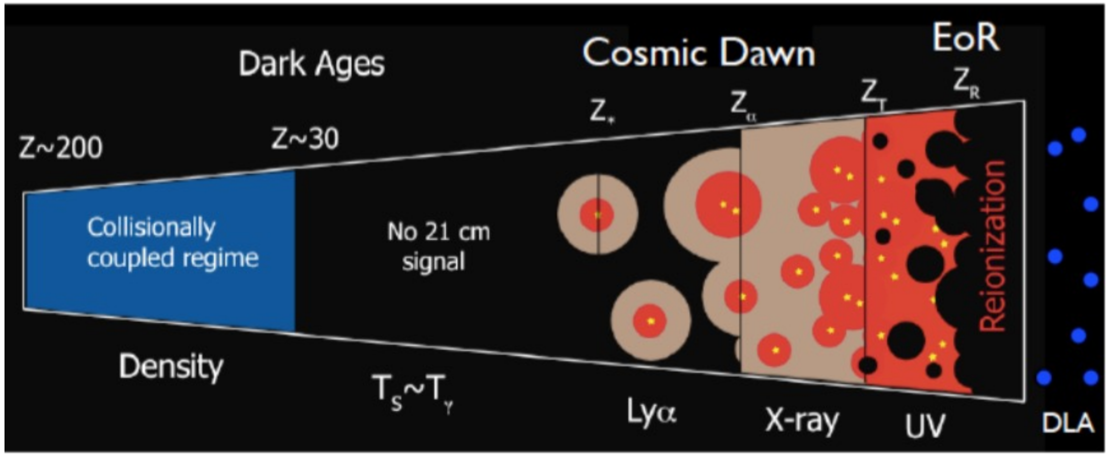

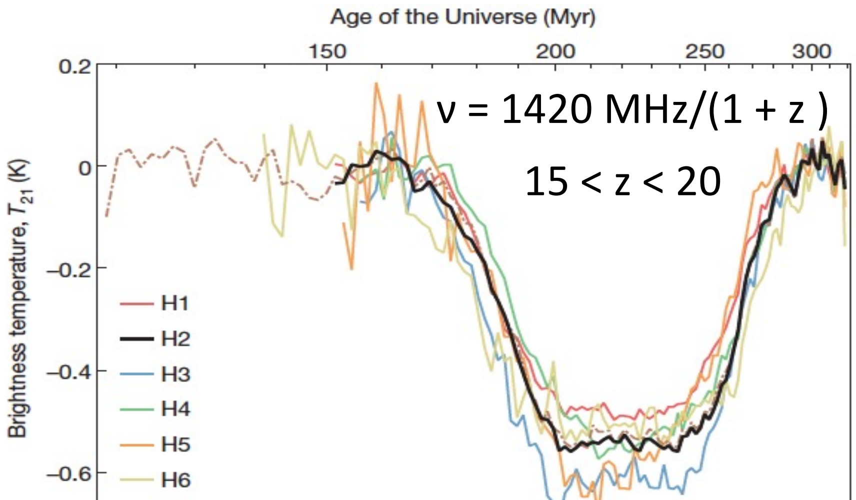

"The low-frequency edge of the observed profile indicates that stars existed and had produced a background of Lyman-α photons by 180 million years after the Big Bang. The high-frequency edge indicates that the gas was heated to above the radiation temperature less than 100 million years later."
Bowman et al. (2018)

the most distant galaxy

Oesch et al. (2016)

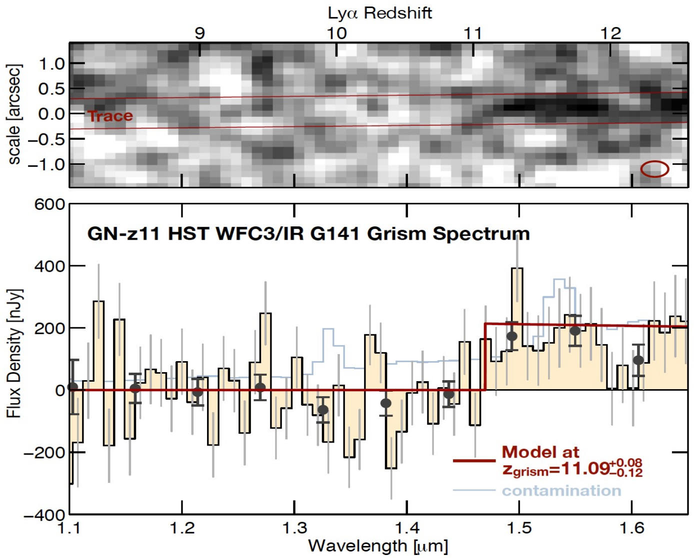

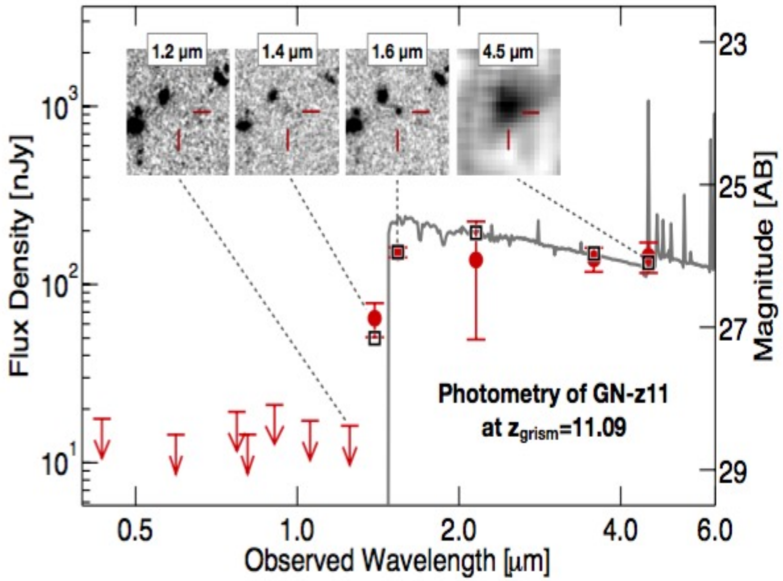

M_{uv} = - 22.1, very little dust extinction (β = -2.5)

$M_{star} = 10^9\ M_{sun}$, t_{age} ~ 40 Myr, SFR = 24 M_{sun}/yr

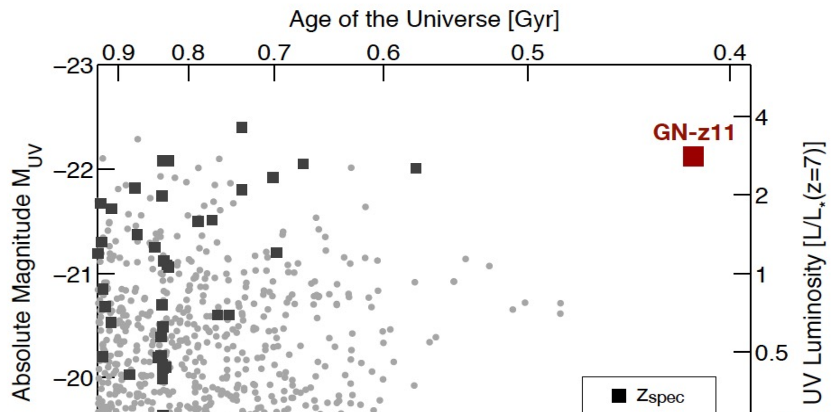

"The spectroscopic measurement of GN-z11 as a high-redshift source proves that massive galaxies of a billion solar masses already existed at less than 500 Myr after the Big Bang and that galaxy build-up was well underway at z > 10."
Oesch et al. (2016)

dust content of z > 7 normal star forming galaxies

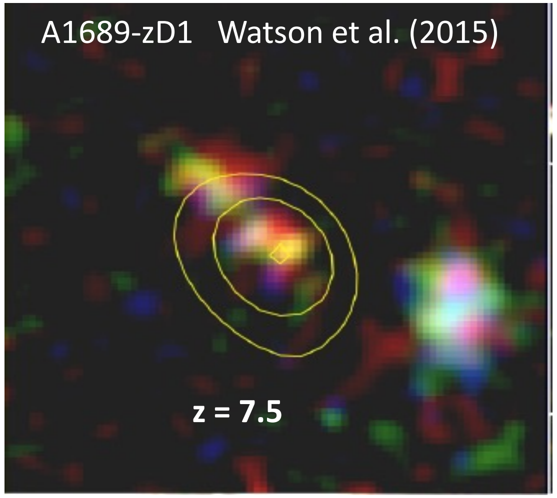

M_{star} ~ 2 10^9 M_{sun} SFR ~ 10 M_{sun}/yr
M_{dust} ~ (3 – 6) 10^7 M_{sun}

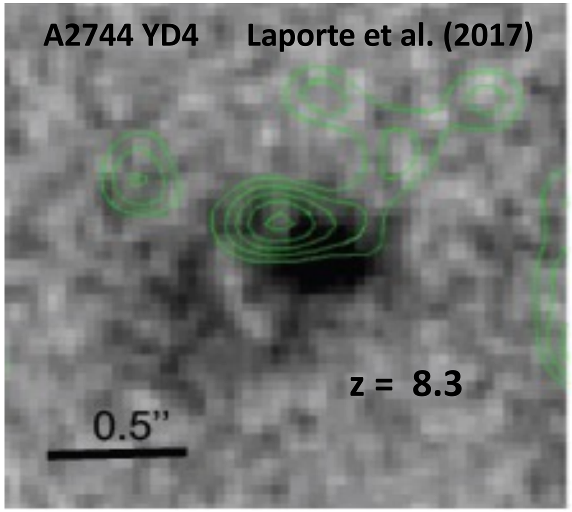

M_{star} ~ 2 10^9 M_{sun} SFR ~ 20 M_{sun}/yr
M_{dust} ~ 6 10^6 M_{sun}

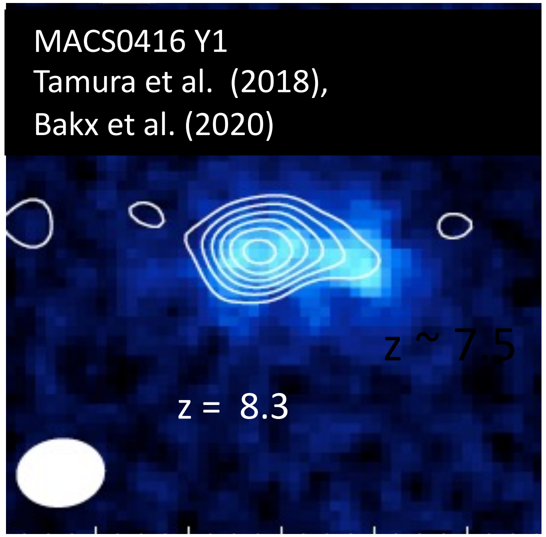

M_{star} ~ (0.3 – 1) 10^{10} M_{sun}
SFR ~ 60 M_{sun}/yr
M_{dust} ~ (7.7 10^6 – 6 10^4) M_{sun}

A1689-zD1 Knudsen et al. (2017)

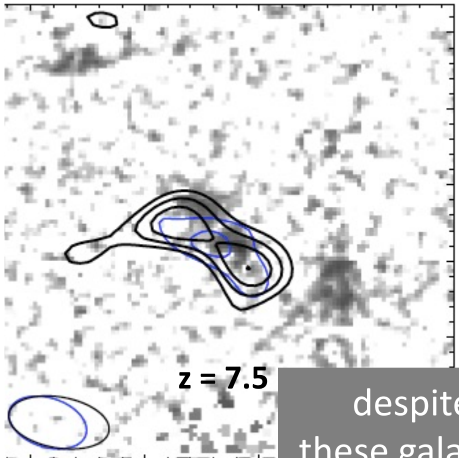

B14-65666 Hashimoto et al. 2018

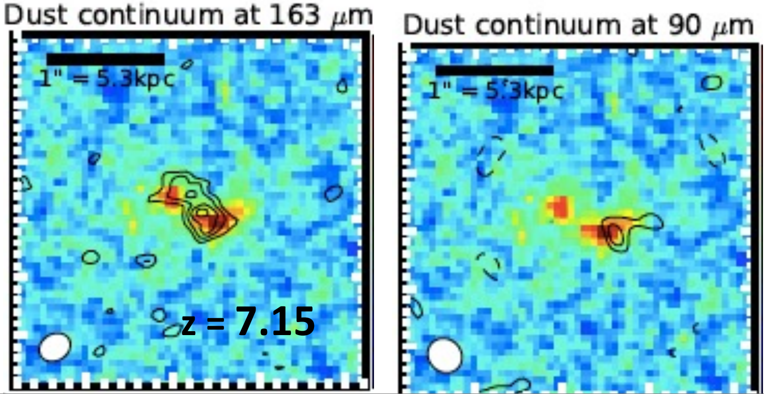

Bowler et al. 2018

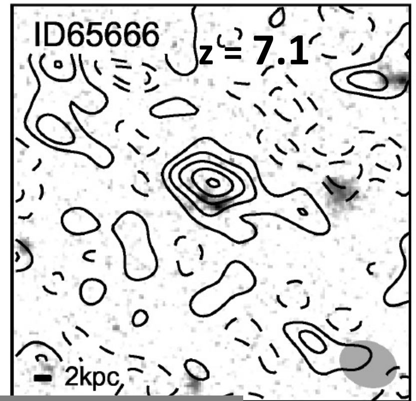

R ~ 50 M_{sun}/yr
0^7 M_{sun}

despite the uncertainties that affect the dust mass determination, the ISM of these galaxies has been already significantly enriched by several stellar generations

the most distant supermassive BHs

a subsample of high-z SMBHs

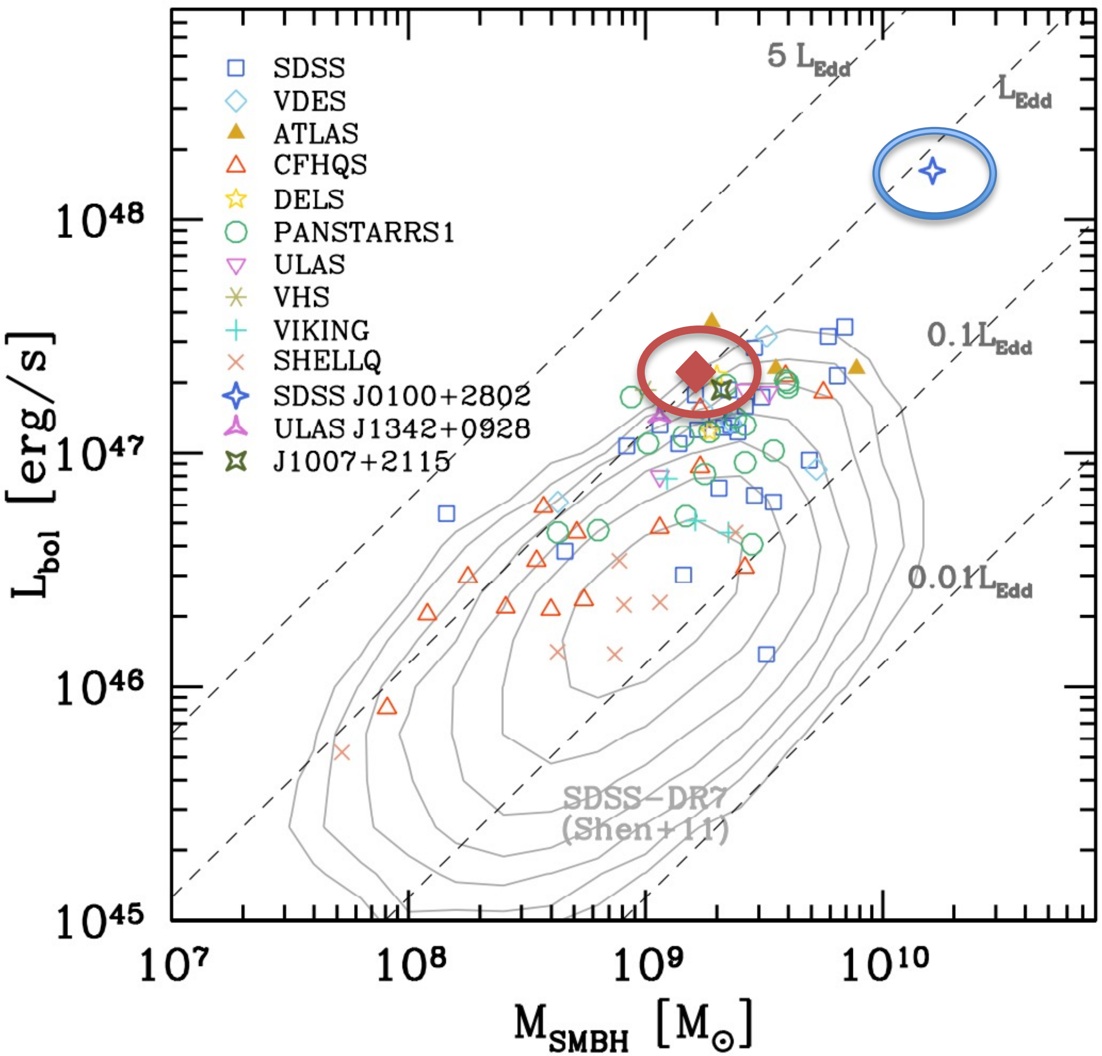

Courtesy of L. Zappacosta

SDSS J0100

$M_{smbh} = 2\ 10^{10}\ M_{sun}$

Wu+2015

J0313-1806

z = 7.64

Wang+2021

z > 6 quasars are powered by fully grown SMBH

building a coherent framework

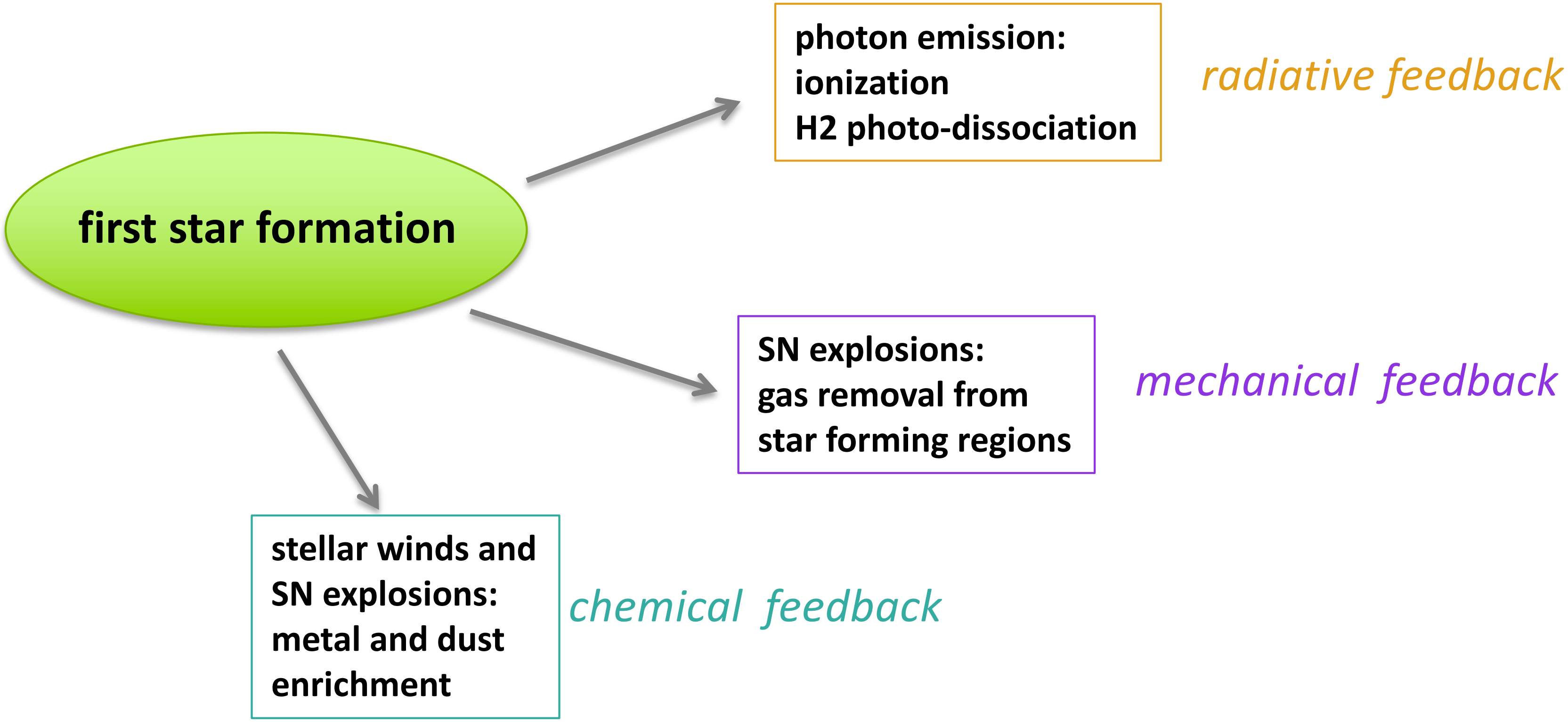

the complex interplay of radiative, mechanical and chemical feedback effects determine the nature and properties of the first galaxies

the formation of the first stars

the first star forming sites in a ΛCDM cosmology

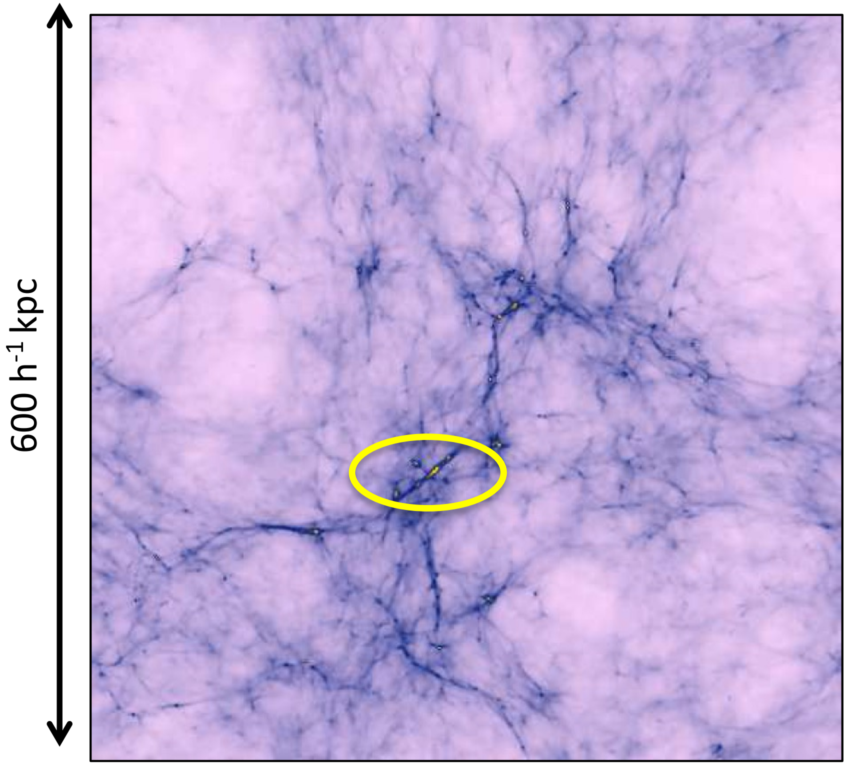

Yoshida et al. 2003

mini-halos with $M = 10^6 - 10^7\ M_{sun}$ @ $z = 20 - 30$

$T_{vir} < 10^4$ K

cooling rate of primordial gas

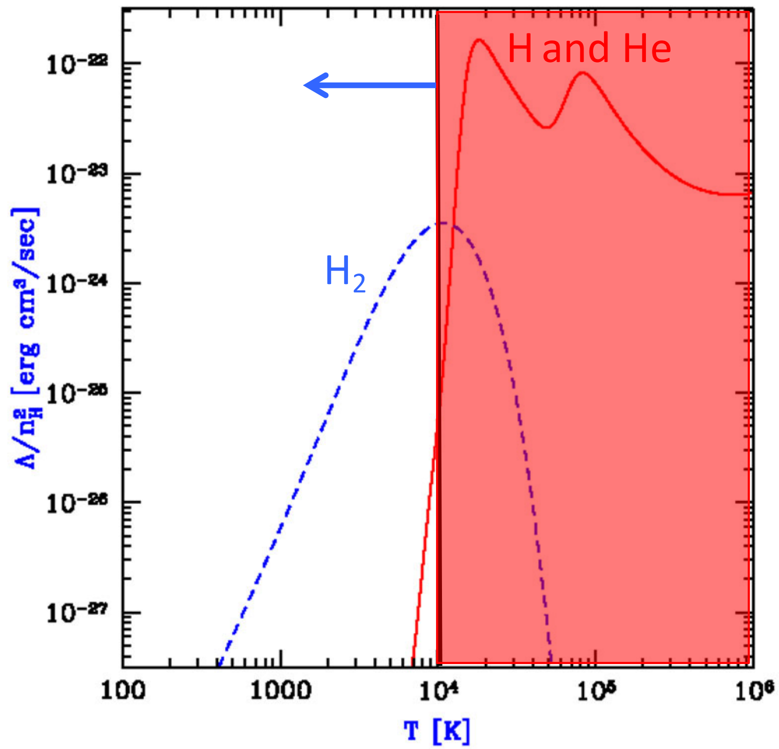

the formation of the first stars relies on H_2 cooling

protostar formation in the early Universe

projected gas distribution around the protostar

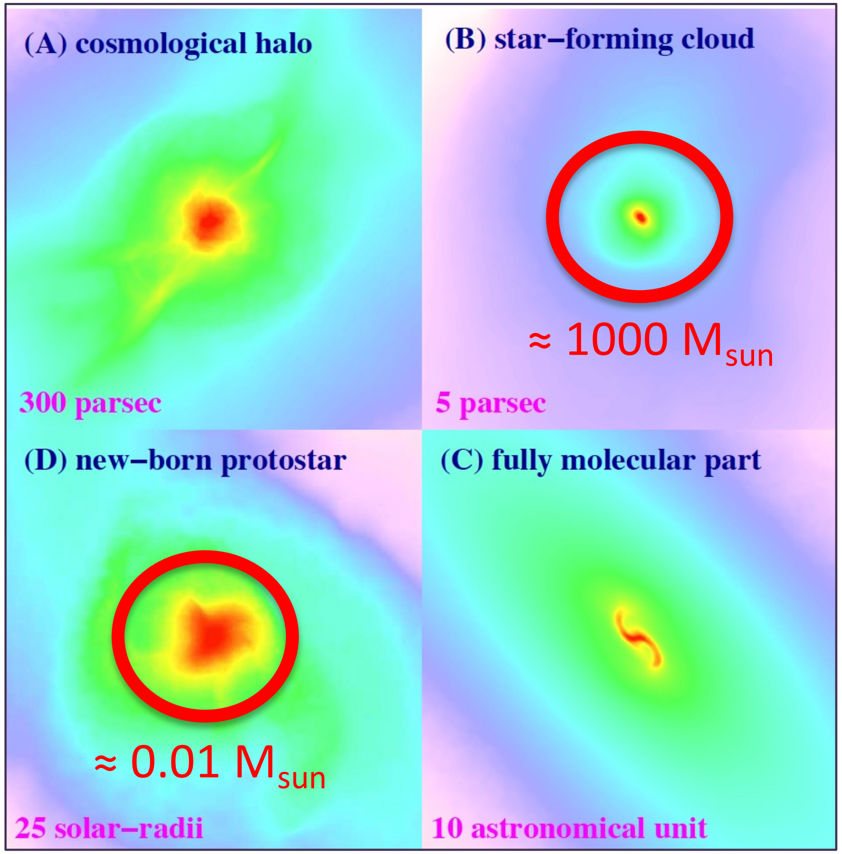

Yoshida et al. 2008

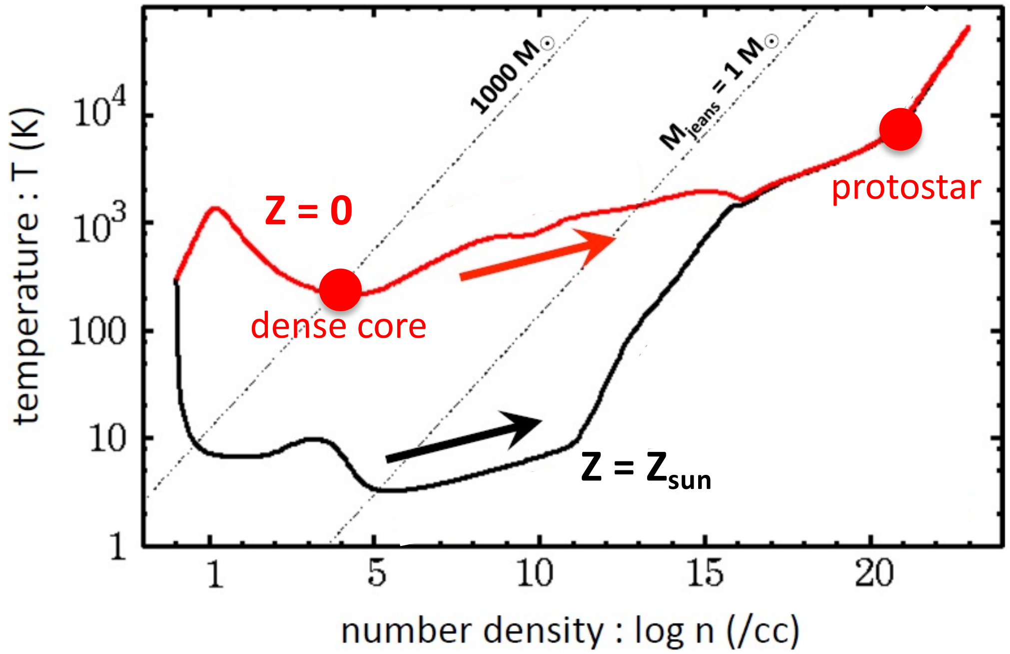

Omukai 2000

H_2 cooling leads to the formation of dense cores at $n \approx 10^4$ cm^{-3}, $T \approx 200$ K

with mass ≈ 1000 M_{sun}

with metal cooling ($Z = Z_{sun}$) dense cores have a mass of mass ≈ 1 M_{sun}

protostellar mass accretion

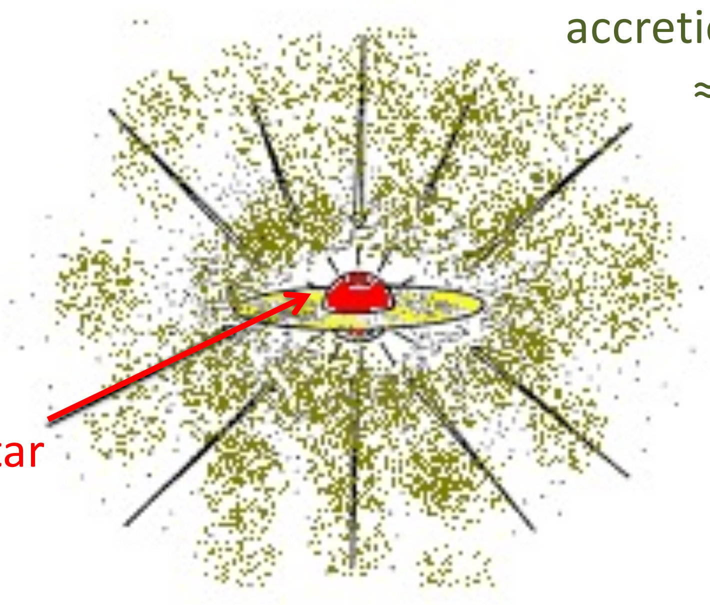

Accretion rate:

$dM/dt \approx M_j/t_{ff} \approx (c_s\ t_{ff})^3\ \rho/t_{ff} \approx c_s^3/G \approx T^{3/2}$

Pop I ($T \approx 10$ K): $10^{-6}\ M_{sun}$/yr

Pop III ($T \approx 200$ K): $10^{-3}\ M_{sun}$/yr

→ much higher accretion rate in Pop III star formation

the final stellar mass is set by UV feedback

2D radiation hydrodynamic simulation of the accretion phase

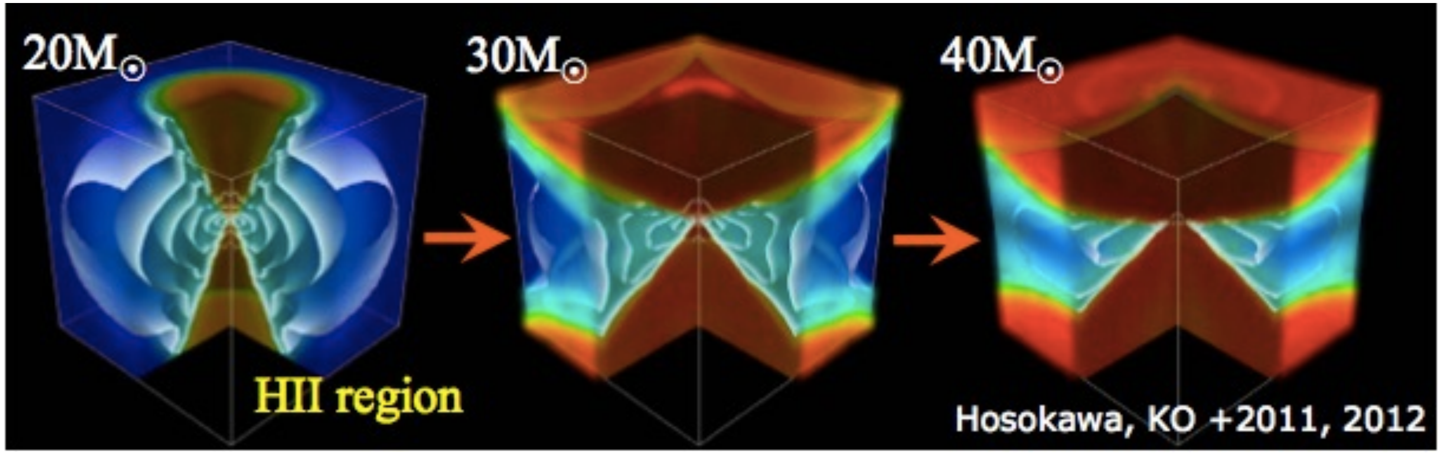

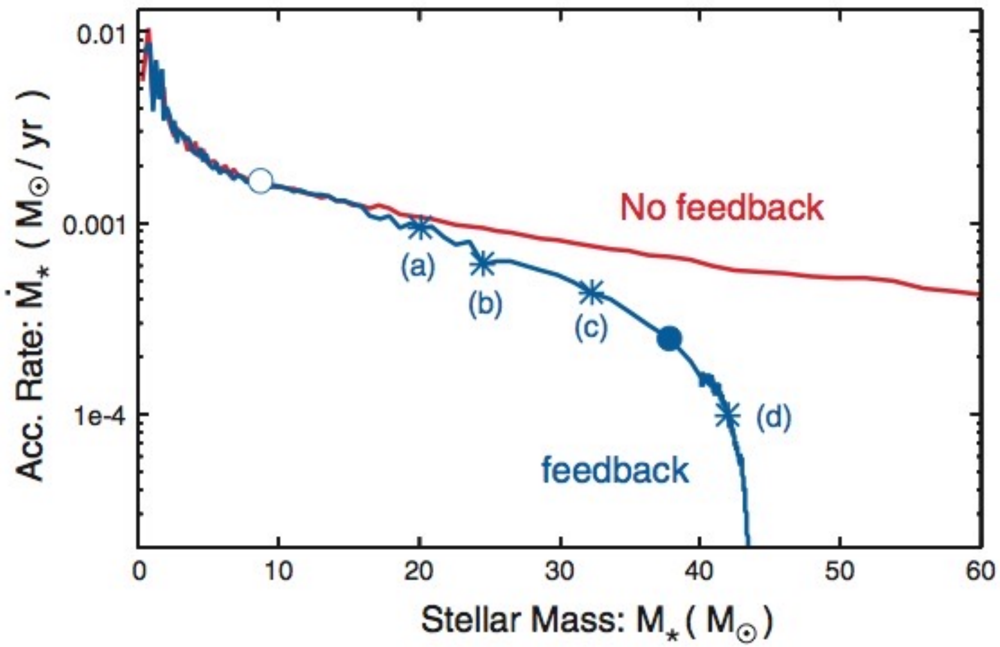

disk photo-evaporation limits the final stellar mass to $M_* \approx 40\ M_{sun}$

but

M_* depends on the environmental conditions

(Hirano+14, 15; Susa+14)

the mass spectrum of Pop III stars

3D cosmological simulation
+ 2D radiation hydrodynamic simulation

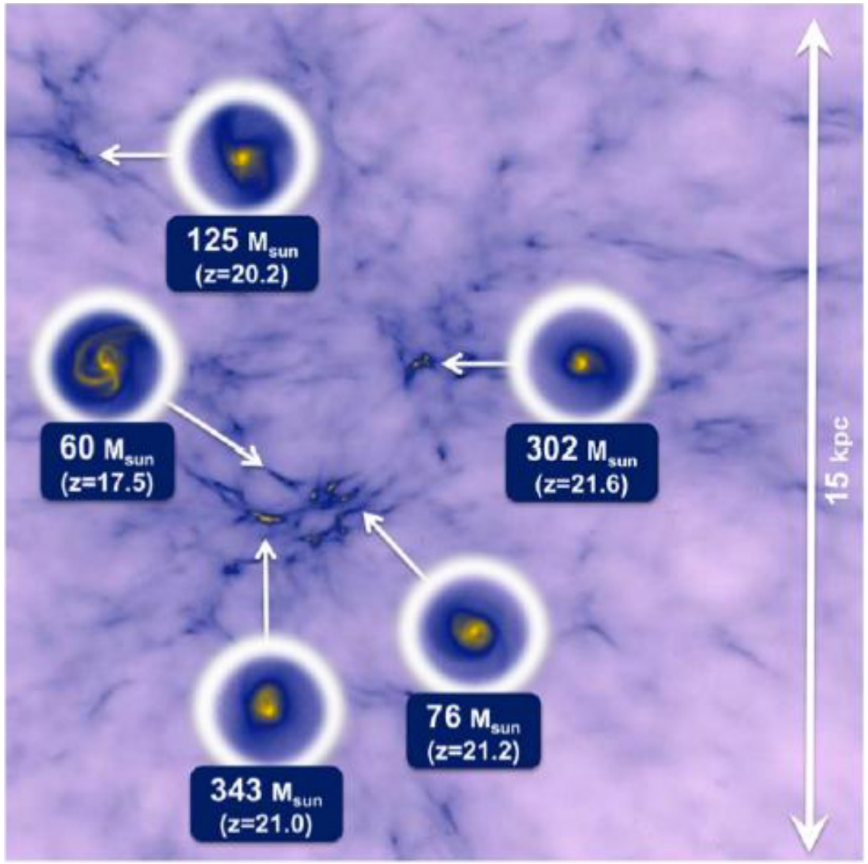

Hirano et al. 2014, 2015

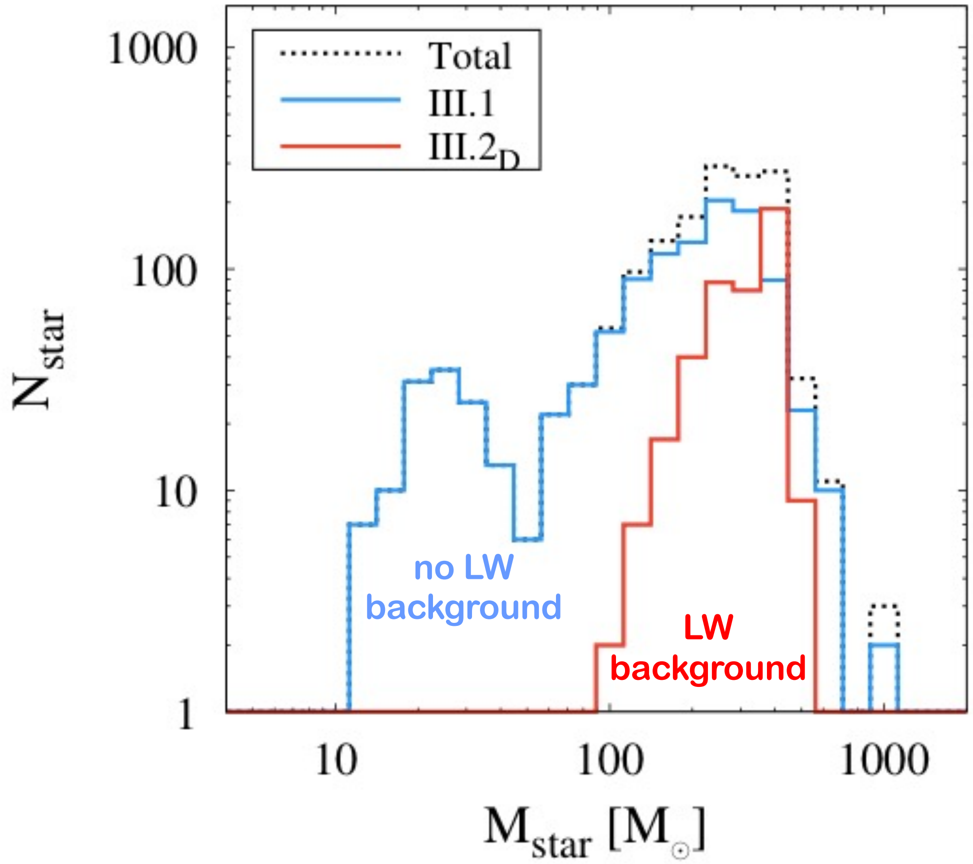

Pop III stars form within a wide mass range: few 10s - 100s up to few 1000s

multiplicity of Pop III stars

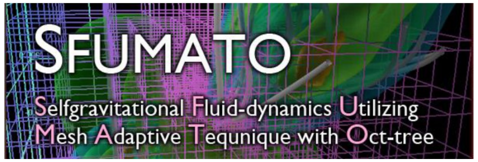

Sugimura et al. (2020)

- ✓ high resolution (AMR) especially in the outer part of the disk, where fragmentation is more active
- ✓ multiple sources of UV radiation (ART)

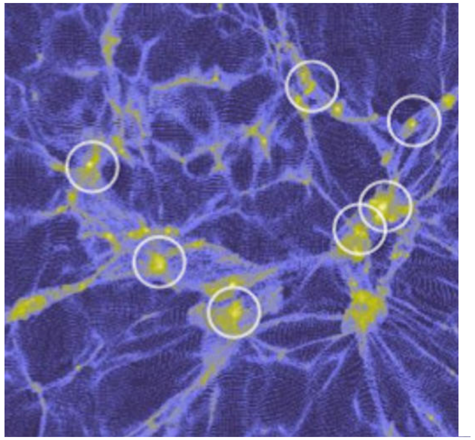

Hirano et al. (2015)

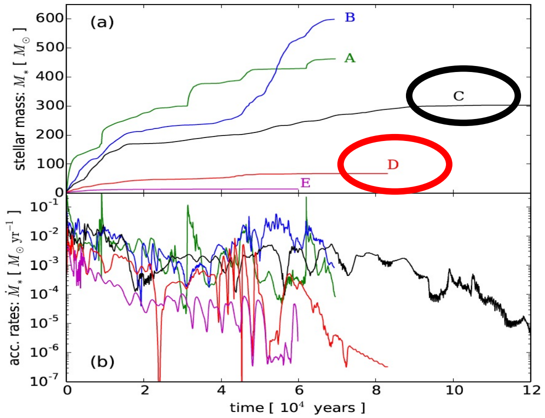

Hosokawa et al. (2016)

minihalo C

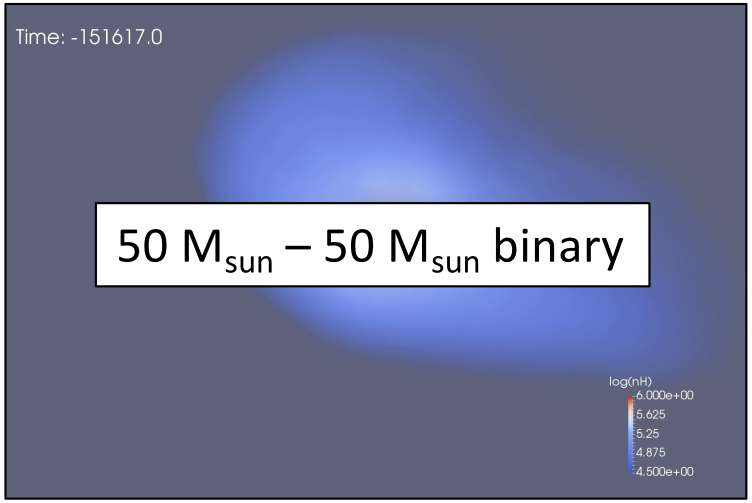

minihalo D

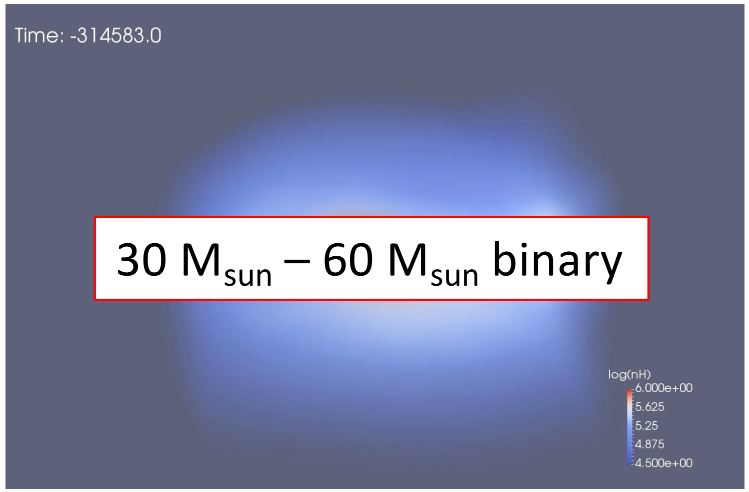

multiple stellar systems with massive binaries are common among Pop III stars

Final fate of the first stars: SN explosion or direct BH formation?

$$\Phi(m) = \frac{dN}{dm} \propto m^{\alpha-1} \exp\left(-\frac{m_{ch}}{m}\right)$$

m_{ch} = 20 M_{sun} α = -1.35 m_* = [10 – 300] M_{sun}

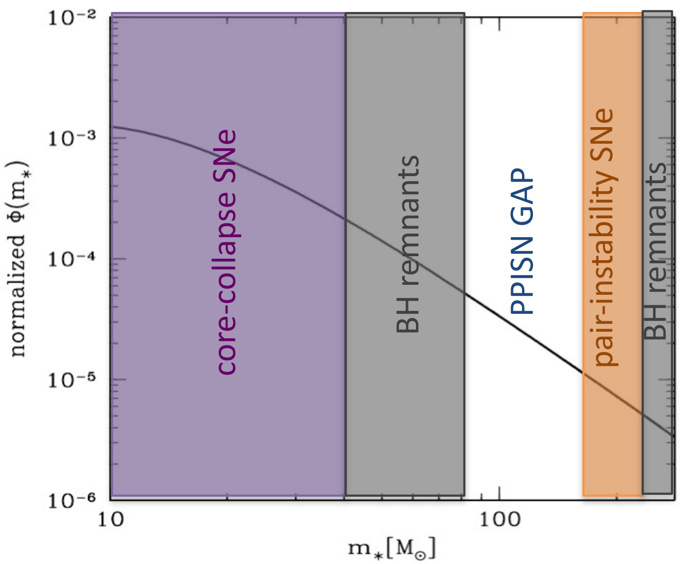

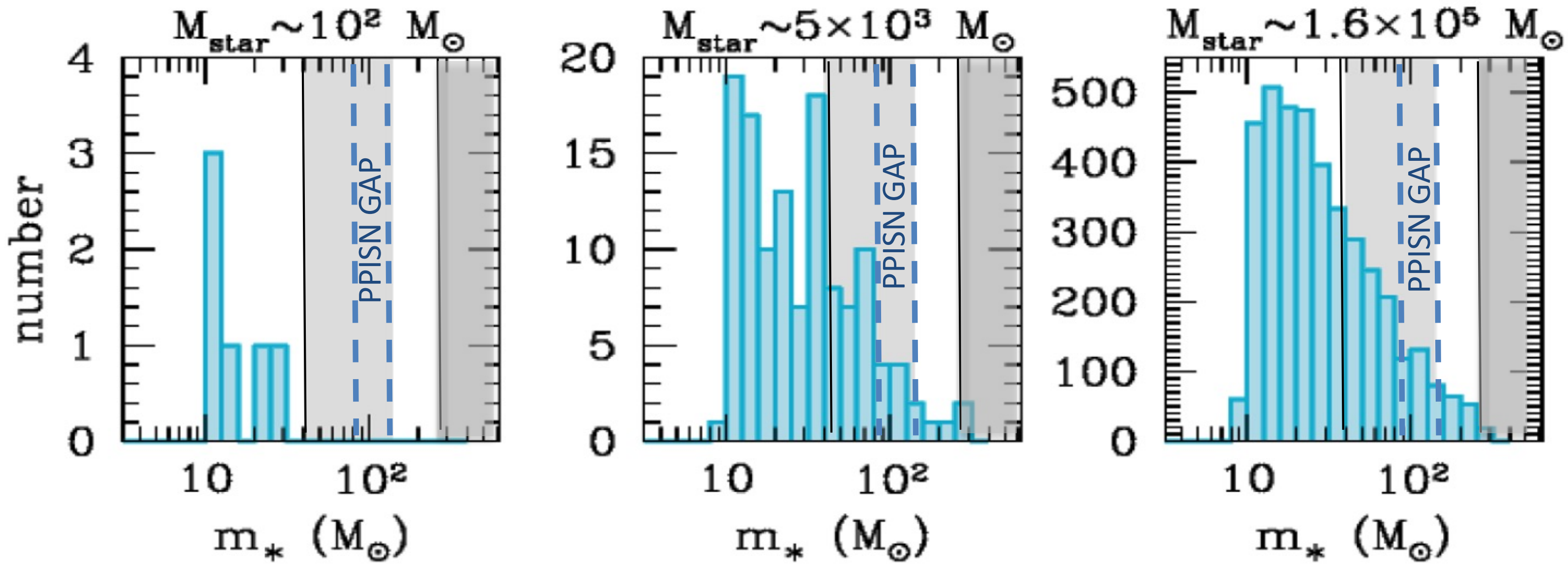

Valiante et al. 2016

fact sheet on the first stars

- ✓ form at $20 < z < 30$ in H_2 cooling mini-halos
- ✓ wide range of possible masses 10s – 1000s M_{sun}
- ✓ poorly constrained mass distribution
- ✓ binary/multiple massive stellar systems
- ✓ BH remnants with masses ≈ 40 – 80 M_{sun} and > 250 M_{sun}
- ✓ Enrichment with heavy elements from core-collapse, PPISN and PISN explosions

second-generation stars

the renaissance simulation (Xu et al. 2016)

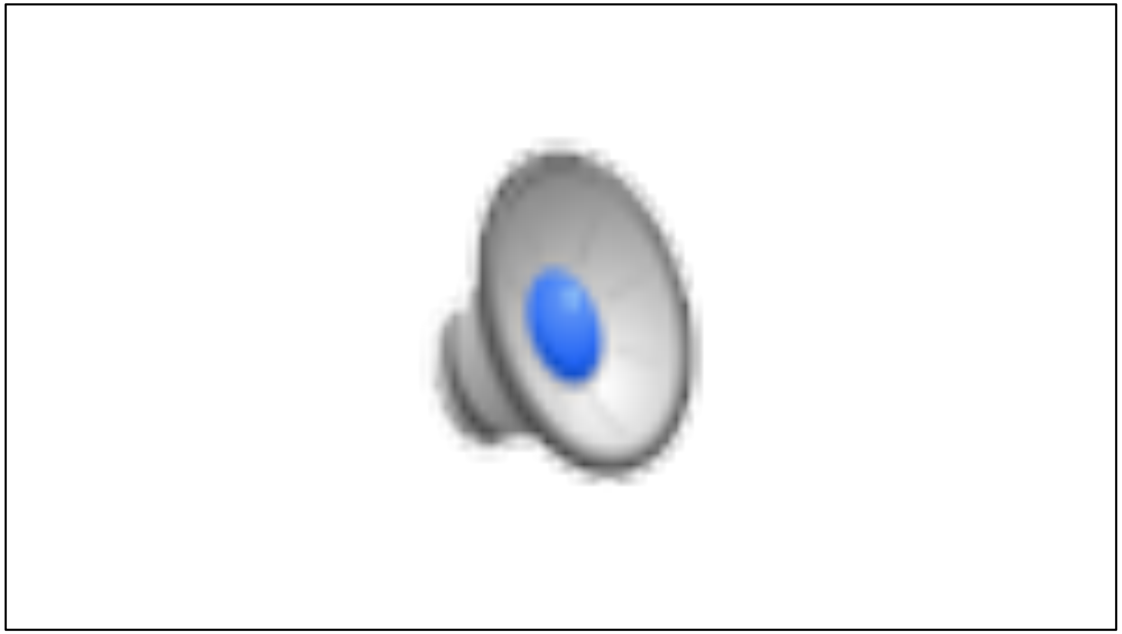

- Emission of UV photons in the Lyman Werner band [11.2 – 13.6] eV → H_2 photo-dissociation
- Supernova explosions pollute the gas with metals and dust

→ the cooling properties of the gas change → the stellar mass spectrum changes

Cooling rate of low-metallicity gas

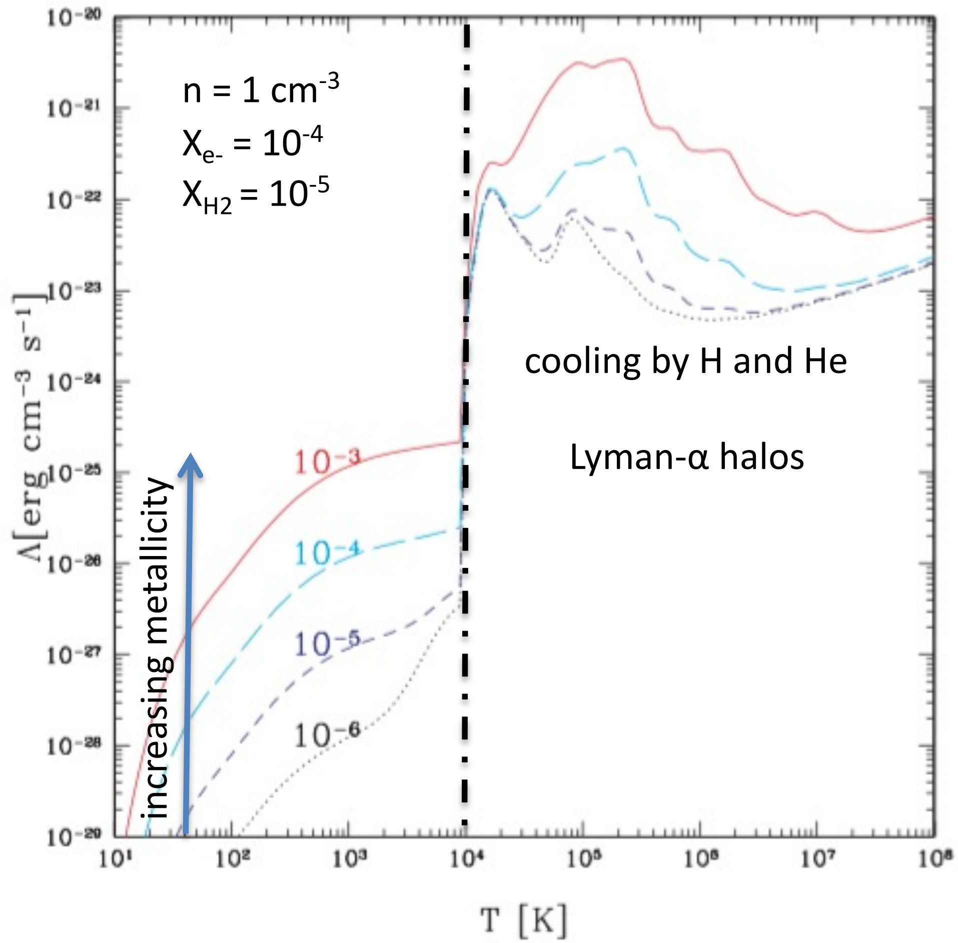

Cooling rate of low-metallicity gas

molecular cooling – primordial gas

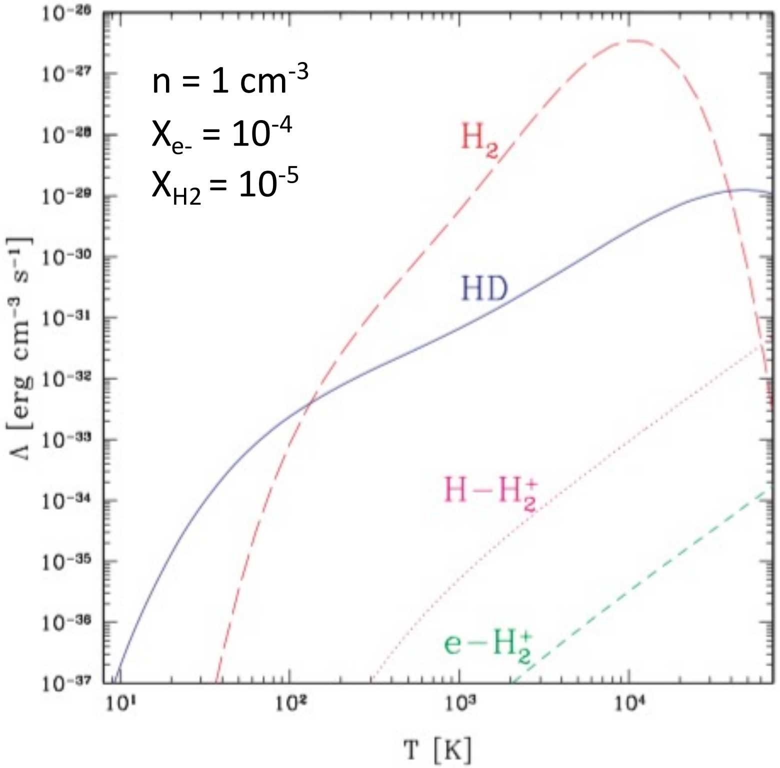

metal cooling – enriched gas

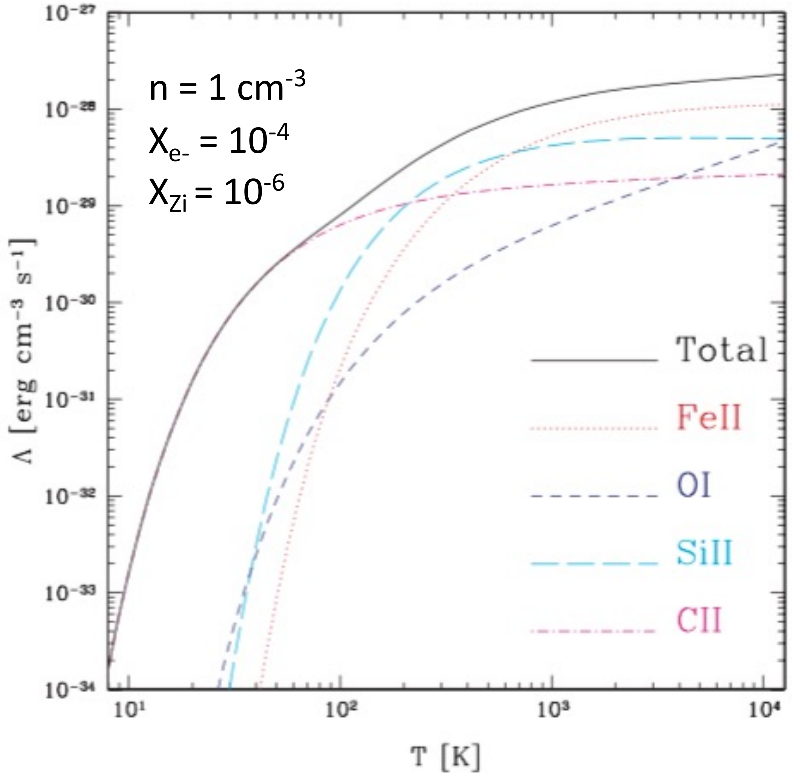

in the first mini-halos ($T_{vir} < 10^4$ K) the gas cools via H_2 and OI / CII

Evolution of star forming clouds

The gas cools when: $t_{cool} = 3nkT/2\Lambda_{cool}(n,T) \ll t_{ff} = (3\pi/32G\rho)^{1/2}$

and the energy deposited by gravitational contraction can not balance radiative losses

The cloud cools and fragments. Fragments form on a scale that ensures pressure equilibrium:

$R_F = \lambda_{Jeans} = c_s\, t_{ff} \approx n^{\Upsilon/2\,-1}$ where $c_s = (\Upsilon kT/\mu m_H)^{1/2}$ and $T \approx n^{\Upsilon-1}$

$M_F \approx n\, R_F^{\eta} \approx n^{\eta\Upsilon/2+(1-\eta)}$ (η = 2 for filaments and = 3 for spherical fragments)

The conditions to stop fragmentation and start gravitational contraction are:

1) cooling becomes inefficient: $t_{cool} > t_{ff}$
2) the Jeans mass does not decrease: $\eta Y/2+(1-\eta) \geq 0$ → $Y \geq 1$ for filaments

$Y \geq 4/3$ for spherical fragments

H_2, metal and dust-driven fragmentation: three different mass-scales

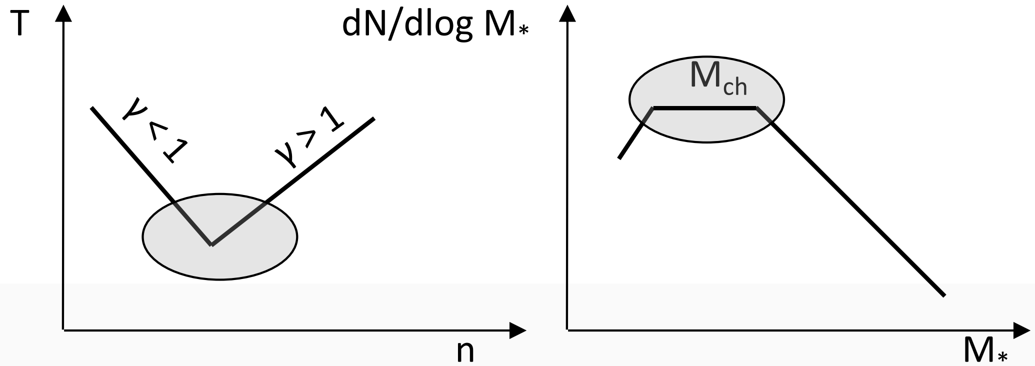

H_2-line cooling:

$M_{jeans} \sim 10^3\ M_{sun}$

Abel+(2002)
Bromm+(2002)
Yoshida+(2008)

metal-line cooling:

$Z > 10^{-4}\ Z_{sun}$

$M_{jeans} > 10\ M_{sun}$

Bromm et al. (2001)
Bromm & Loeb (2003)
Santoro & Shull (2004)

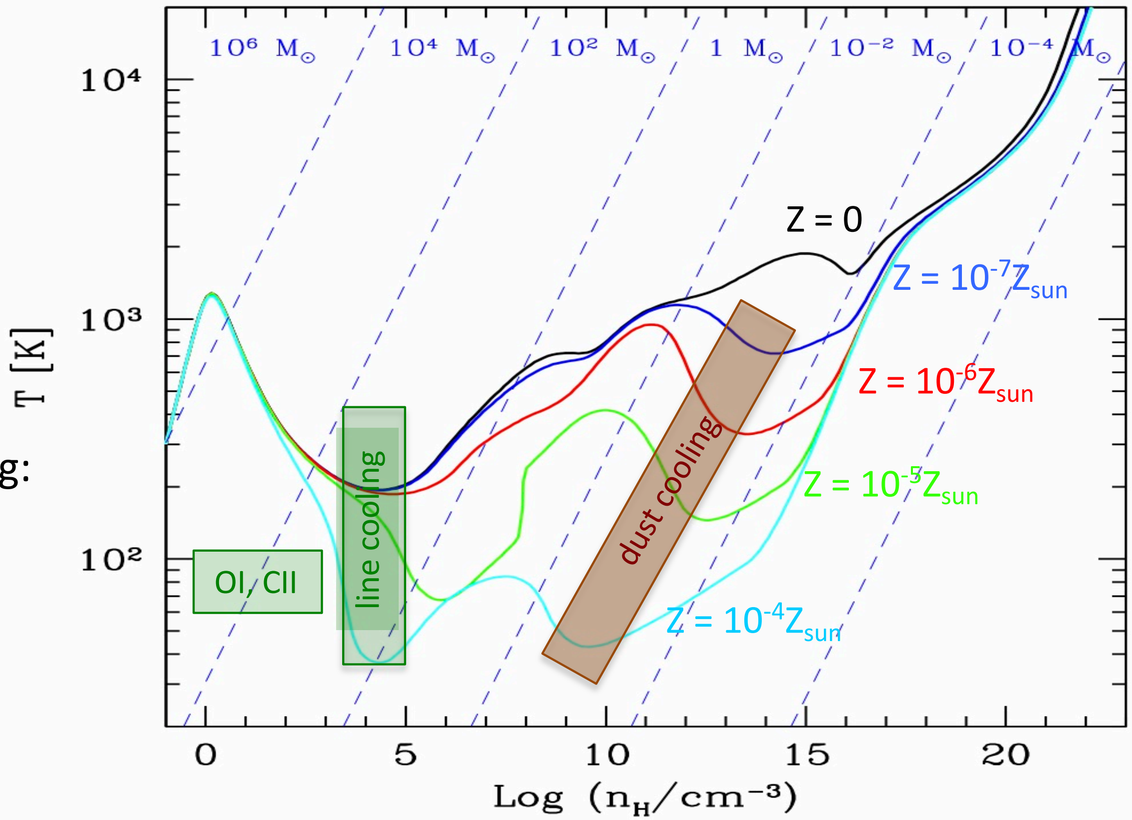

dust cooling:

$Z > 10^{-6}\ Z_{sun}$

$M_{jeans} < 1\ M_{sun}$

RS et al. (2002,2003,2006),
Omukai et al. (2005)

The formation of the first low-mass stars: critical metallicity or dust-to-gas ratio?

RS, Omukai, Bianchi, Valiante (2011)

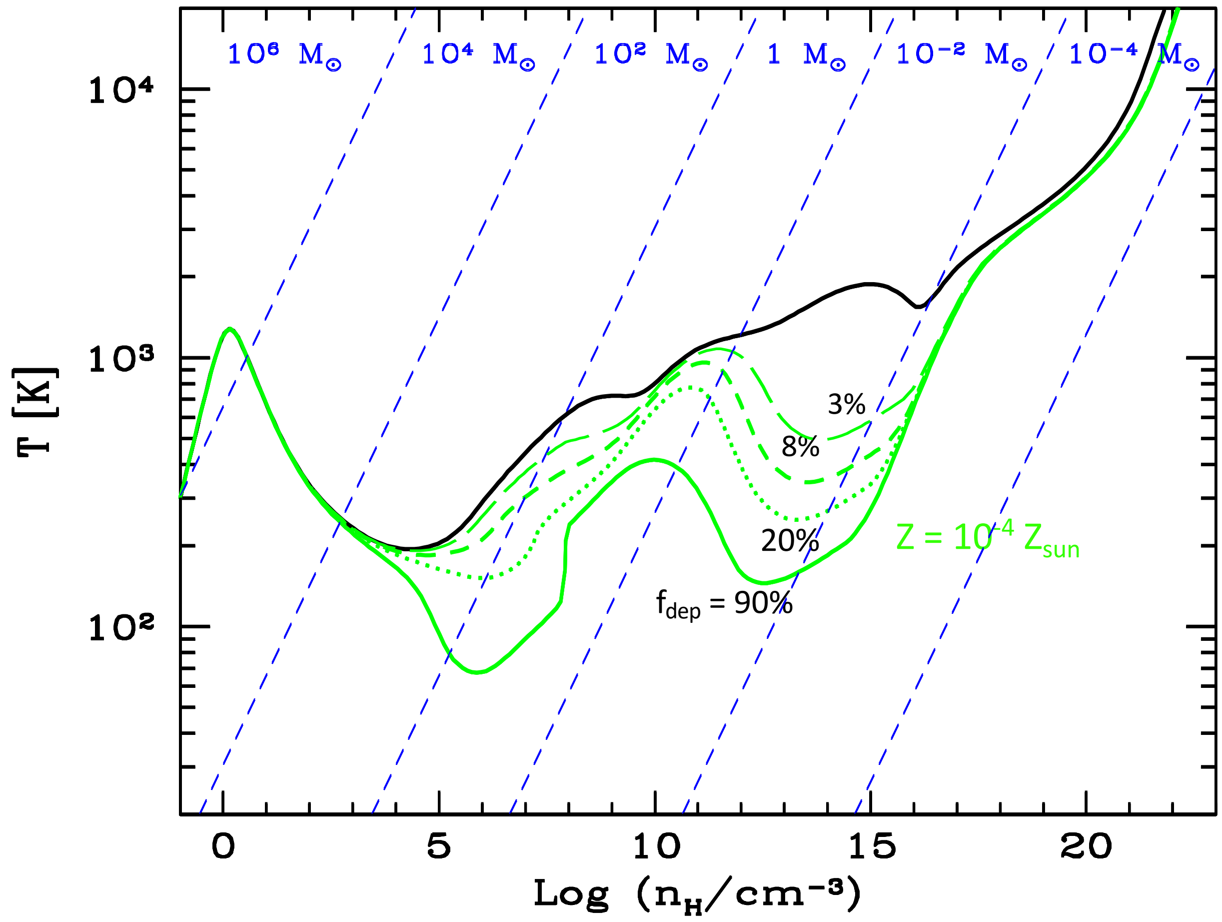

$f_{dep}=M_{dust}/(M_{met}+M_{dust})$

dust cooling depends on the absolute metallicity AND dust depletion factor → dust-to-gas ratio

low mass star formation: critical dust-to-gas ratio

- 20 M_{sun} Z = 0
- 35 M_{sun} Z = $10^{-4} Z_{sun}$
- 20 M_{sun} Z = $10^{-4} Z_{sun}$
- CCSN Schneider+06
- PISN Schneider+06
- Local ISM Omukai+05

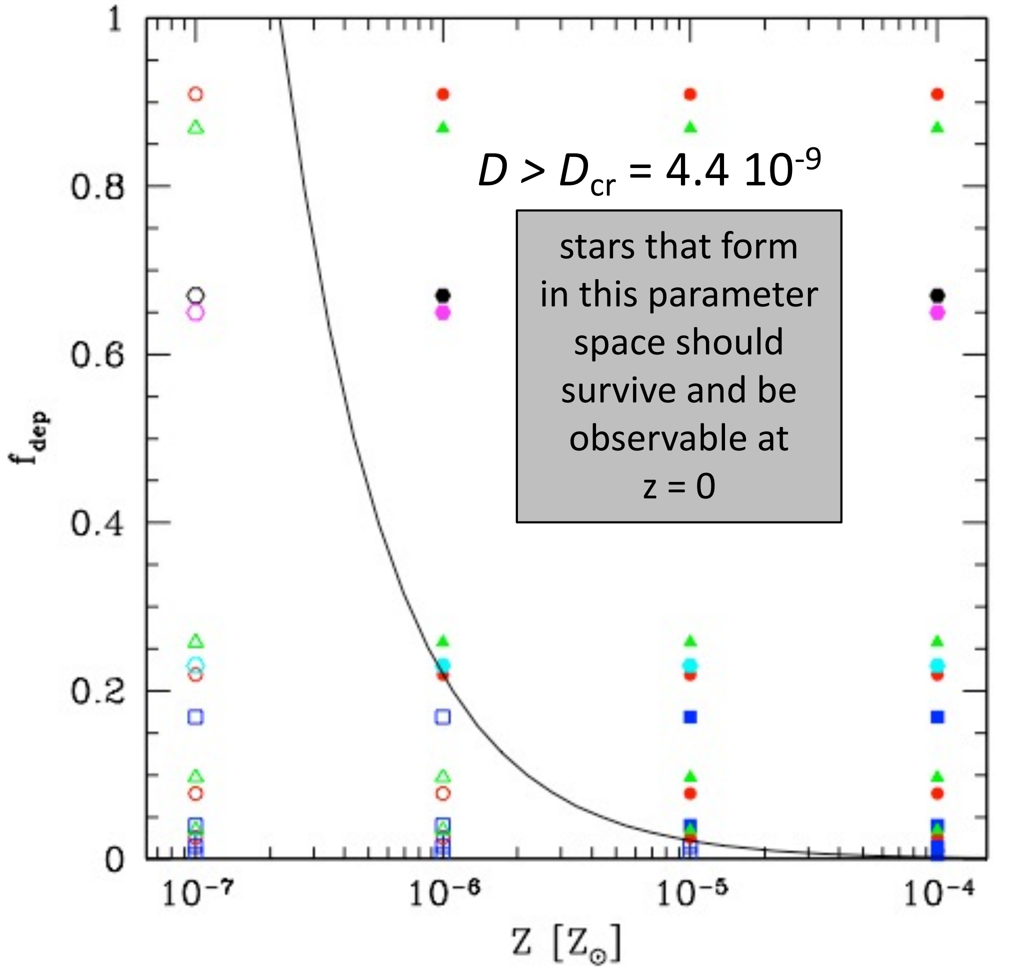

Energy transfer rate between gas and dust > Compressional heating rate

total grain cross section per unit dust mass ←

$$\mathcal{SD}_{cr} > 1.4 \times 10^{-3} \mathrm{cm}^2/\mathrm{gr} \left[\frac{T}{10^3 \mathrm{K}}\right]^{-1/2} \left[\frac{n_\mathrm{H}}{10^{12} \mathrm{cm}^{-3}}\right]^{-1/2}$$

RS, Omukai, Bianchi, Valiante (2011)

simulating the birth of a second generation star

numerical simulations of the entire formation sequence of a 2nd-generation star through the feedback effects of photo-ionization and metal-enrichment by a Pop III SN

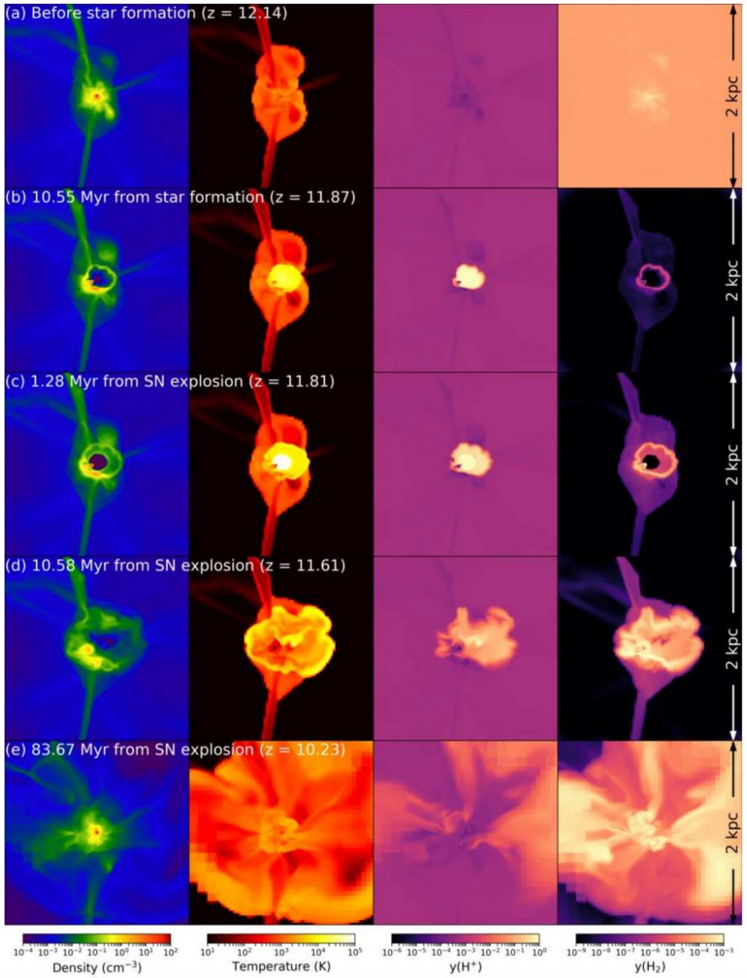

In a minihalo with M_h = 1.77 10^6 M_{sun} a 13 M_{sun} Pop III star forms at z = 12.1

after ≈ 11 Myr, the star explodes as a core-collapse SN

after ≈ 84 Myr, the gas falls back into the central region of the mini-halo, enriching it with Z = 2.6 10^{-4} Z_{sun} ([Fe/H] = -3.42)

Chiaki & Wise (2019), see also Chiaki et al. (2020)

simulating the birth of a second generation star

numerical simulations of the entire formation sequence of a 2nd-generation star through the feedback effects of photo-ionization and metal-enrichment by a Pop III SN

The recollapsing cloud undergoes molecular coolung (HD, CO, OH) and H_2 reformation

dust grains grow by accreting gas-phase metals and trigger dust cooling

knotty filaments appear in the central 100 AU region, leading to the formation of low-mass metal poor 2nd generation star

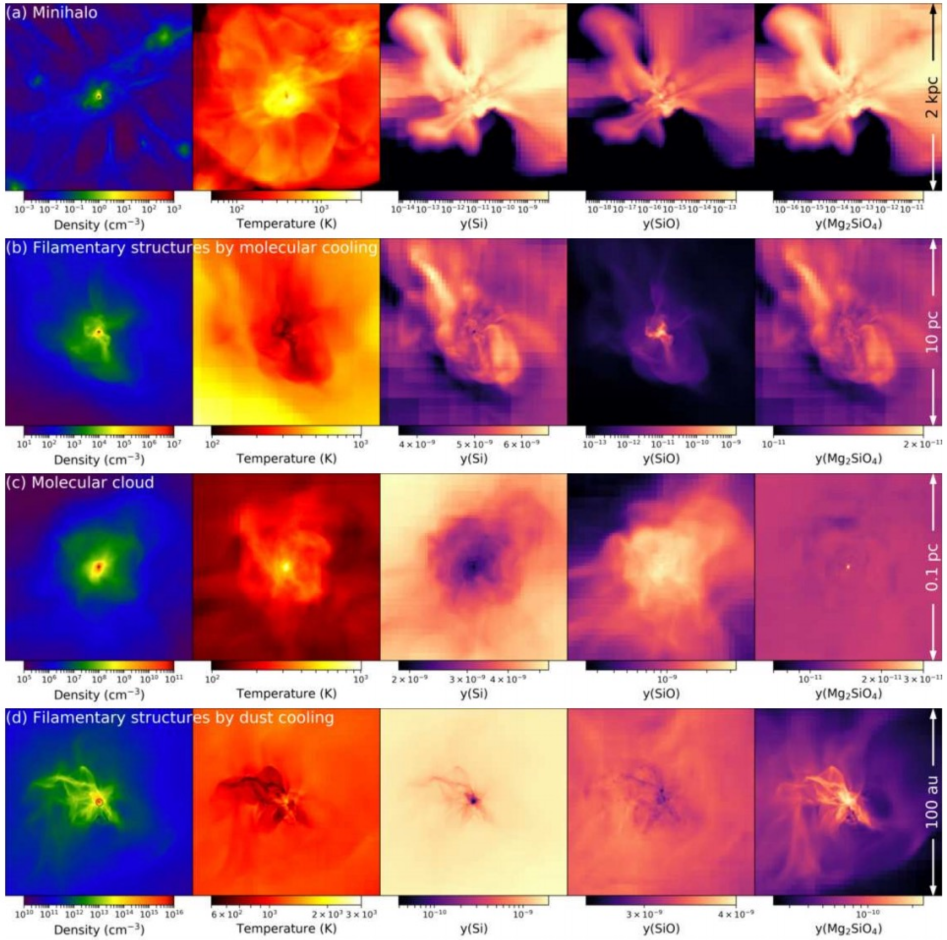

Chiaki & Wise (2019), see also Chiaki et al. (2020)

galactic archaeology

How can we test these ideas? By looking at the most metal poor stars in the local neighbourhood

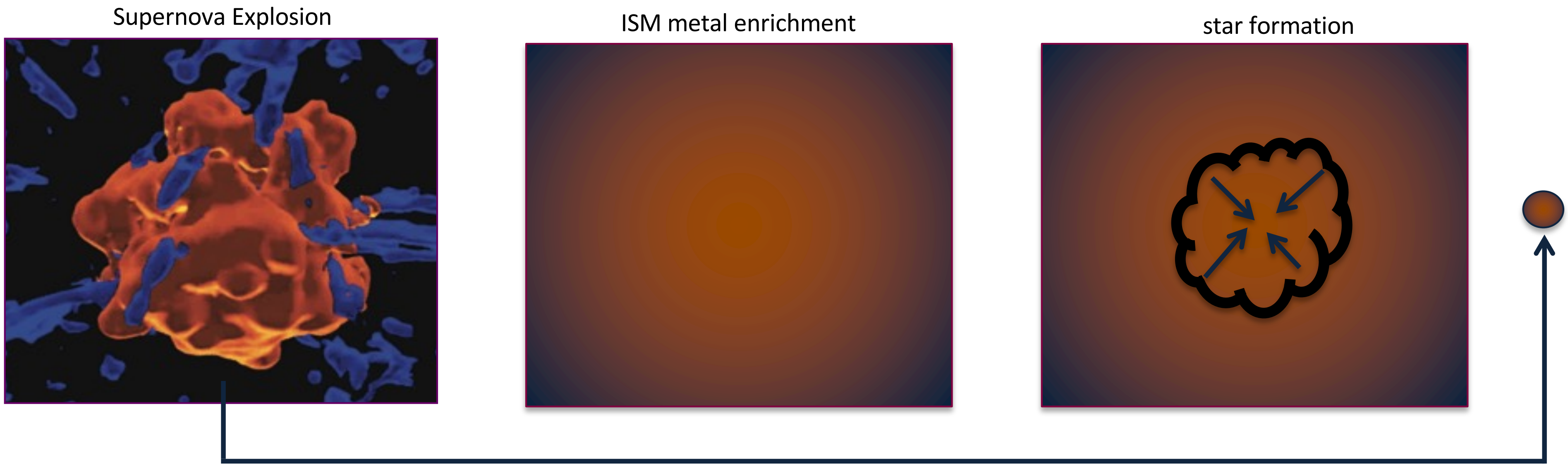

Example of comparing theoretical yields with elemental abundances in extremely metal-poor stars

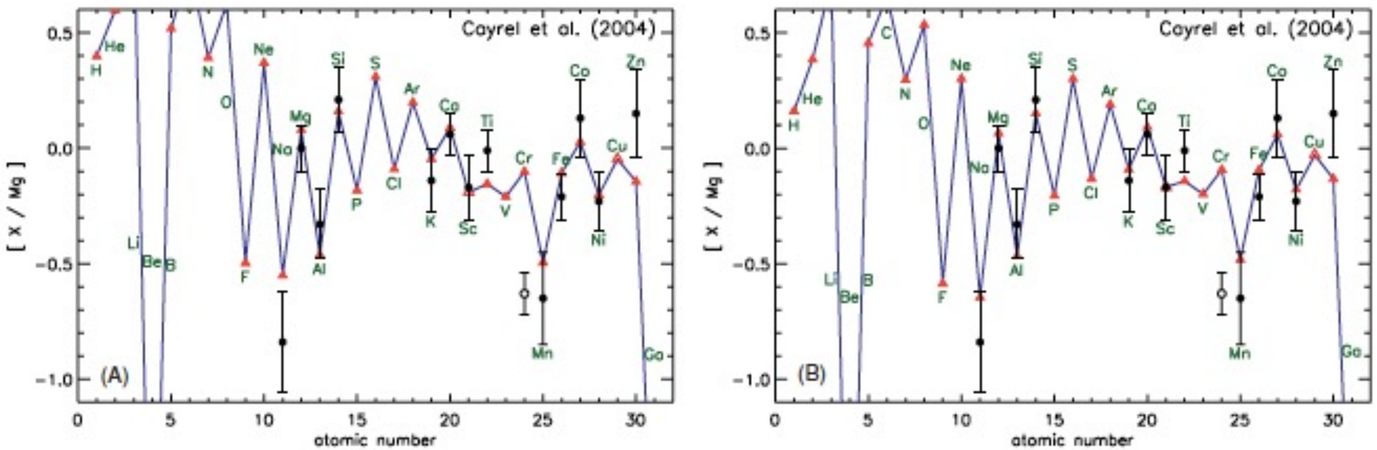

ASSUMPTION: observed metal-poor stars are *mono-enriched* (i.e. enriched by 1 SN)

A metallicity dependent IMF?

3D simulations of a turbulent core with different initial metallicities, to predict the stellar IMF

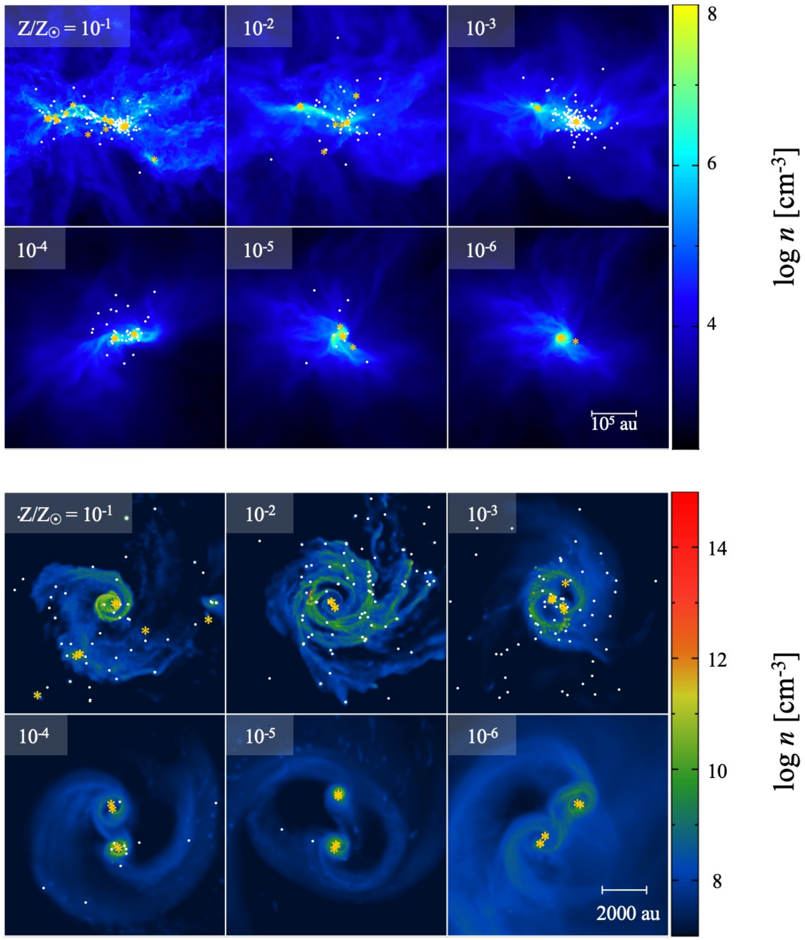

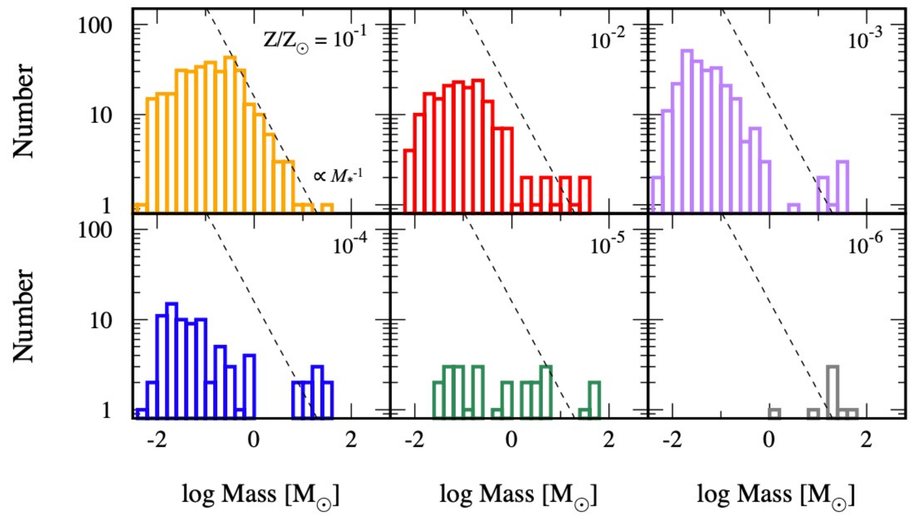

Chon, Omukai, RS (2021)

fact sheet on second generation stars

- ✓ form at $z < 30$ in H_2 cooling mini-halos and/or Lyman-α cooling halos

- ✓ metallicity-dependent mass distribution: when $Z < Z_{cr}$ the mass function is still top-heavy, when $Z > Z_{cr}$ the IMF is Chabrier-like.

- ✓ When $Z_{cr} = 10^{-5}\ Z_{sun}$ dust-driven fragmentation appears but the IMF may still be top-heavy up to $Z_{cr} = 10^{-2}\ Z_{sun}$ due to inefficient cooling and turbulence decay

do we reliably track the metal and dust content of galaxies at various redshifts?

Dwek+98, Hirashita+02; Inoue 03; Morgan & Edmunds 03; Calura+08; Zhukovska+08; Valiante+09, +11,+14; Asano+13; Calura +14; Zhukovska 2014; Feldmann+15; Pipino+11; Calura+13; Rowlands+14; Michałowski+15; Shimizu+14; Mancini+15, 16; de Bennassuti+16; Khakaleva-Li & Gnedin 16; Grassi+2016, Zhukovska+16; Aoyama+17,18, Popping+17, McKinnon+17, Ginolfi+18, Vogelsberger+18, Wilkins+18, Gall & Hjorth 18, Kimm+18, Katz+18, De Rossi & Bromm 2019; Lesniewska & Michalowski 2019; Graziani+ 2020

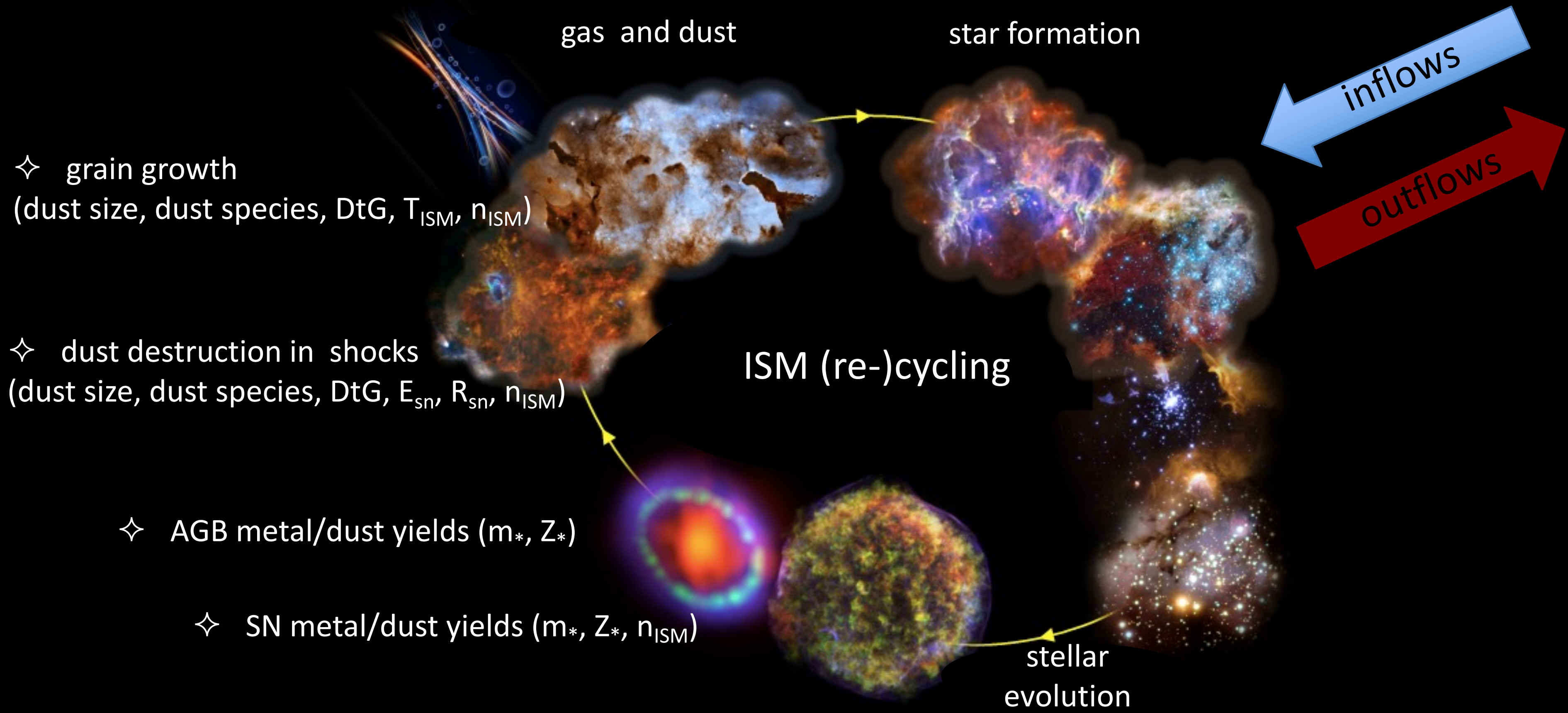

metal yields and stellar lifetimes

The mass of a given element produced by a star depends on the stellar mass and metallicity

$\mathbf{m_{met,i}(m, Z)}$

with i = C, N, O, Mg, Si, Fe, etc.

In a similar way, the mass of a given grain species is:

$\mathbf{m_{dust,j}(m,Z)}$

with j = AC, SiO_2, Mg_2SiO_4, $MgSiO_3$, Fe_3O_4, etc.

Stellar evolution models allow us to compute stellar yields for the main metal/dust factories:
Intermediate mass stars during their **Asymptotic Giant Branch (AGB)** phase and
supernova explosions (core-collapse SN, PISN, SNIa,…)

Cosmic stellar yields

Given a star formation history, ψ(t), and a stellar IMF, φ(m), the mass of metals and dust returned to the ISM per unit time can be computed as:

$$Y_{met}(t) = \int_{m_\tau}^{m_{up}} dm\, m_{met}(m, Z)\, \Phi(m)\, \Psi(t - \tau_m)$$

$$Y_{dust}(t) = \int_{m_\tau}^{m_{up}} dm\, m_{dust}(m, Z)\, \Phi(m)\, \Psi(t - \tau_m)$$

where:

$$m_{met}(m, Z) = \sum_i m_{met,i}(m, Z) \qquad m_{dust}(m, Z) = \sum_j m_{dust,j}(m, Z)$$

is the total mass in heavy elements (i = C, N, O…) and dust grains (i = AC, SiO_2, Mg_2SiO_4, $MgSiO_3$, Fe_3O_4, ...) and the intergral accounts for the contribution of all stars with a mass $m \geq m_\tau$ and a lifetime:

$$\tau_m = \tau(m, Z)$$

stellar lifetimes & timing arguments

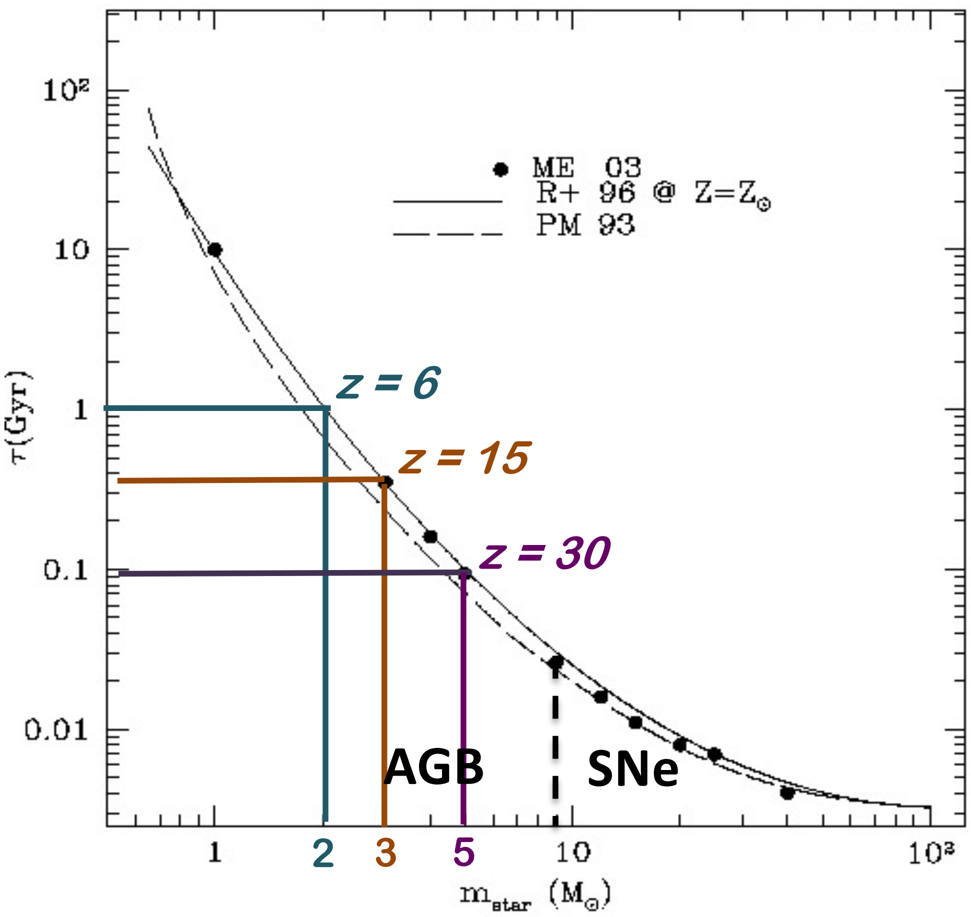

core-collapse SNe enrich on very short timescales: < 40 Myr

massive AGB stars (> 2 M_{sun}) can contribute to enrichment at z > 6

Pop III stellar yields

Chemical evolution for a single stellar population (SSP): all stars form in a single burst at t = 0

Larson IMF with α = -1.35 $$\Phi(m) = \frac{dN}{dm} \propto m^{\alpha-1} exp\left(-\frac{m_{ch}}{m}\right)$$

de Bennassuti+2017

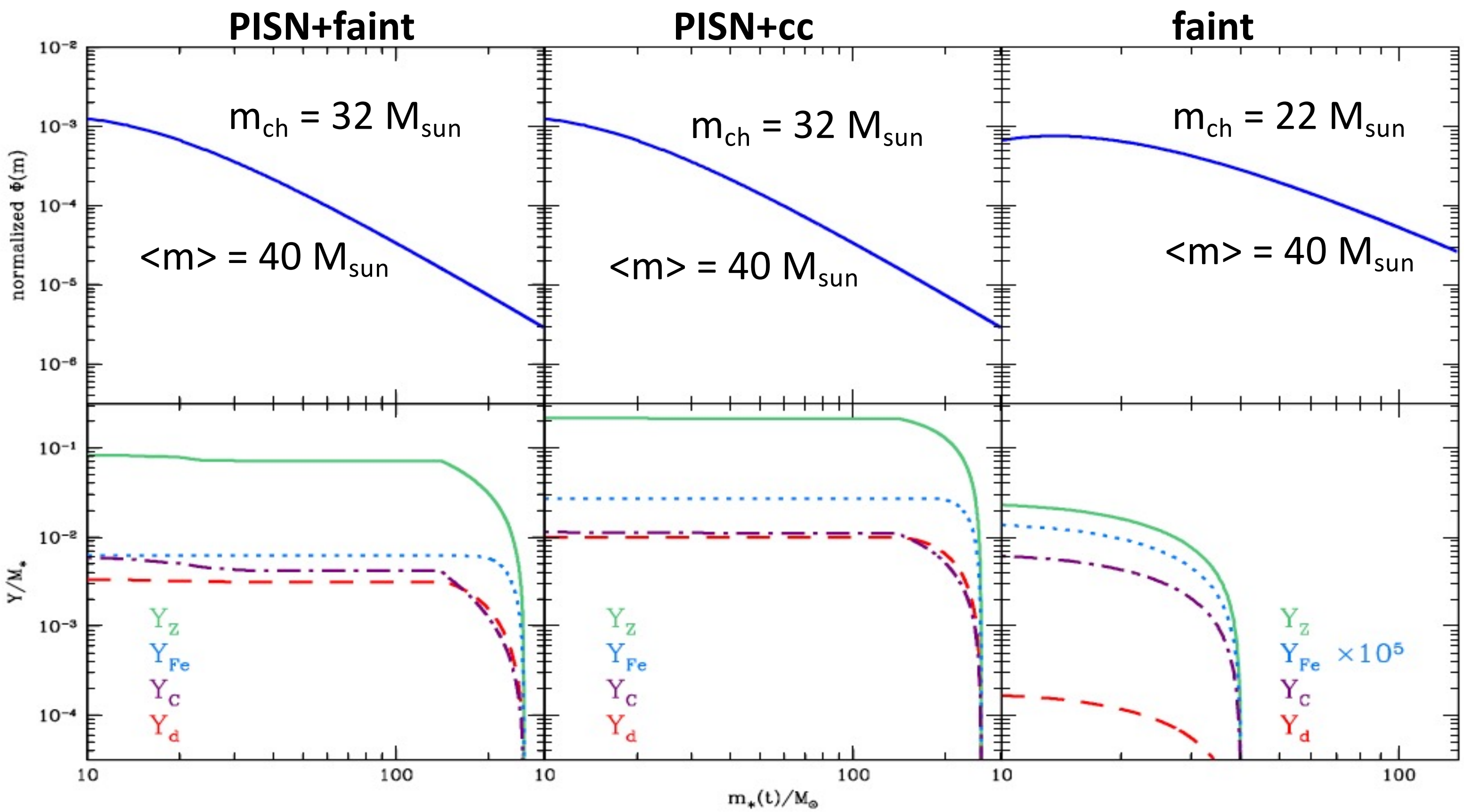

Pop II stellar yields

Chemical evolution for a single stellar population (SSP): all stars form in a single burst at t = 0

de Bennassuti+2017

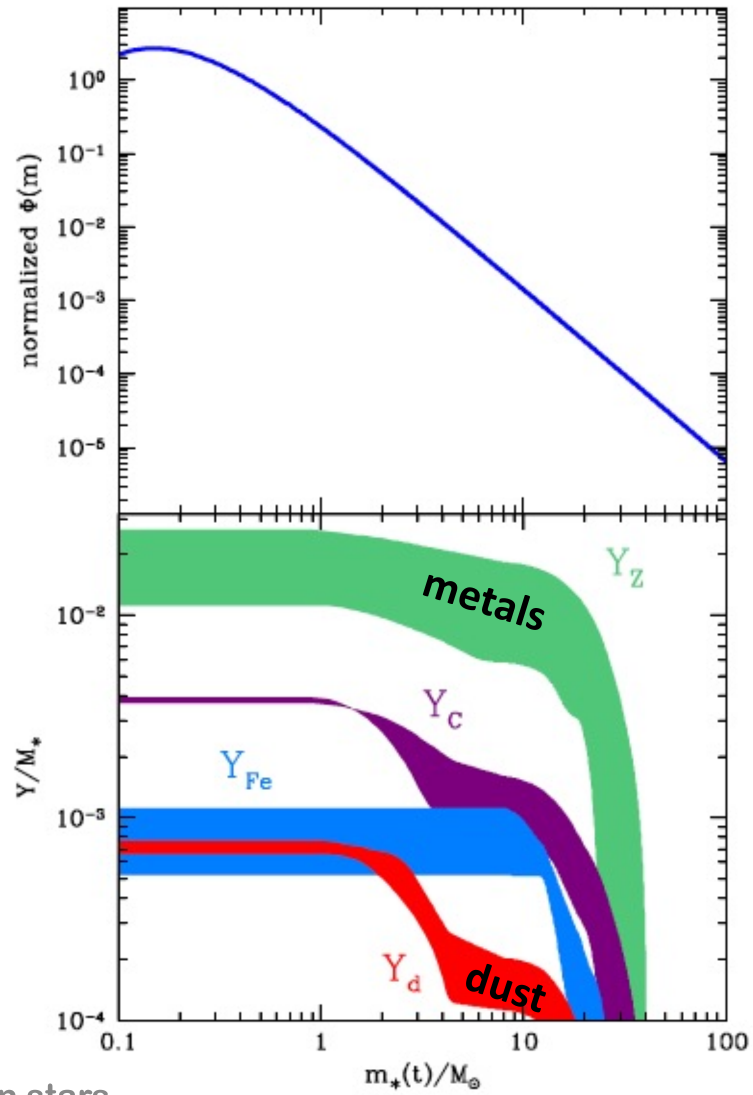

Larson IMF with $m_{ch} = 0.35\ M_{sun}$ and $\alpha = -1.35$

$$\Phi(m) = \frac{dN}{dm} \propto m^{\alpha-1} exp\Big(-\frac{m_{ch}}{m}\Big)$$

Stars with $m < 8\ M_{sun}$:

metal yields from van den Hoek & Groenewegen (1997)

dust yields from Zhukovska et al. (2008)

Stars with $12\ M_{sun} \leq m \leq 40\ M_{sun}$:

metal yields from Woosley & Weaver (1995)

dust yields from Bianchi & Schneider (2007)

Coloured regions show variations of the cosmic yield when the stellar metallicity varies in the range $10^{-4}\ Z_{sun} \leq Z \leq 1\ Z_{sun}$

physical conditions for dust formation

Classical nucleation theory: condensation occurs under super-saturation conditions

two-steps process:

1. formation of stable seed clusters
2. accretion of seed clusters to form grains

the gas must be metal-rich with physical conditions allowing condensation

$$T < T_{cond} = 1000 – 2000\ K$$
$$n > 10^9\ cm^{-3}$$

winds of Asymptotic Giant Branch stars

supernova ejecta

Asymptotic Giant Branch (AGB) stars

stars with masses < 8 M_{sun} at the end of He-burning

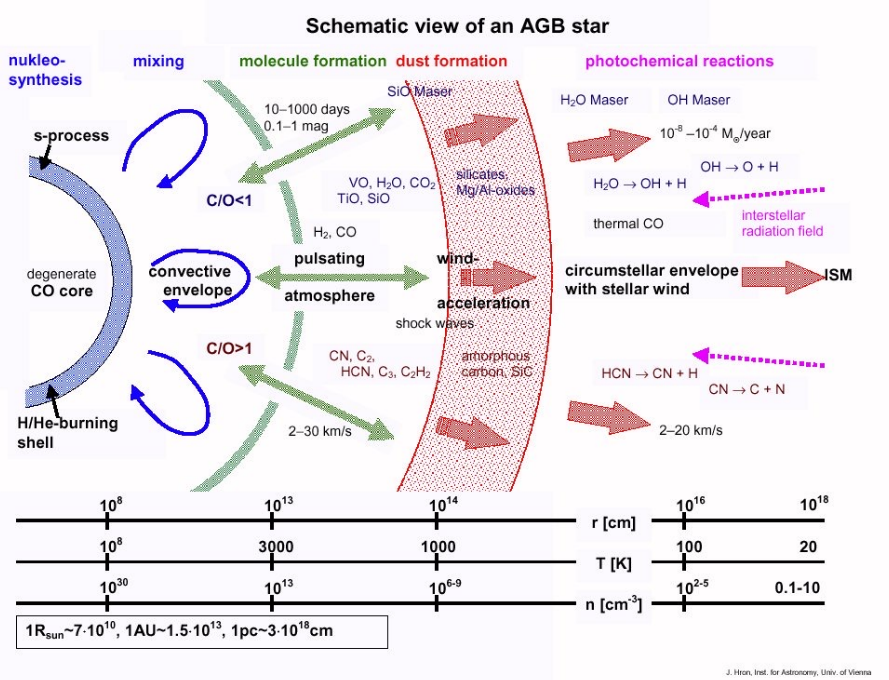

stellar tracks in the H-R diagram

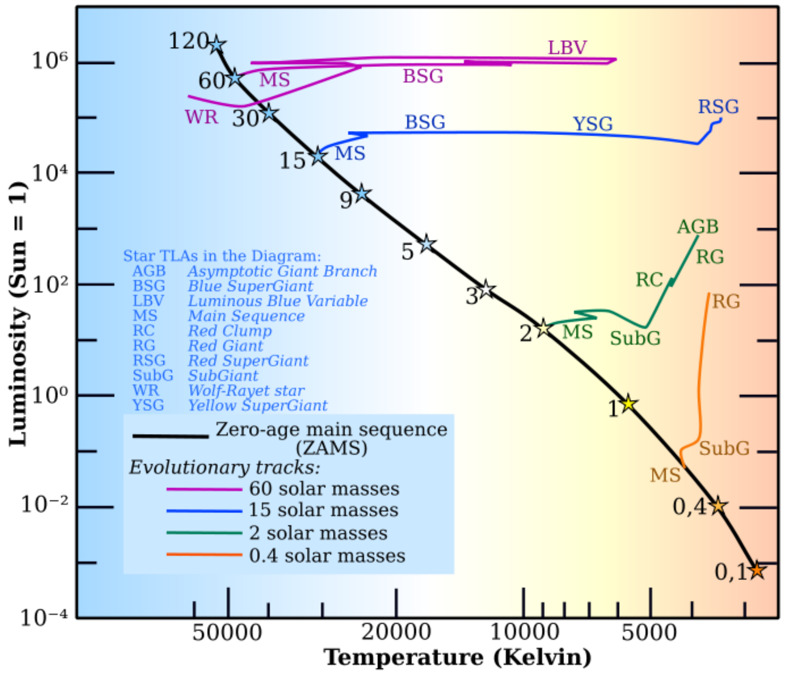

1. convection dredges up elements from the CO core
2. pulsations “lift” the gas in the atmosphere, dust forms and accelerates the wind

dust formation in AGB stars

Ferrarotti & Gail 01; 02; 06; Zhukovska+08; Nanni+13,14,15; Ventura+12a,b, 14; Di Criscienzo+13; Dell'Agli+14,19

1. model for the time-dependent physical and chemical conditions of the stellar surface
2. model for the physical conditions in the stellar winds
3. grain nucleation

Two fundamental processes affect the chemical composition of the stellar surface:

- Third Dredge Up (TDU) : occurs following each thermal pulse, penetration of the bottom of the external mantle in a region enriched by He-burning → **surface C enrichment**

- Hot Bottom Burning (HBB): occurs in the inter-pulse phase, the outer region of the CNO burning layer of the core is coupled to the bottom of the external mantle → **C (and O) surface depletion**

grid of AGB/SAGB stars with $1\ M_{sun} \leq M \leq 8\ M_{sun}$ and $3x10^{-4} \leq Z \leq 0.02$

dust yields from AGB stars: stellar mass dependence

transition from carbon dust to silicate production at M ≈ 3 M_{sun}

Z = 0.001

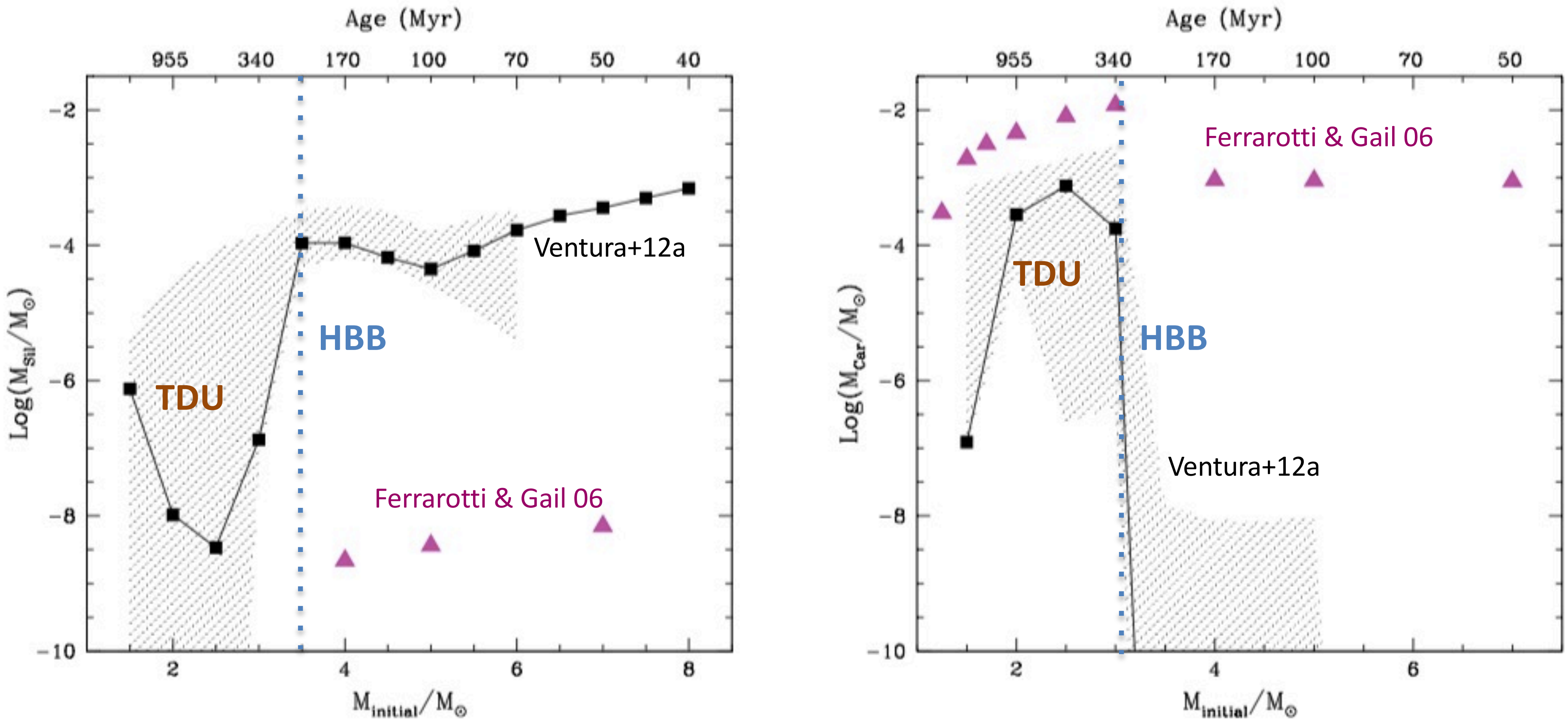

dust yields from AGB stars: metallicity dependence

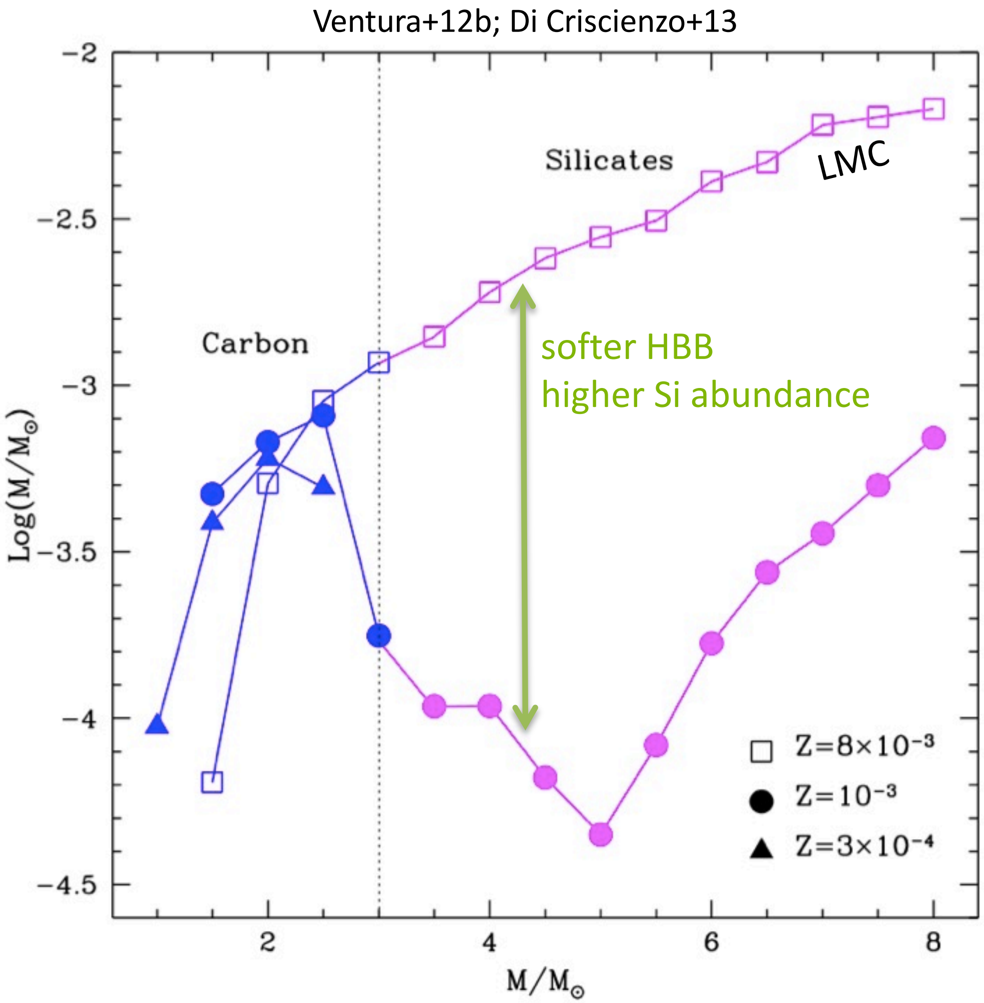

- ✓ Silicates are produced by > 3 M_{sun} stars
- ✓ Silicate dust production increases with Z
- ✓ No silicates are produced when Z < 0.001
- ✓ Carbon dust is produced by < 3 M_{sun} stars and does not depend on Z
- ✓ When $Z < 10^{-4}$ HBB is present even at M < 2 M_{sun} → no AGB dust

dust formation in Supernovae (SNe)

dust has been observed to form in the ejecta of SN1987A since 450 days after the explosion

(Wooden et al. 1993, Bouchet et al. 2006, Matsuura et al. 2011, Indebetouw et al. in prep)

FIR emission: dust condensed in the ejecta
M_{dust} = [0.4 - 0.7] M_{sun}
$T_{dust} \approx 20$ K

Matsuura et al. 2011

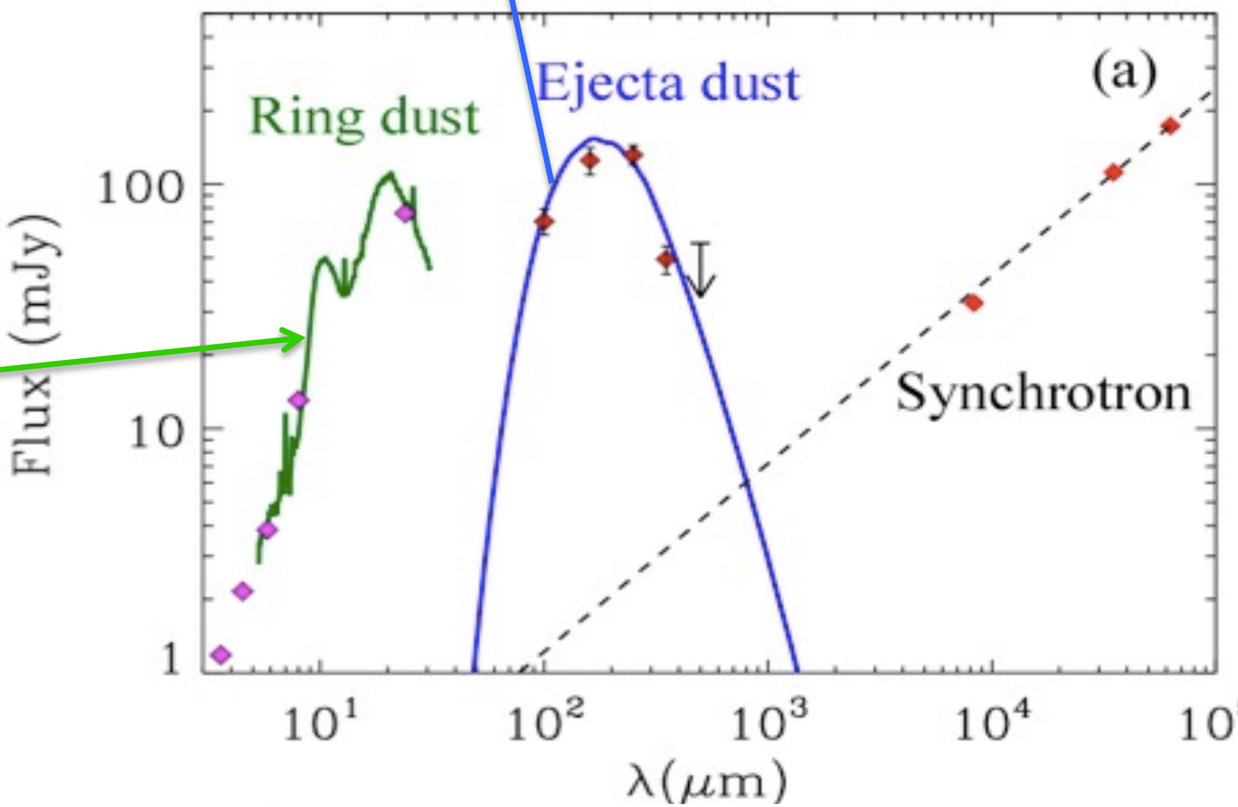

Bouchet et al. 2006

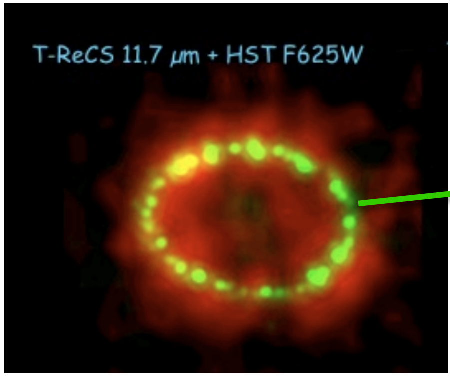

MIR emission: dust in the ring ejected by the progenitor
$M_{dust} \approx 10^{-6}$ M_{sun}
$T_{dust} \approx 160$ K

models for dust formation in SNe

Kozasa & Hasegawa 1987; Todini & Ferrara 2001; Nozawa et al 2003; Schneider, Ferrara & Salvaterra 2004;
Bianchi & Schneider 2007; Chercheneff & Dwek 2010; Fallest et al. 2011; Sarangi & Cherchneff 2013; Marassi+2014, 2015, 2016; Schneider+2021

1. model for the evolution of the progenitor star (mass, metallicity, rotation)
2. model for the explosion (explosion energy, mass cut/fallback, mixing of the ejecta)
3. grain nucleation

sequence of events in a supernova explosion

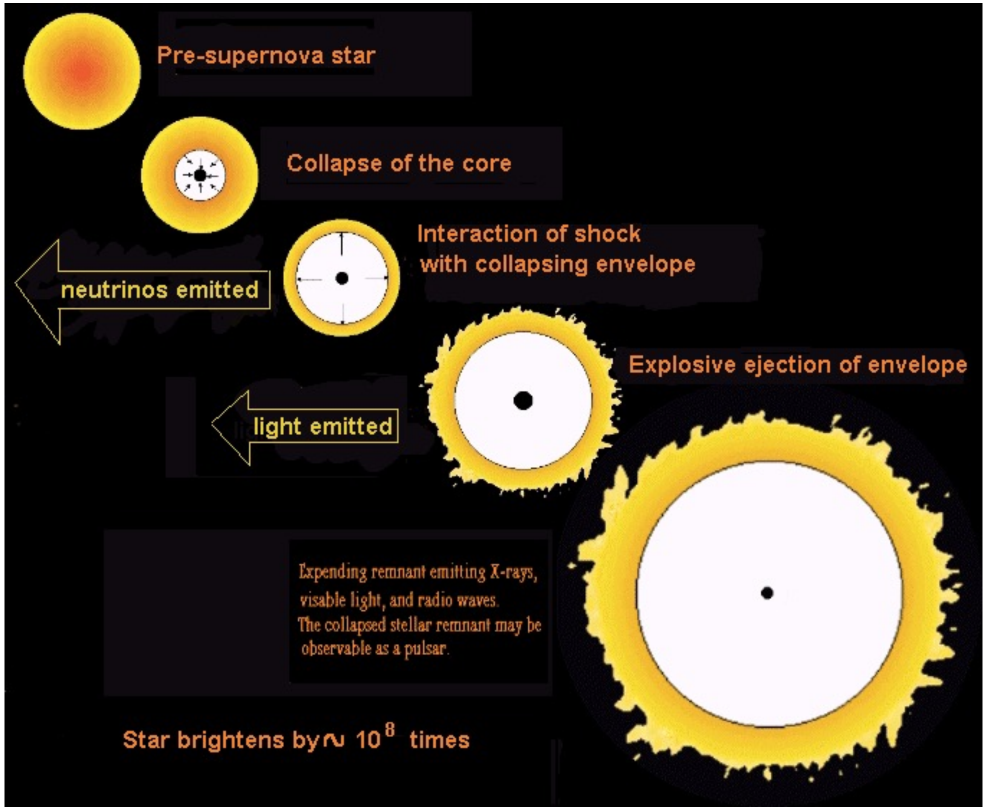

Models use "artifical explosions": energy, mass-cut, M_{Ni56}

- **Explosions @ fixed energy**
- **Calibrated models**

models for dust formation in SNe

Kozasa & Hasegawa 1987; Todini & Ferrara 2001; Nozawa et al 2003; Schneider, Ferrara & Salvaterra 2004;
Bianchi & Schneider 2007; Chercheneff & Dwek 2010; Fallest et al. 2011; Sarangi & Cherchneff 2013; Marassi+2014, 2015, 2016; Schneider+2021

1. model for the evolution of the progenitor star (mass, metallicity, rotation)
2. model for the explosion (explosion energy, mass cut/fallback, mixing of the ejecta)
3. grain nucleation

pre-supernova structure

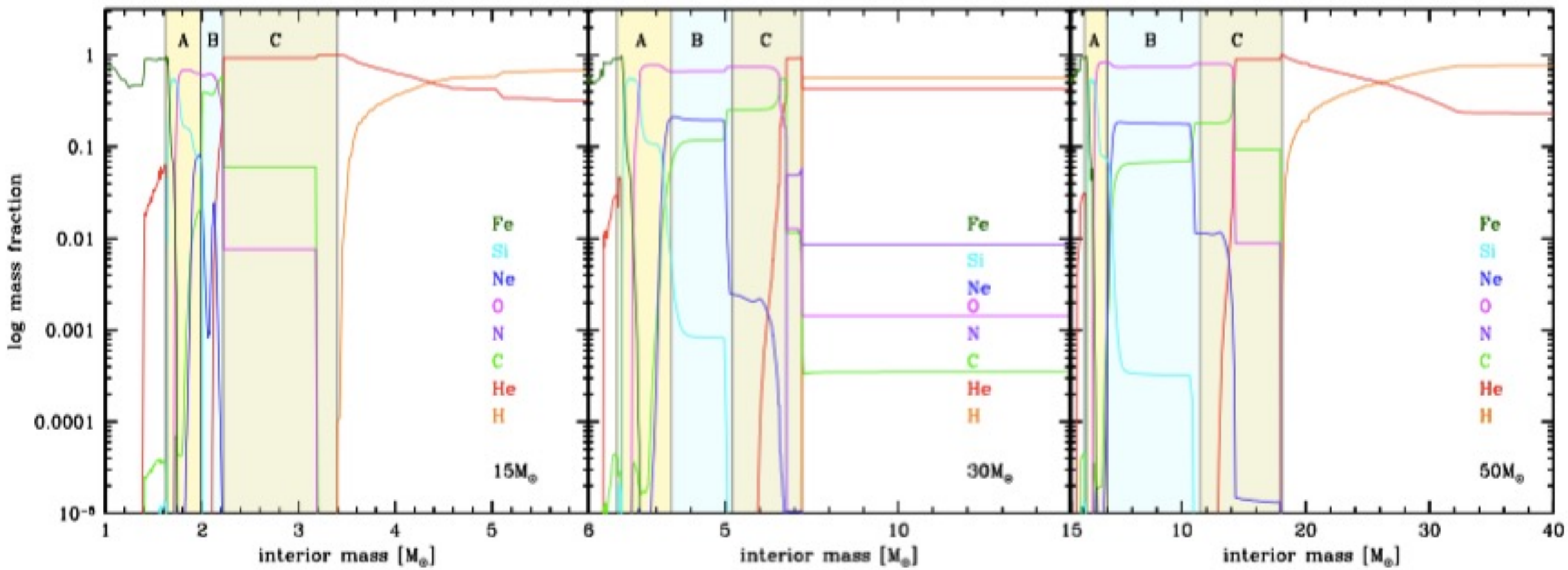

models for dust formation in SNe

Kozasa & Hasegawa 1987; Todini & Ferrara 2001; Nozawa et al 2003; Schneider, Ferrara & Salvaterra 2004;
Bianchi & Schneider 2007; Chercheneff & Dwek 2010; Fallest et al. 2011; Sarangi & Cherchneff 2013; Marassi+2014, 2015, 2016; Schneider+2021

1. model for the evolution of the progenitor star (mass, metallicity, rotation)
2. model for the explosion (explosion energy, mass cut/fallback, mixing of the ejecta)
3. grain nucleation

turbulence mixing during ejecta expansion

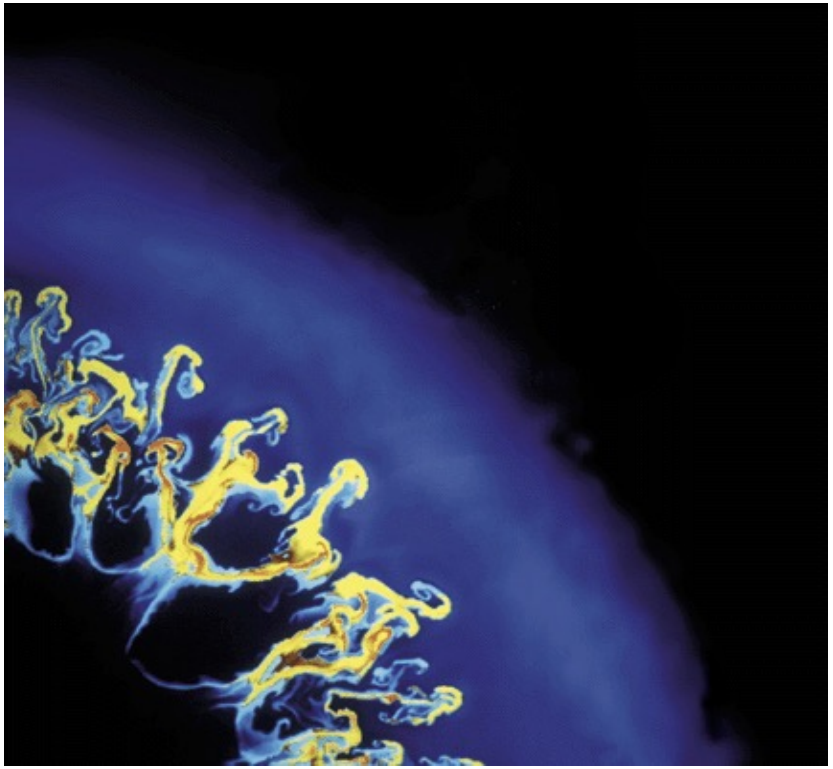

SN1987a: observations of Y-rays from Co^{56} decay 6 months before expected ←→ mixing of heavy elements from innermost to the outer layers

- **fully mixed models**
- **unmixed/stratified models**

models for dust formation in SNe

Kozasa & Hasegawa 1987; Todini & Ferrara 2001; Nozawa et al 2003; Schneider, Ferrara & Salvaterra 2004;
Bianchi & Schneider 2007; Chercheneff & Dwek 2010; Fallest et al. 2011; Sarangi & Cherchneff 2013; Marassi+2014, 2015, 2016; Schneider+2021

1. model for the evolution of the progenitor star (mass, metallicity, rotation)
2. model for the explosion (explosion energy, mass cut/fallback, mixing of the ejecta)
3. grain nucleation

$$\ln S = -\frac{\Delta G_r}{RT} + \sum_i \nu_i \ln P_i,$$

nucleation current:

$$J = \alpha\Omega\left(\frac{2\sigma}{\pi m_1}\right)^{1/2} c_1^2 \exp\left[-\frac{4\mu^3}{27(\ln S)^2}\right]$$

$$\Omega = \tfrac{4}{3}\pi a_0^3 \qquad \mu = 4\pi a_0^2\sigma/k_B T$$

Solid compound	Chemical reaction
AC	$C(g) \rightarrow C(s)$
Al_2O_3	$2Al + 3O \rightarrow Al_2O_3$
Fe	$Fe(g) \rightarrow Fe(s)$
Fe_3O_4	$3Fe + 4O \rightarrow Fe_3O_4$
$MgSiO_3$	$Mg + SiO + 2O \rightarrow MgSiO_3$
Mg_2SiO_4	$2Mg + SiO + 3O \rightarrow Mg_2SiO_4$
SiO_2	$SiO + O \rightarrow SiO_2$

critical cluster size:

$$r(0) = r_* = \frac{2\sigma\Omega}{k_B T \ln S},$$

grain accretion rate:

$$\frac{dr}{dt} = \alpha\Omega v_1 c_1(t),$$

Two critical parameters:

sticking coefficient α

number of monomers in a critical cluster $\mathcal{N} = r_*^3/a_0^3$

SN dust yields

Kozasa & Hasegawa 1987; Todini & Ferrara 2001; Nozawa et al 2003; Schneider, Ferrara & Salvaterra 2004;
Bianchi & Schneider 2007; Chercheneff & Dwek 2010; Fallest et al. 2011; Sarangi & Cherchneff 2013; Marassi+2014, 2015; Schneider+2021

fixed energy explosion models (1.2 10^{51} erg) and fully mixed ejecta

dependence on mass and parameters

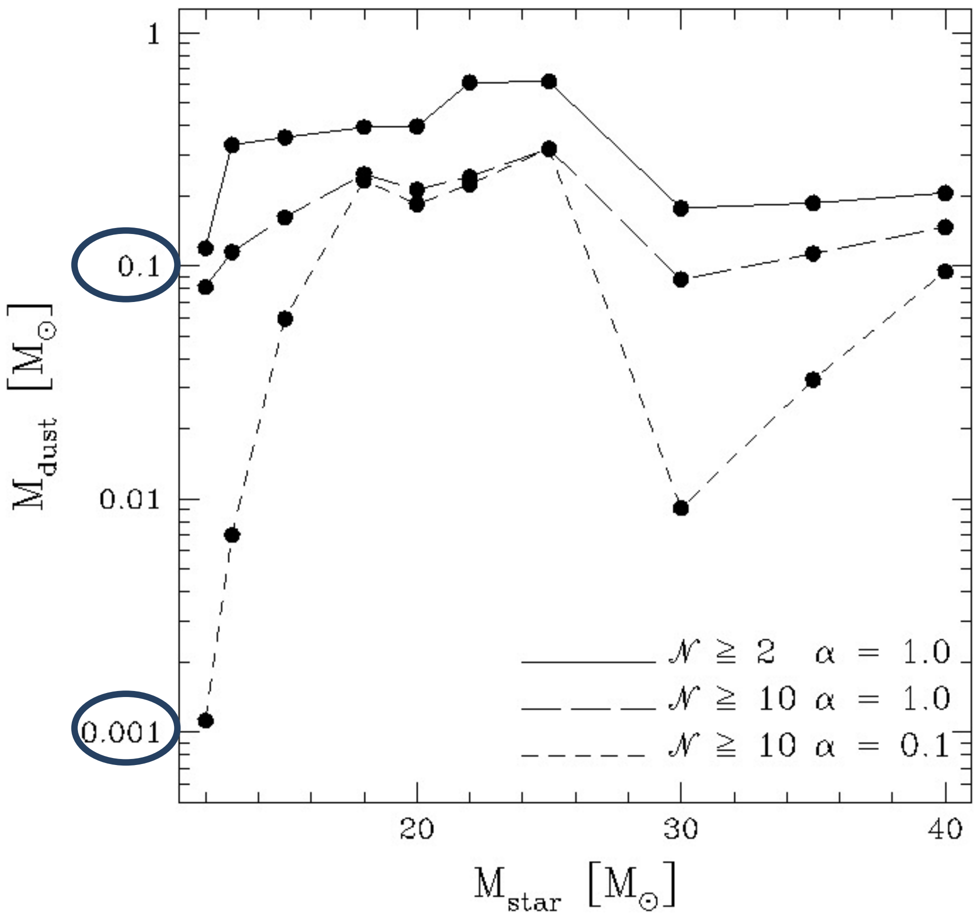

Bianchi & Schneider (2007)

dependence on metallicity

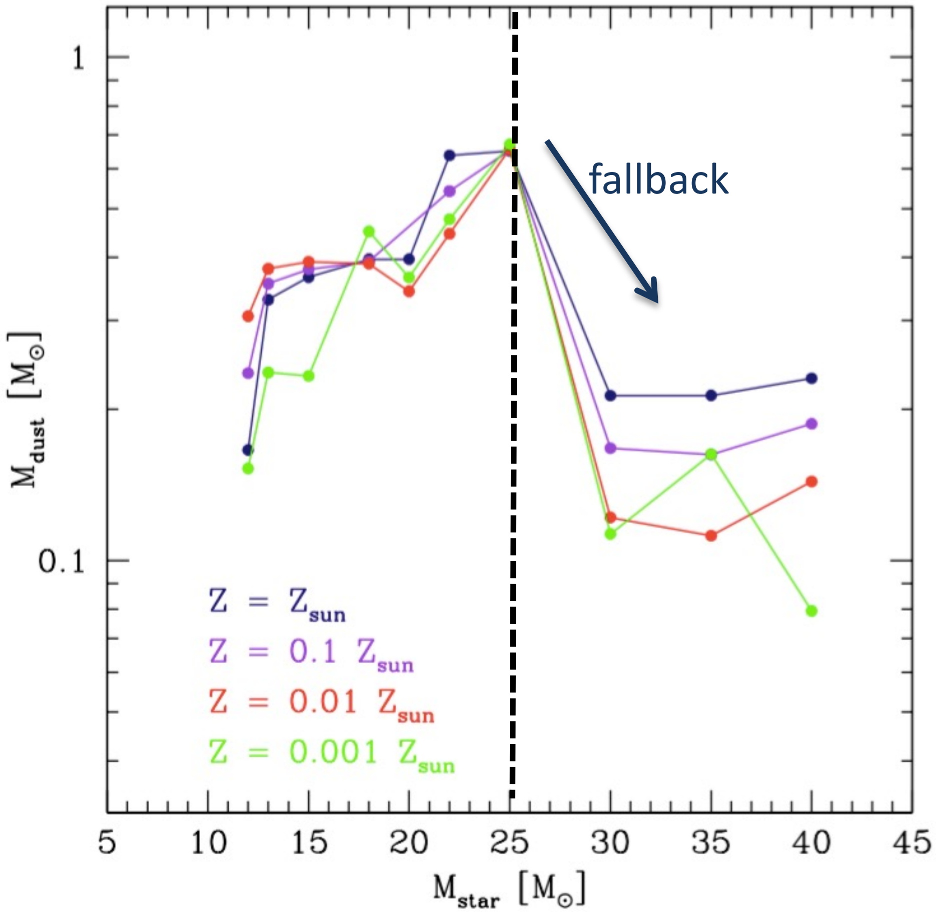

Population III SN dust yields

13 – 80 M_{sun} SN models from Chieffi & Limongi (2002)

calibrated explosion models and fully mixed ejecta

metals and dust yields for Z = 0 non-rotating core-collapse SN models

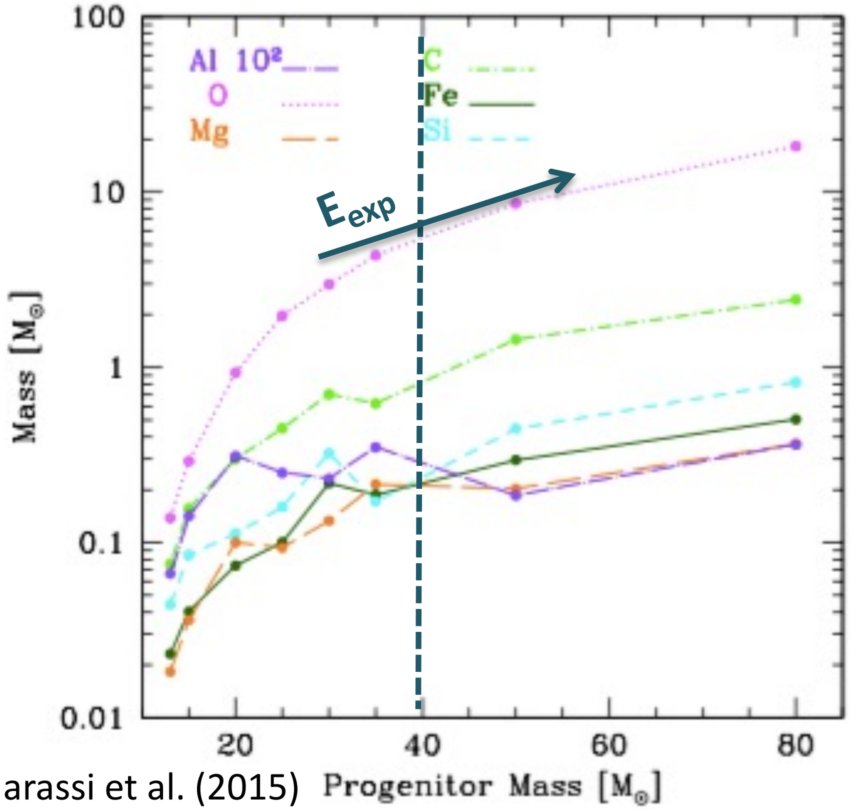

Marassi et al. (2015)

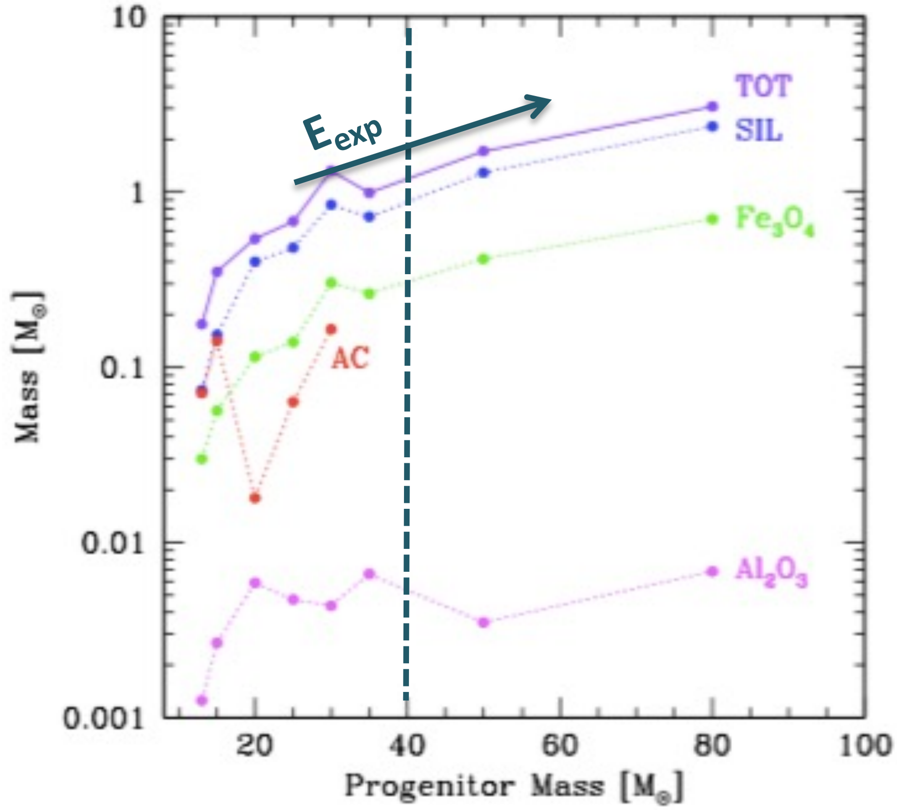

explosion models calibrated to reproduce the "average" elemental abundances of metal-poor stars in the Galactic halo

SN dust yields: dependence on rotation

13 – 80 M_{sun} SN models from Chieffi & Limongi (2013)

fixed energy explosion models (1.2 10^{51} erg) and fully mixed ejecta

non-rotating models

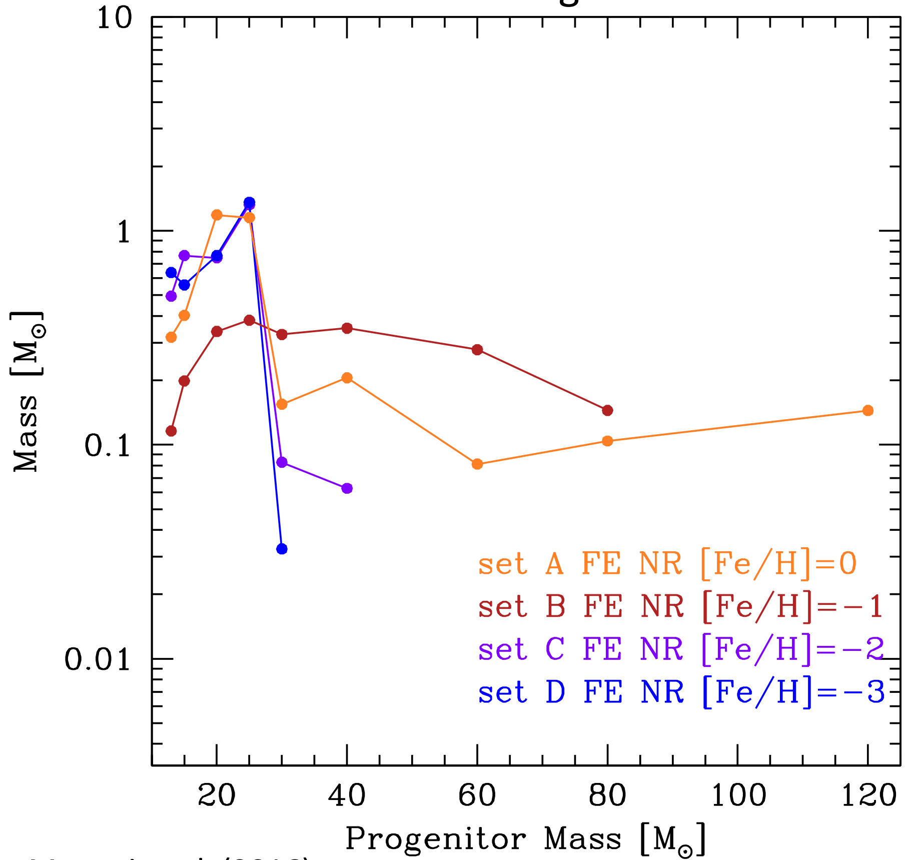

Marassi et al. (2016)

rotating models (v_{eq} = 300 km/s)

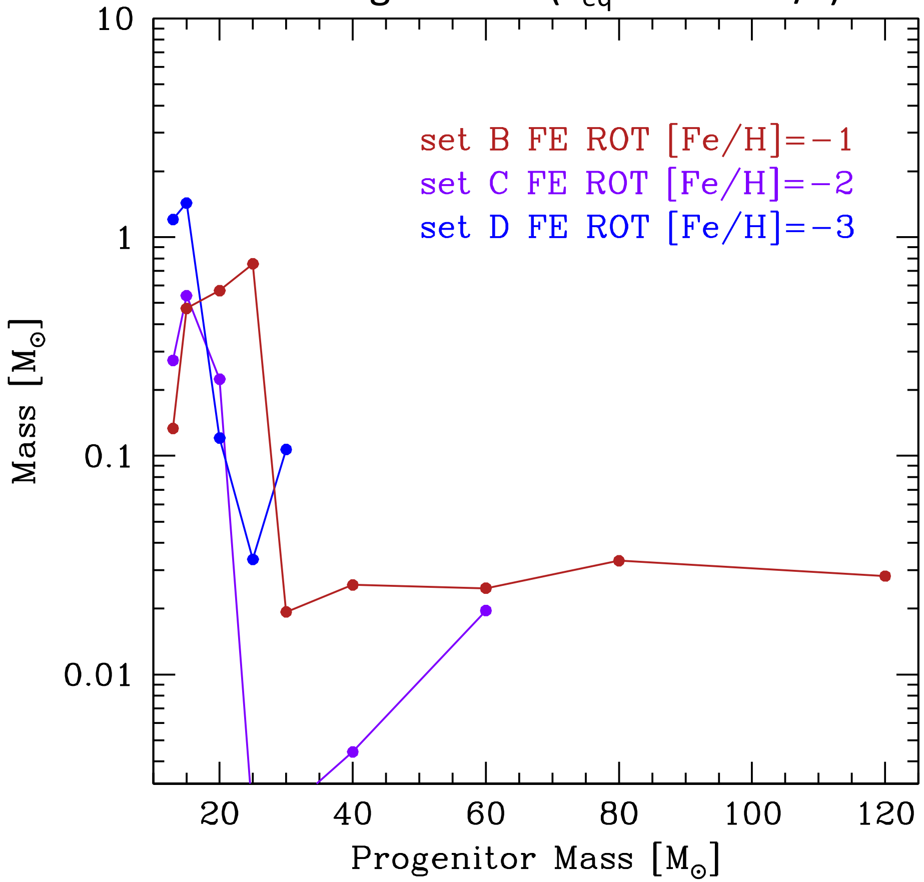

rotating pre-SN models are more compact: stronger fallback and less dust produced

SN dust yields: reverse shock destruction

Nozawa et al 2006, 2007; Bianchi & Schneider 2007; Silvia et al. 2010, 2012; .Marassi et al. 2014, 2015; Bocchio et al. 2016

evolution of the SN forward and reverse shock

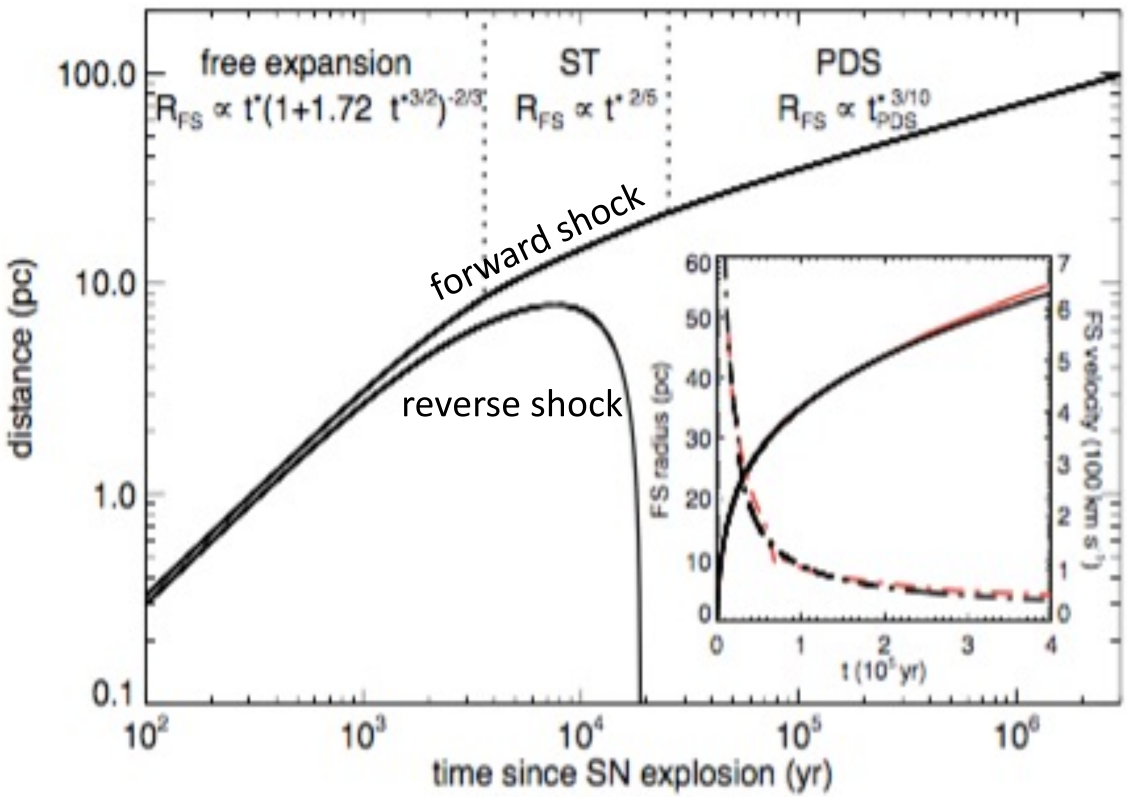

Different physical processes:

- **Sputtering** due to grain-gas interaction
- **Sublimation** due to collisional heating
- **Shattering** due to grain-grain collisions
- **Vapourisation**

the passage of the reverse shock has a strong effect on the SN dust size distribution and mass

SN dust yields: reverse shock destruction

Nozawa et al 2006, 2007; Bianchi & Schneider 2007; Silvia et al. 2010, 2012; .Marassi et al. 2014, 2015; Bocchio et al. 2016

modification of grain size distribution

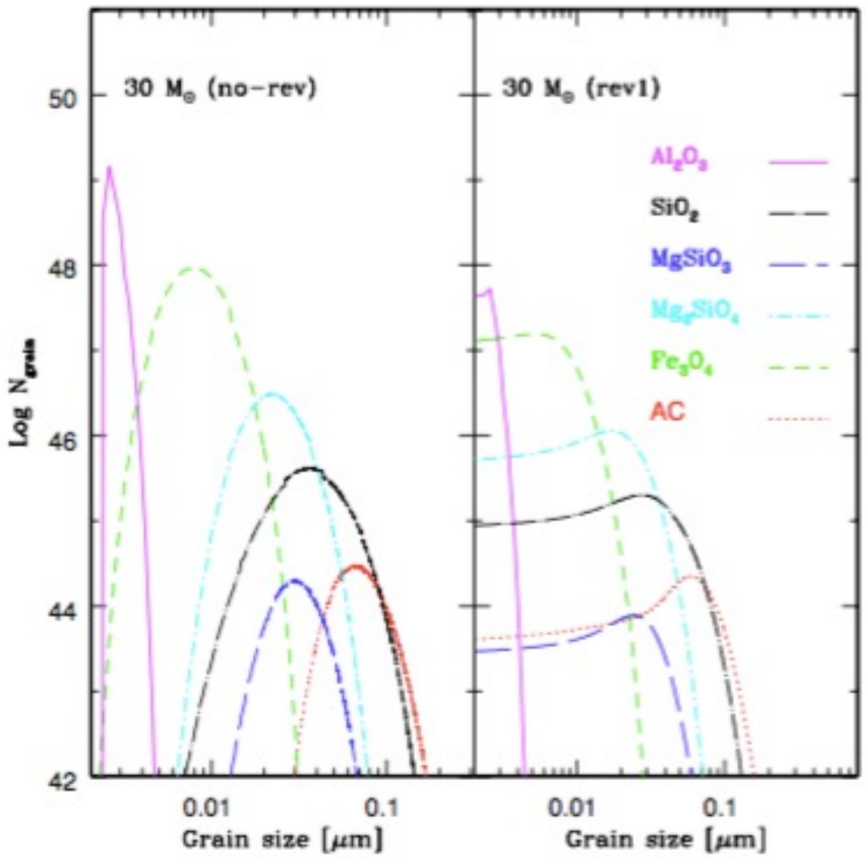

Marassi et al. 2015

SN dust mass surviving the reverse shock

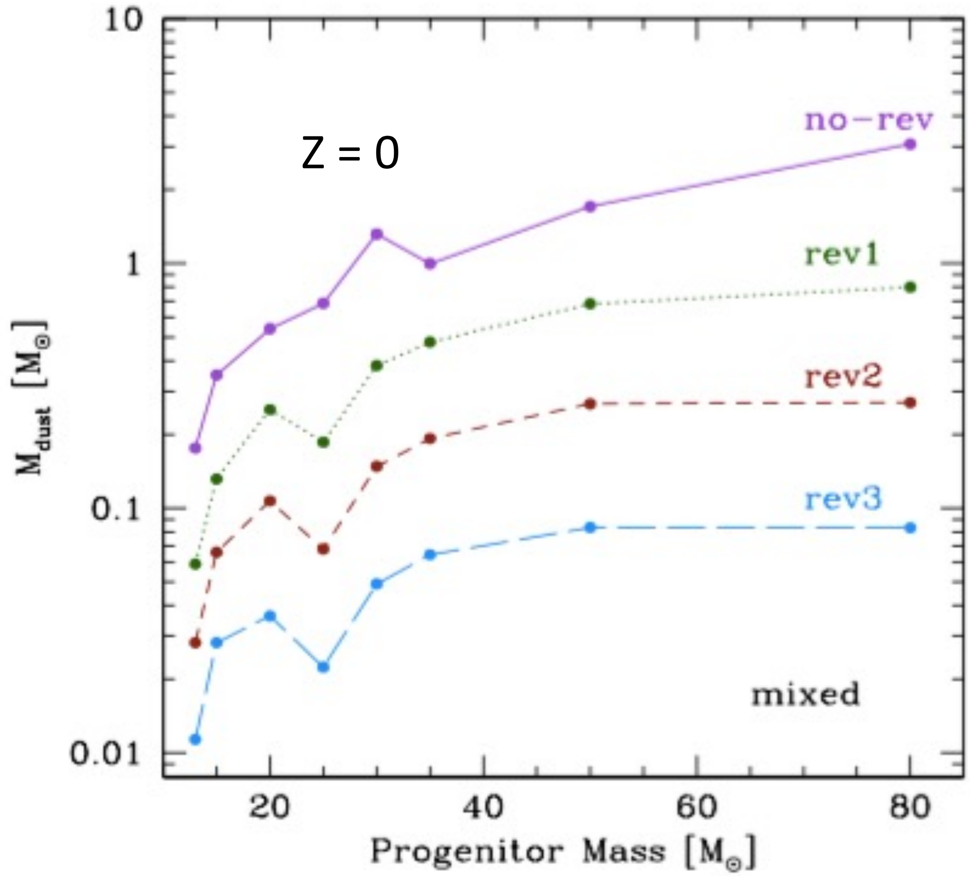

Bianchi & Schneider 2007

SN dust yields: comparison with observations

updated from Schneider+14

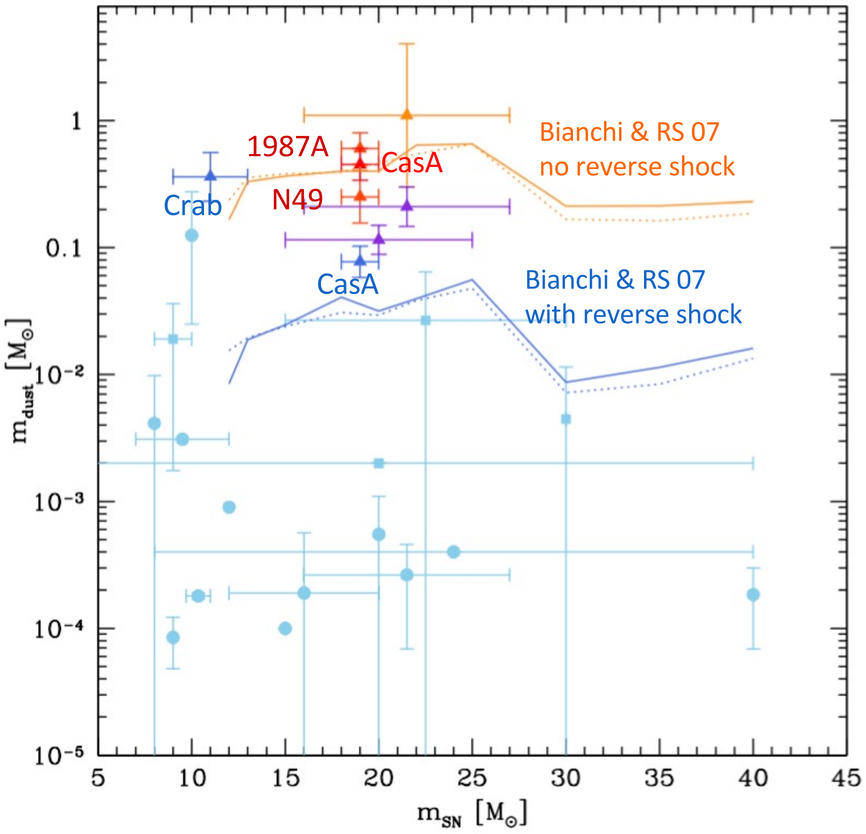

Gall+11, Gomez+12, Dunne+09, Barlow+10, Matsuura+11, Otsuka+10, de Looze+17, Temim+17, Bevan+17

Marassi+14,15; Bocchio+16

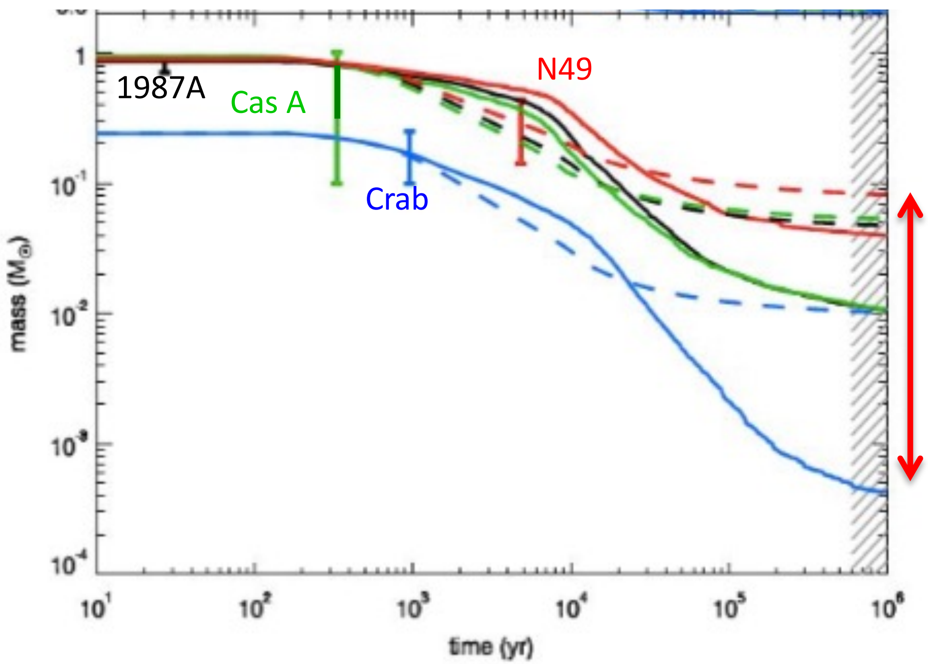

Nozawa et al 2006, 2007; Bianchi & Schneider 2007; Silvia et al. 2010, 2012; Marassi et al. 2014, 2015; Bocchio et al. 2016; Micelotta+2016; Martinez-Gonzalez et al. 2019; Slavin et al. 2020

theoretical SN dust yields are in broad agreement with available data

the mass of SN dust that will enrich the ISM << than observed in SN remnants with $t_{age} < 10^4$ yr

the contribution of AGB and SN to early dust enrichment

all stars are formed in a single burst at t = 0 with a Salpeter IMF:

AGB dust yields from ATON code (Ventura+12,13)

SN yields from Bianchi & Schneider (2007)

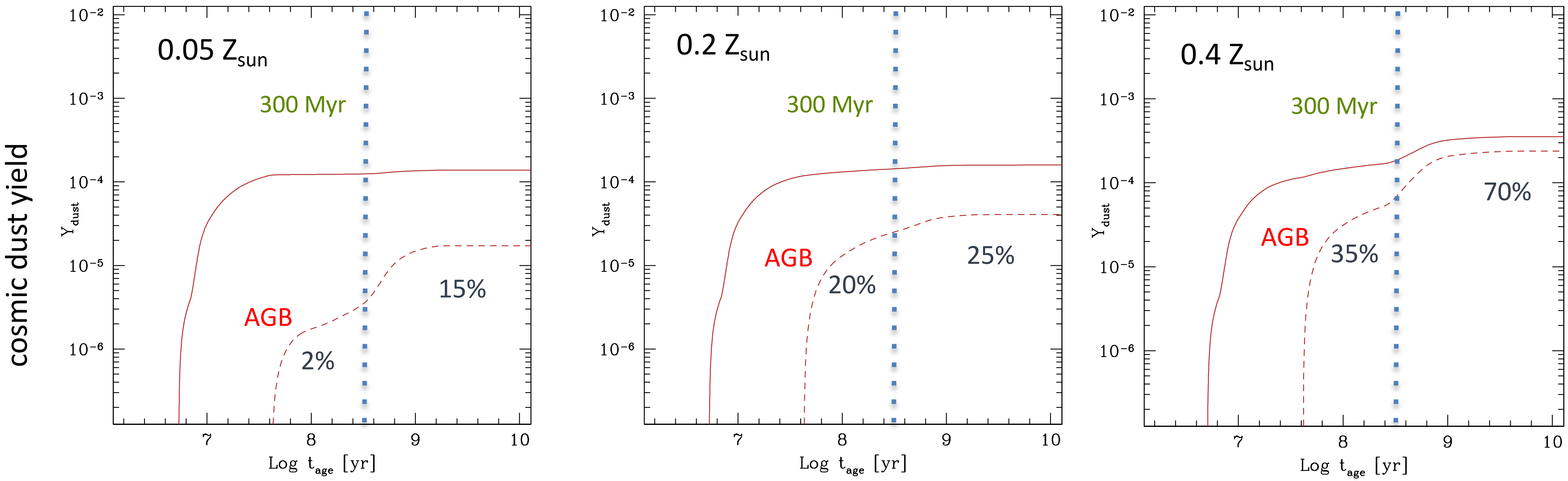

when $Z \leq 0.2\ Z_{sun}$ AGB dust is always sub-dominant wrt to SN dust

AGB contribution to the total dust budget becomes > 30% only when the $Z > 0.2\ Z_{sun}$ and starts to dominate at > 500 Myr

the contribution of AGB stars to early dust enrichment

all stars are formed in a single burst at t = 0 with a Salpeter IMF:

AGB dust yields from ATON code (Ventura+12,13)

SN yields from Bianchi & Schneider (2007)

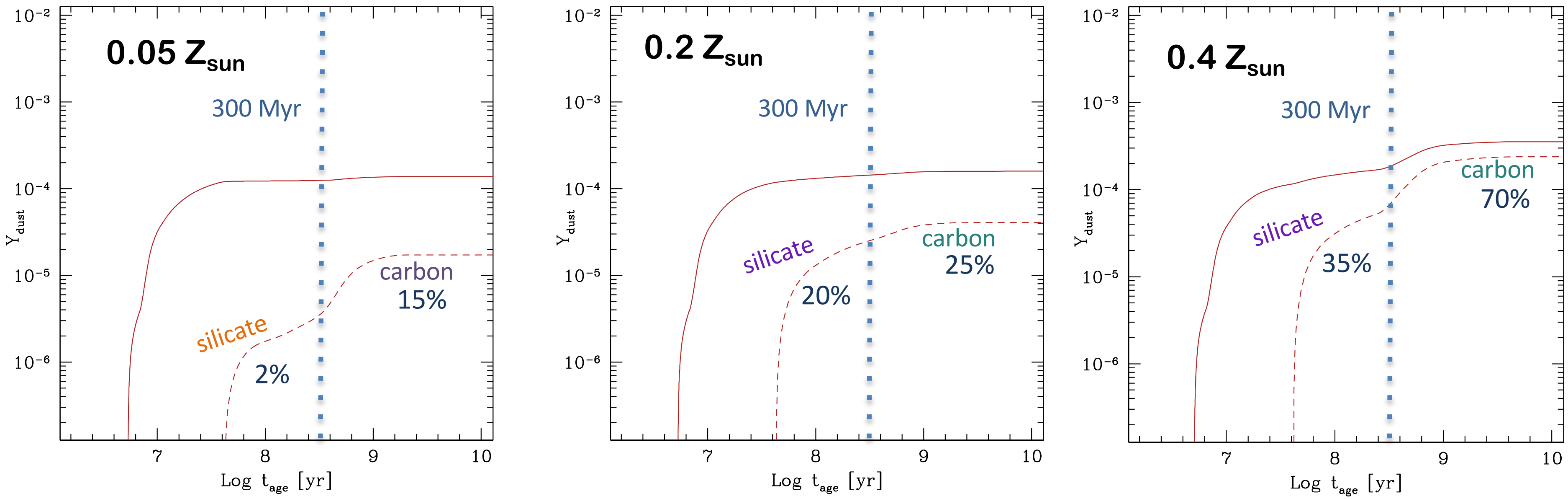

if SN at low Z produce mostly silicate dust, we expect to see only silicate features in young (< 300 Myr) starbursts and the presence of carbon features (PAHs) may be an indication of the growing AGB contribution to the total dust mass at > 300 Myr

chemical enrichment in a cosmological context

GAMESH: semi-analytical galaxy formation model +
dark matter simulation coupled to the radiative transfer code CRASH

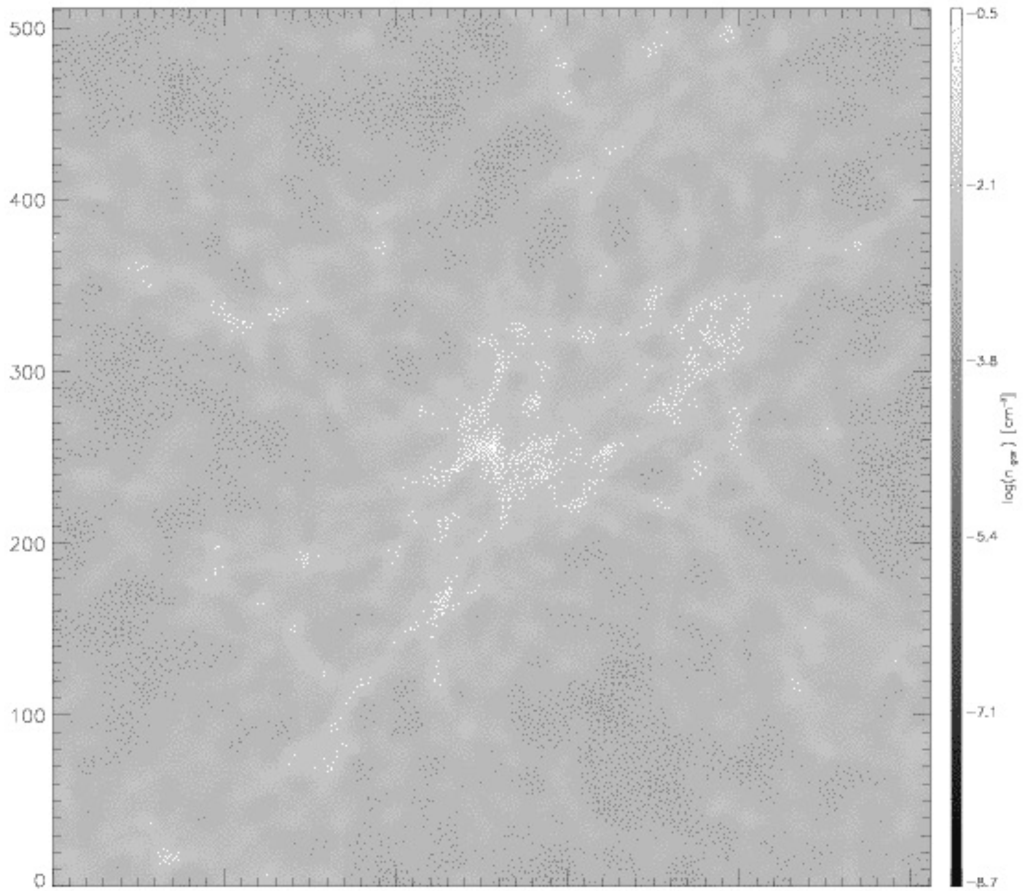

Dark matter simulation of the Milky Way galaxy in Planck cosmology GCD+ code with multi-resolution technique (Kawata & Gibson 2003):

Low-res spherical region of R_l ~ 20 h^{-1} Mpc taken from a low-res cosmological simulation

High-res spherical region of R_h ~ 2 h^{-1} Mpc with M_p = 3.4 x 10^5 M_{sun}

where does Galactic dust come from?

stellar dust production along the build-up of the MW

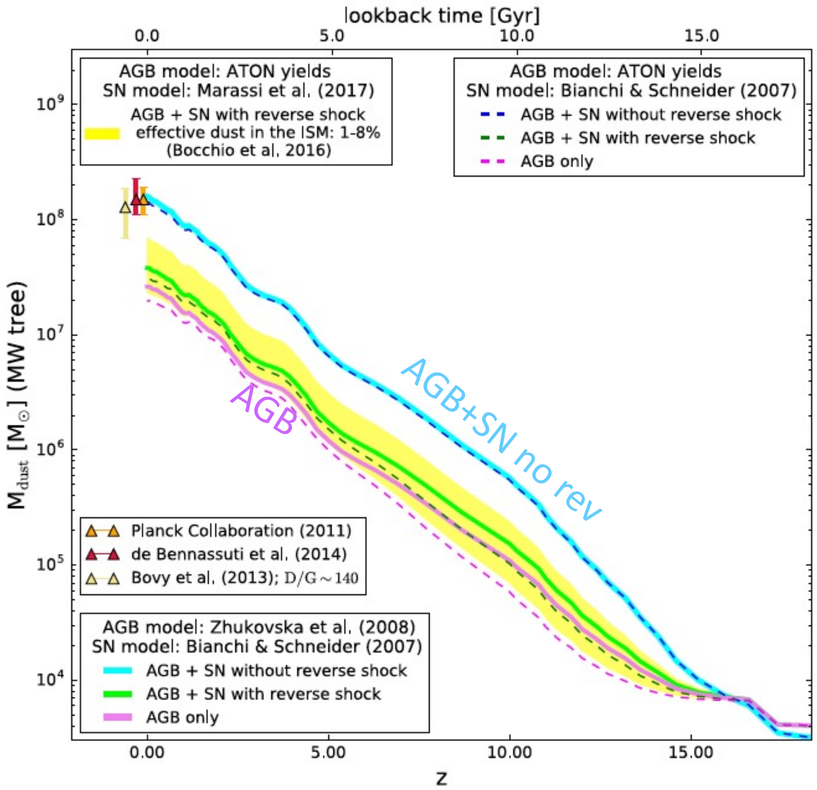

dust-to-gas mass ratio vs metallicity: stellar dust sources

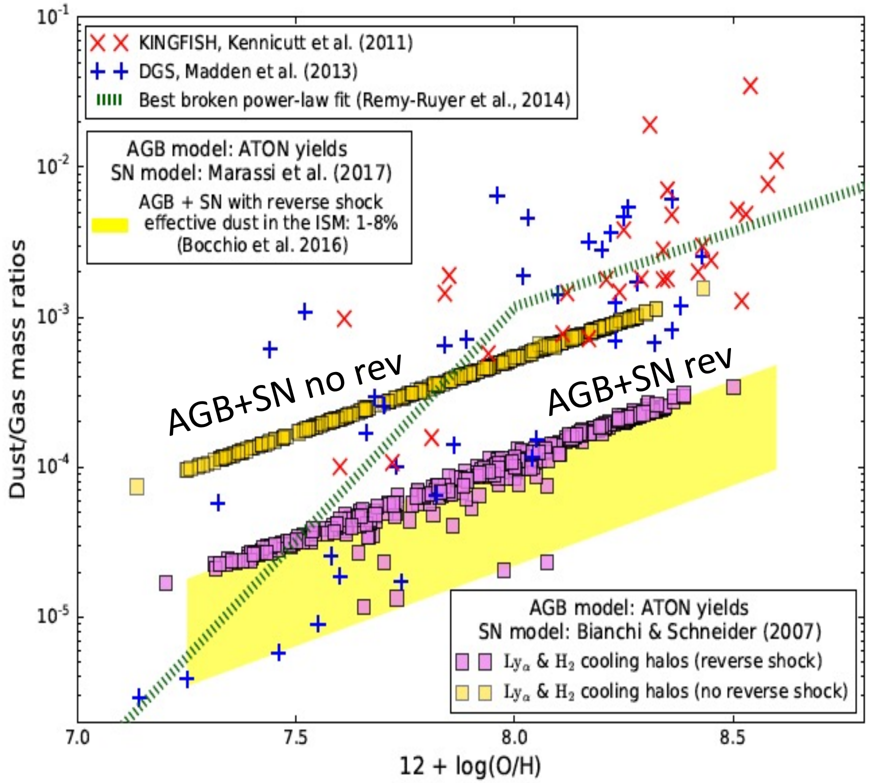

Ginolfi, Graziani, RS et al. 2018

- the injected and surviving dust mass is a factor 4-5 smaller than observed in the MW (unless no reverse shock)
- models with stellar dust only can not reproduce the observed scaling relations between the dust-to-gas mass and Z

these conclusions are independent of the adopted dust yields

Remy-Ruyer et al. 2014; Asano+2013; Zhukovska+2014; Schneider+14; Feldman+15; Popping+16, Galliano+18

grain destruction by interstellar shocks

increasing gas velocity →

DEPLETIONS AND DUST DESTRUCTION

Element	$A_\odot$[a]	Galactic Warm/Cold[b]	23 Ori HV/WLV/SLV[b]	ζ Ori HV/A/DE[c]	Percent Destroyed[d]
C............	8.55	−0.4/−0.4	>−0.2/−0.31/−0.31	−0.12/.../...	60–67
N	7.97	−0.1/−0.1	.../−0.15/−0.15	0.08/.../...	...
Al...........	6.48	−1.1/−2.4	−0.5/−1.36/−1.71	−0.82/−1.43/−1.84	9–13
Si	7.55	−0.4/−1.3	−0.1/−0.52/−0.89	−0.39/−0.59/−0.72	0–20
Fe	7.51	−1.4/−2.2	.../−1.49/−1.92	−0.97/−1.46/−1.85	6–8

Welty et al. 2002

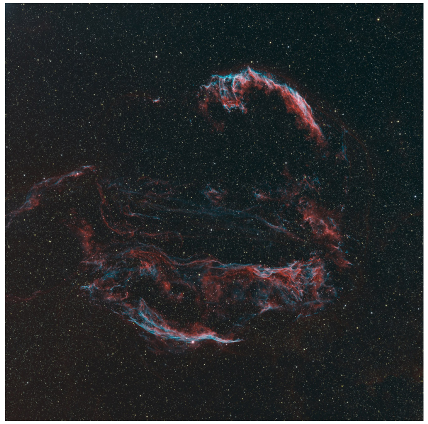

$$\tau_d = \frac{\tau_{SN} M_{ISM}}{\int \epsilon(v_s) dM_s(v_s)}$$

$\tau_{SN} = 1/R_{SN}$ $\quad R_{SN}$ = SN rate $\quad M_s(v_s) = 6800\ M_{sun}\ E_{51}/(v_s/100\ \mathrm{km/s})^2$

grain destruction efficiency:
depends on grain properties and v_s

In the Milky Way:
$\tau_{SN} = 125$ yr $\quad M_{ISM} = 4.5\ 10^9\ M_{sun}$

$$\tau_d = \begin{cases} (6.2 \pm 5.6) \times 10^7\ \mathrm{yr} & \text{for carbonaceous grains} \\ (3.1 \pm 2.7) \times 10^8\ \mathrm{yr} & \text{for silicate grains} \end{cases}$$

Bocchio+2014

→ Grains have a short lifetime (< 60 - 300 Myr) in the MW ISM

grain growth in dense metal-enriched gas

Asano+12; Hirashita & Kuo 2011

$$\left(\frac{\mathrm{d}M_\mathrm{d}}{\mathrm{d}t}\right)_\mathrm{acc} = \eta N \pi \langle a^2 \rangle \alpha \rho_Z^\mathrm{gas} \langle v \rangle = M_d/\tau_{acc}$$

spherical grains approximation:

$$m_\mathrm{d} = \frac{4\pi \langle a^3 \rangle \sigma}{3} \qquad N = \frac{M_\mathrm{d}}{m_\mathrm{d}} = \frac{3M_\mathrm{d}}{4\pi \langle a^3 \rangle \sigma} \qquad \rho_Z^\mathrm{gas} = \rho_\mathrm{ISM}^\mathrm{eff} Z(1-\delta) \quad \delta = M_d/M_Z$$

$\alpha = 1$ $\sigma = 3$ gr/cm^3 (silicates)

$$\tau_\mathrm{acc} = \frac{4\langle a^3 \rangle \sigma}{3\langle a^2 \rangle \alpha \rho_\mathrm{ISM}^\mathrm{eff} Z \langle v \rangle} = 20 \text{ Myr } (\bar{a}/0.1\ \mu\text{m})\ (n_H/100 \text{ cm}^{-3})^{-1}\ (T/50\text{K})^{-1/2}\ (Z/Z_{sun})^{-1}$$

$$\tau_{acc} = \tau_{acc,0}\,(Z/Z_{sun})^{-1}$$

In the MW galaxy:

Cold Neutral Medium (CNM): $n = 50 - 100$ cm^{-3} and $T = 50 - 100$ K → $\tau_{acc,0} = 20 – 30$ Myr

Molecular gas (MC): $n = 10^2 - 10^4$ cm^{-3} and $T = 10 - 20$ K → $\tau_{acc,0} = 0.4 – 30$ Myr

chemical evolution with dust

$$\frac{dM_*(t)}{dt} = \mathrm{SFR}(t) - \frac{dR(t)}{dt},$$

stellar mass

$$\frac{dM_{\rm ISM}(t)}{dt} = -\mathrm{SFR}(t) + \frac{dR(t)}{dt} + \frac{dM_{inf}(t)}{dt} - \frac{dM_{ej}(t)}{dt} - (1-\epsilon_r)\frac{dM_{accr}(t)}{dt}$$

gas mass

$$\frac{dM_Z(t)}{dt} = -Z_{\rm ISM}(t)\mathrm{SFR}(t) + \frac{dY_Z(t)}{dt} + Z_{\rm vir}(t)\frac{dM_{inf}(t)}{dt} - Z_{ISM}(t)\frac{dM_{ej}(t)}{dt} - Z_{\rm ISM}(t)(1-\epsilon_r)\frac{dM_{accr}(t)}{dt}$$

metal mass

$$\frac{dM_d(t)}{dt} = -Z_d(t)\mathrm{SFR}(t) + \frac{dY_d(t)}{dt} - \frac{M_d^{diff}(t)}{\tau_d} + \frac{M_d^{mc}(t)}{\tau_{acc}} - Z_d(t)(1-\epsilon_r)\frac{dM_{accr}}{dt}$$

dust mass

$$\tau_{\rm acc} \approx 20\,\mathrm{Myr} \times \left(\frac{\bar{a}}{0.1\,\mu\mathrm{m}}\right)\left(\frac{\mathrm{n}}{100\,\mathrm{cm}^{-3}}\right)^{-1}\left(\frac{\mathrm{T}}{50\,\mathrm{K}}\right)^{-1/2}\left(\frac{\mathrm{Z}}{\mathrm{Z}_\odot}\right)^{-1}$$

$$\tau_d = \frac{M_{\rm ISM}(t)}{\epsilon_d M_{swept} R'_{\rm SN}}$$

the lifecycle of dust in the Milky Way

average over 50 independent merger trees

1 – σ

de Bennassuti et al 2014

global properties of the MW

2-phase structure of the ISM

Pop III and Pop II SFRs

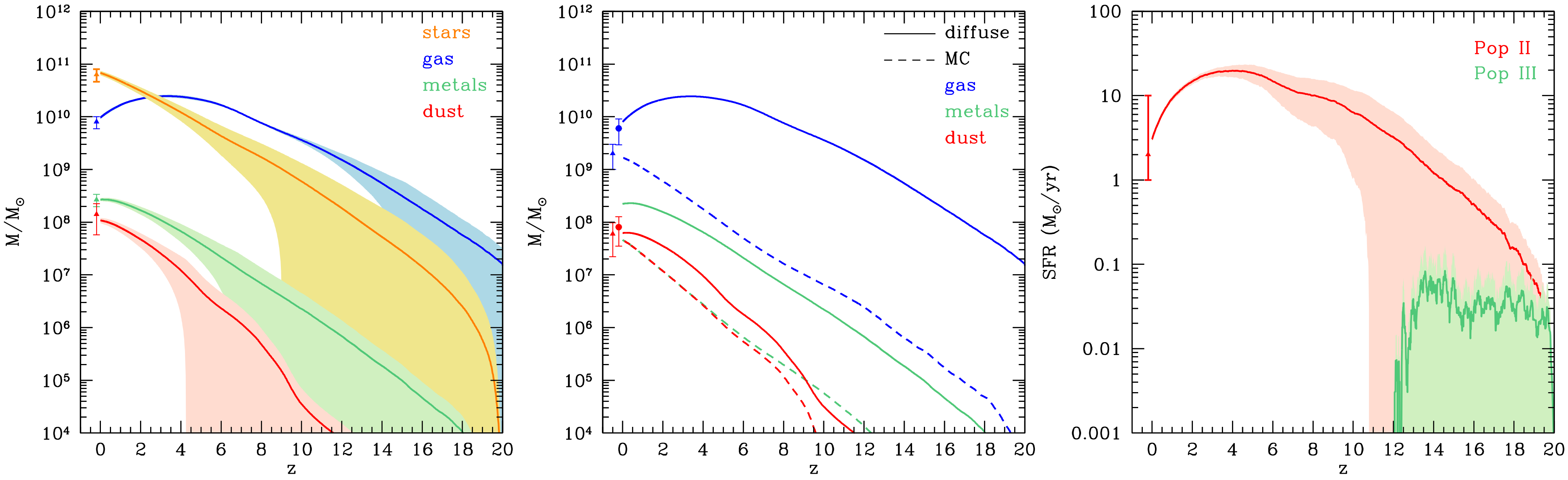

the existing dust mass is well reproduced and the predicted depletion factors are 1 for the MC phase and 0.3 for the diffuse phase → consistent with observed depletion (Jenkins 2009)

the MW and its dusty progenitors

de Bennassuti et al 2014

dust-to-gas ratio versus metallicity

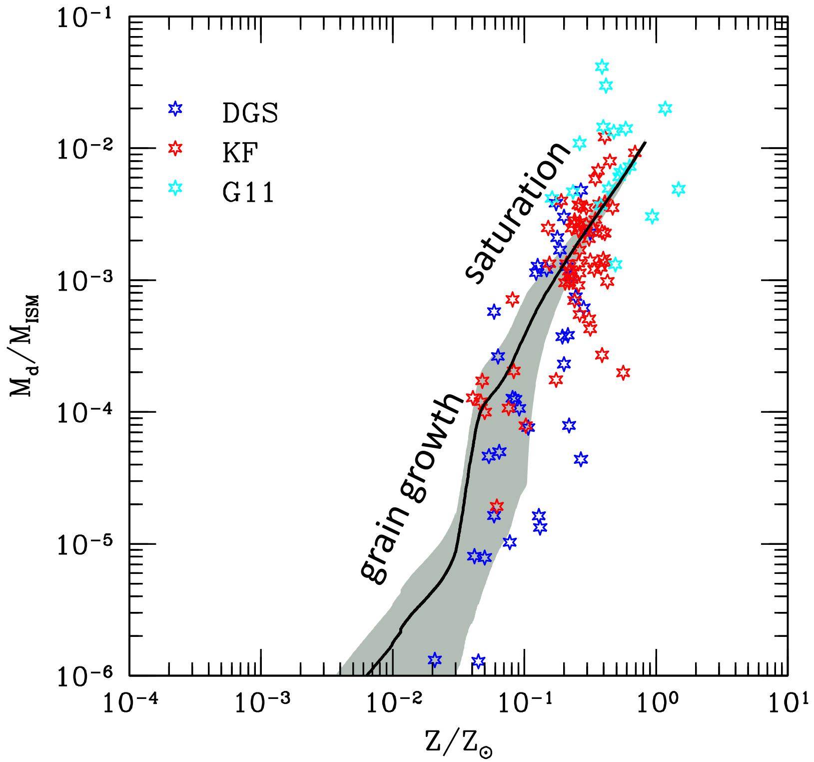

data points:
Local dwarfs Galametz et al. (2011)
Madden et al. (2013),
Remy-Ruyer et al. (2014)

dust mass evolution

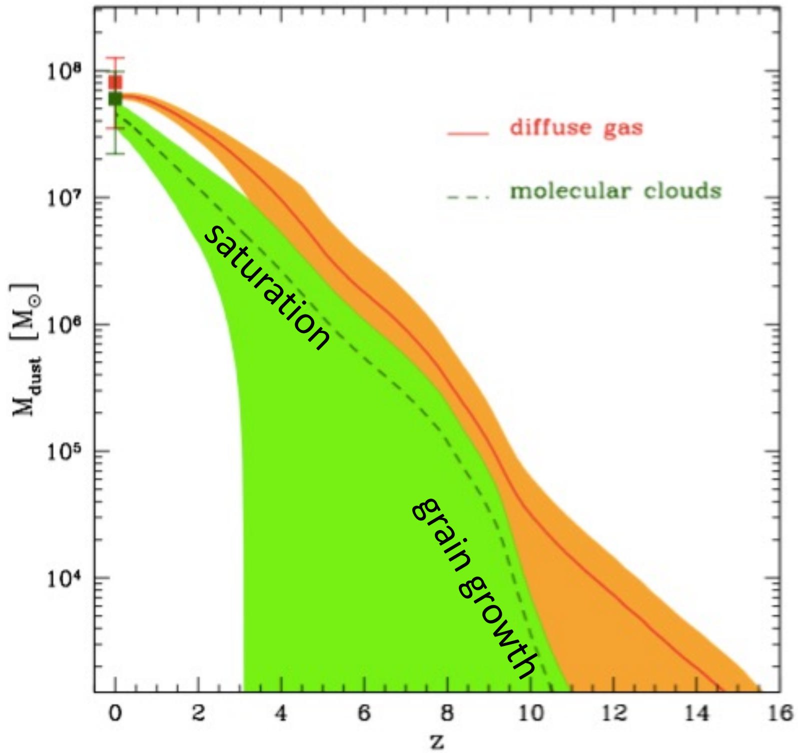

grain growth provides the dominant contribution to the existing dust mass in the MW

summary and take-home messages

- dust grains form at the end of stellar evolution: AGB stars and SNe
- dust yields depend on poorly constrained parameters
  (stellar evolution and nucleation theory)
- the relative importance of AGB stars and SNe as dust factories depends on:
  the stellar initial mass function, the star formation history and metallicity
- the dust content is different in different phases of the ISM as a consequence
  of grain processing by SN-shocked gas and grain growth in dense metal-enriched clouds
- due to the short destruction timescales, grain growth is a fundamental source of dust in the MW and it is required to reproduce observed dust-to-gas scaling relations

the spectral energy distribution of a dusty star forming galaxy

Arp 220: a proto-typical Ultra Luminous Infrared Galaxy (ULIRG)

HST image

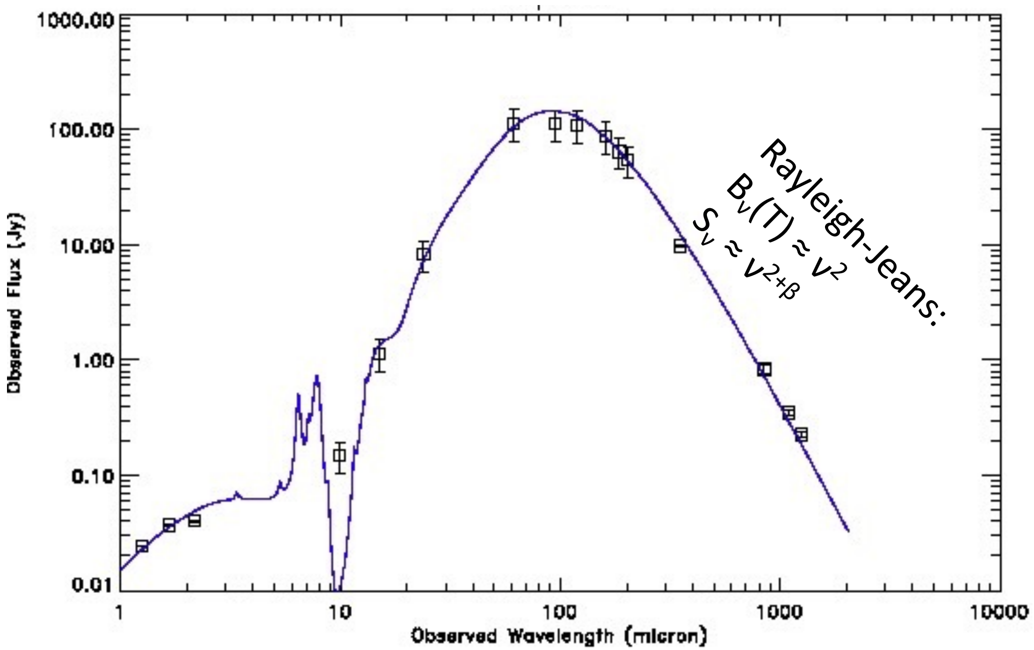

$S_\nu \approx (1 - e^{-\tau(\nu)}) B_\nu(T_{dust}) / 4\pi D_L^2(z)$ where $\tau(\nu) = k_\nu \Sigma_{dust}$ and $k_\nu = k_0 (\nu/\nu_0)^\beta$

at rest-frame FIR wavelengths: optically thin emission $\tau(\nu) << 1$:

$S_\nu \approx k_\nu B_\nu(T_{dust}) / 4\pi D_L^2(z)$ ←→ single temperature modified black body approximation

inferring dust masses from rest-frame FIR flux

$$M_{\rm dust} = \frac{S_{\nu_0}\, d_{\rm L}^2(z)}{(1+z)\,\kappa_{\rm d}(\nu)\, B(\nu, T_{\rm d})}$$

$$L_{\rm FIR} = 4\pi M_{\rm dust} \int \kappa_{\rm d}(\nu)\, B(\nu, T_{\rm d})\, d\nu$$

Ref.	κ_0 [cm^2/gr]	λ_0 [μm]	β
a	7.5	230	1.5
b	30	125	2.0
c	0.4	1200	1.6
d	34.7	100	2.2
e	40	100	1.4

z = 6.4 QSO SDSS J1148

$T_{\rm d}$ [K]	$M_{\rm dust}$ [$M_\odot$]	$L_{\rm FIR}$ [$L_\odot$]
58	3.16×10^8	2.32×10^{13}
49	2.91×10^8	2.09×10^{13}
56	4.29×10^8	2.27×10^{13}
47	4.78×10^8	2.02×10^{13}
60	1.86×10^8	2.38×10^{13}

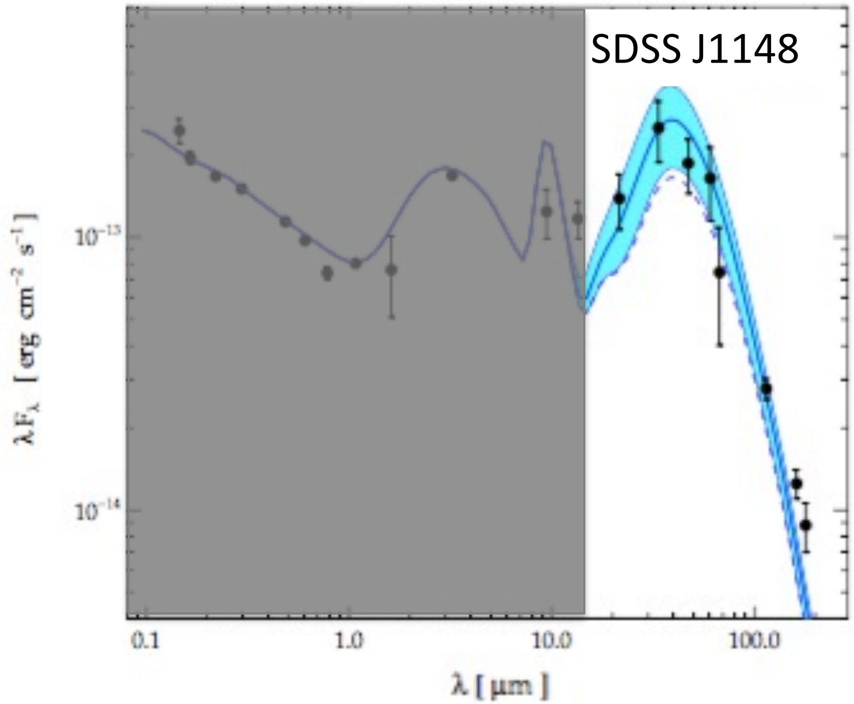

observed dust masses are uncertain

with one/two data-points there is a strong degeneracy between dust temperature and emissivity

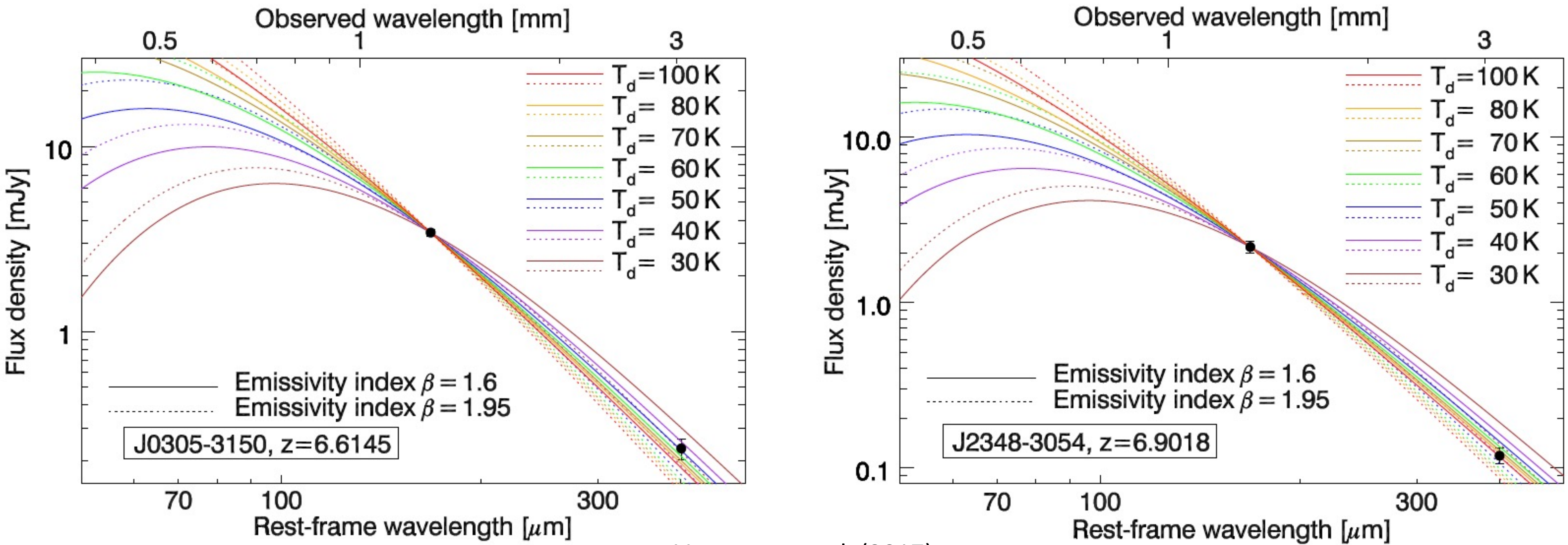

Venemans et al. (2017)

single temperature component fits

quasar	T_d	β	M_{dust}
J0305 (z=6.6)	[28 – 47]K	1.6 – 1.95	[4.5 – 24] 10^8 M_{sun}
J2348 (z= 6.9)	[40 – 94]K	1.6 – 1.95	[2.7 – 15] 10^8 M_{sun}

observed dust masses are uncertain

with one/two data-points there is a strong degeneracy between dust temperature and emissivity

ALMA observations of MACS0416_Y1 (z=8.3)

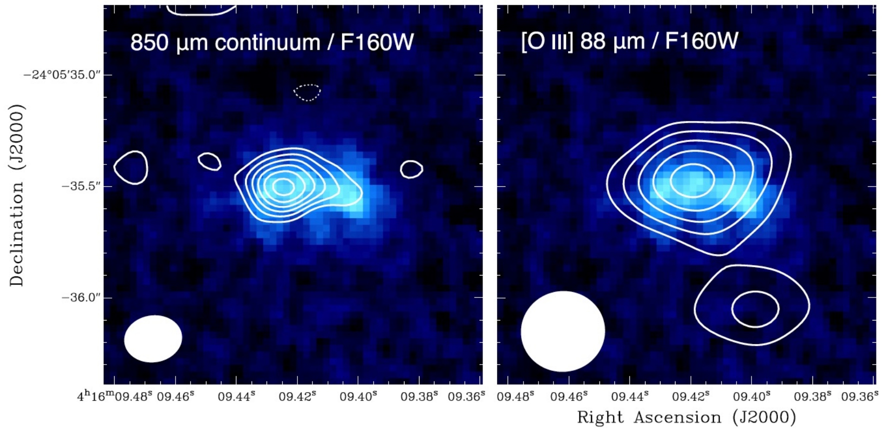

Tamura et al. (2019)

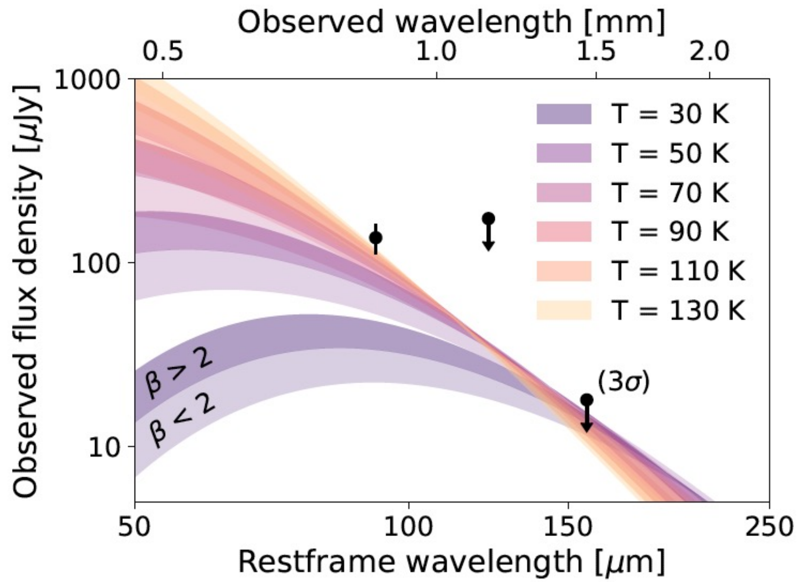

Bakx et al. (2020)

single temperature component fits

LBG - MACS0416_Y1 (z=8.3)	**T_d**	**β**	**M_{dust}**
Tamura et al (2019)	[40 – 50]K	1.5	[3.6 – 8.2] 10^6 M_{sun}
Bakx et al. (2020)	[60 – 121]K	1.5 – 2.5	[2.5 – 5.2] 10^5 M_{sun}

the dust mass in "extreme" galaxies at z ≈ 6: dusty SF galaxies and quasar hosts

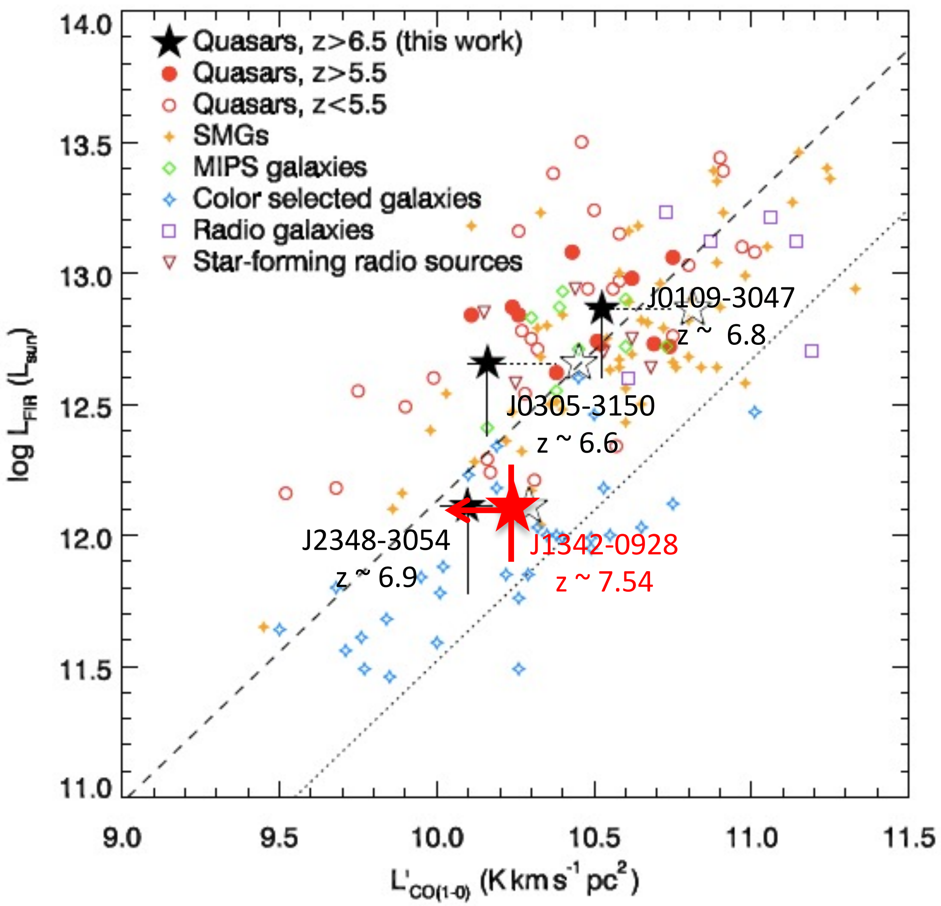

Venemans et al. 2017a,b

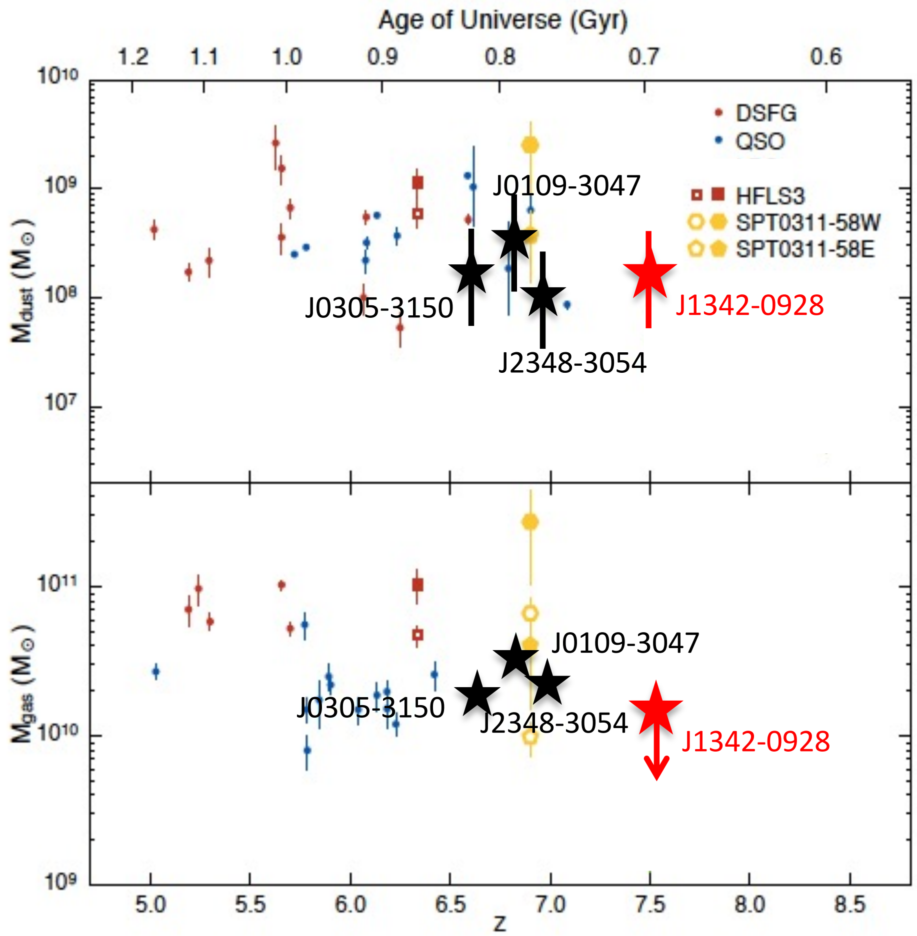

Marrone et al. 2017

Valiante et al. 2014, 2015

dust content of z > 7 normal star forming galaxies

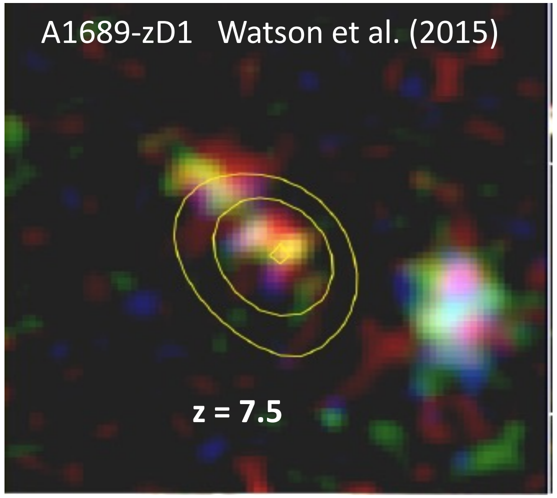

M_{star} ~ 2 10^9 M_{sun} SFR ~ 10 M_{sun}/yr
M_{dust} ~ (3 – 6) 10^7 M_{sun}

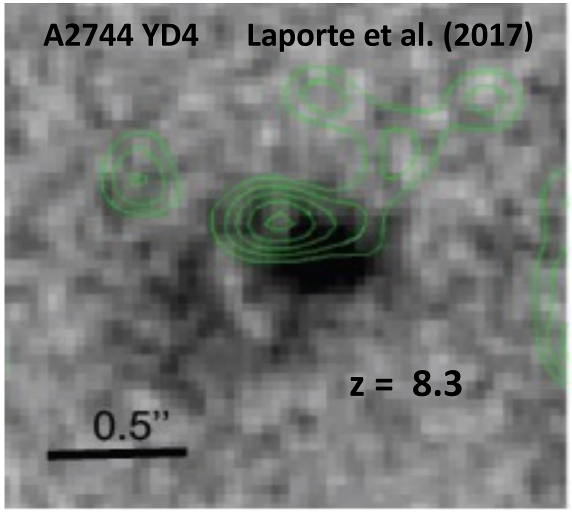

M_{star} ~ 2 10^9 M_{sun} SFR ~ 20 M_{sun}/yr
M_{dust} ~ 6 10^6 M_{sun}

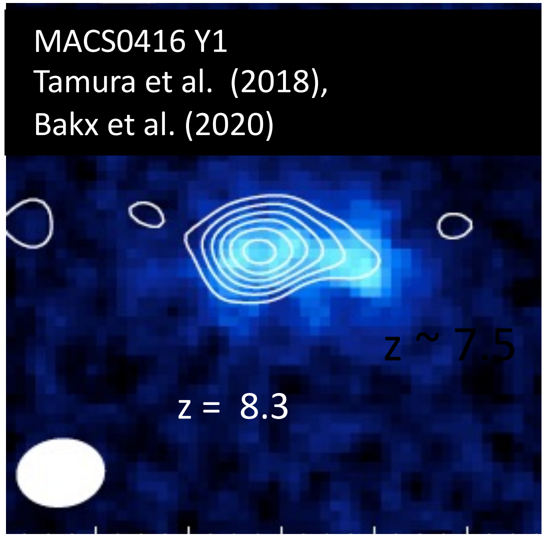

M_{star} ~ (0.3 – 1) 10^{10} M_{sun}
SFR ~ 60 M_{sun}/yr
M_{dust} ~ (7.7 10^6 – 6 10^4) M_{sun}

A1689-zD1 Knudsen et al. (2017)

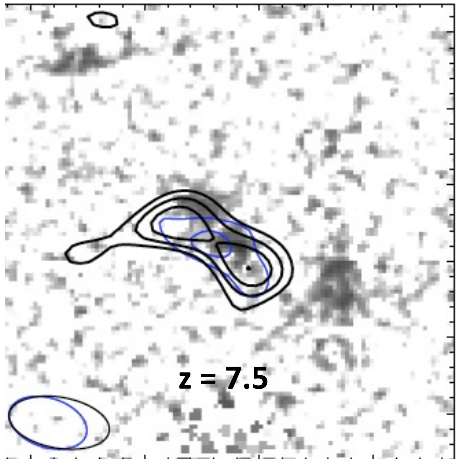

B14-65666 Hashimoto et al. 2018

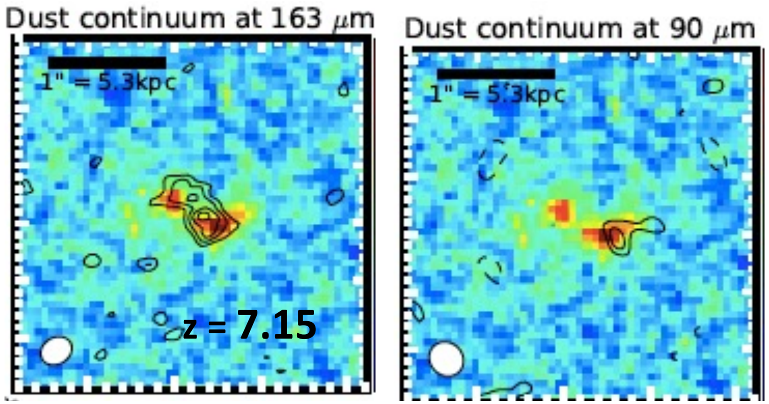

M_{star} ~ 2.1 10^9 M_{sun} SFR ~ 143 M_{sun}/yr
M_{dust} ~ (1 – 6) 10^7 M_{sun}

Bowler et al. 2018

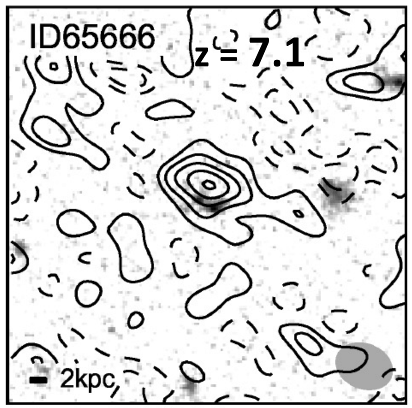

M_{star} ~ 10^9 M_{sun} SFR ~ 50 M_{sun}/yr
M_{dust} ~ 2 10^7 M_{sun}

the dust mass in “normal” SF galaxies at z ≈ 6

Shimizu+14; Mancini, RS+2015, 2016; Khakaleva-Li & Gnedin 2016; Zhukowska+ 2016; Grassi+ 2016; McKinnon+ 2016
Aoyama+2016; Graziani+ 2020

the dust mass in some “normal” galaxies at 5 < z < 8.4 compared to local galaxies

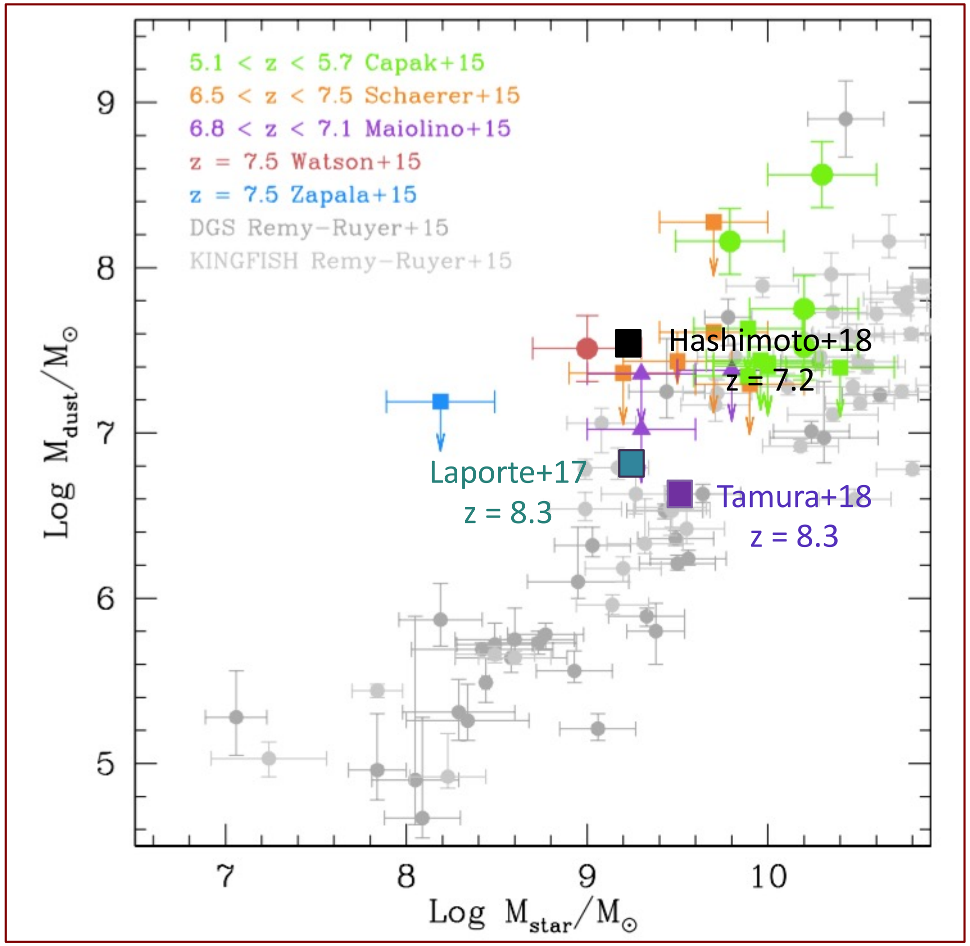

“normal” star forming galaxies at z > 6 have a dust-to-stellar mass relation consistent with local galaxies

dust mass budget

dust yield per SN and AGB stars required to explain the observed dust masses

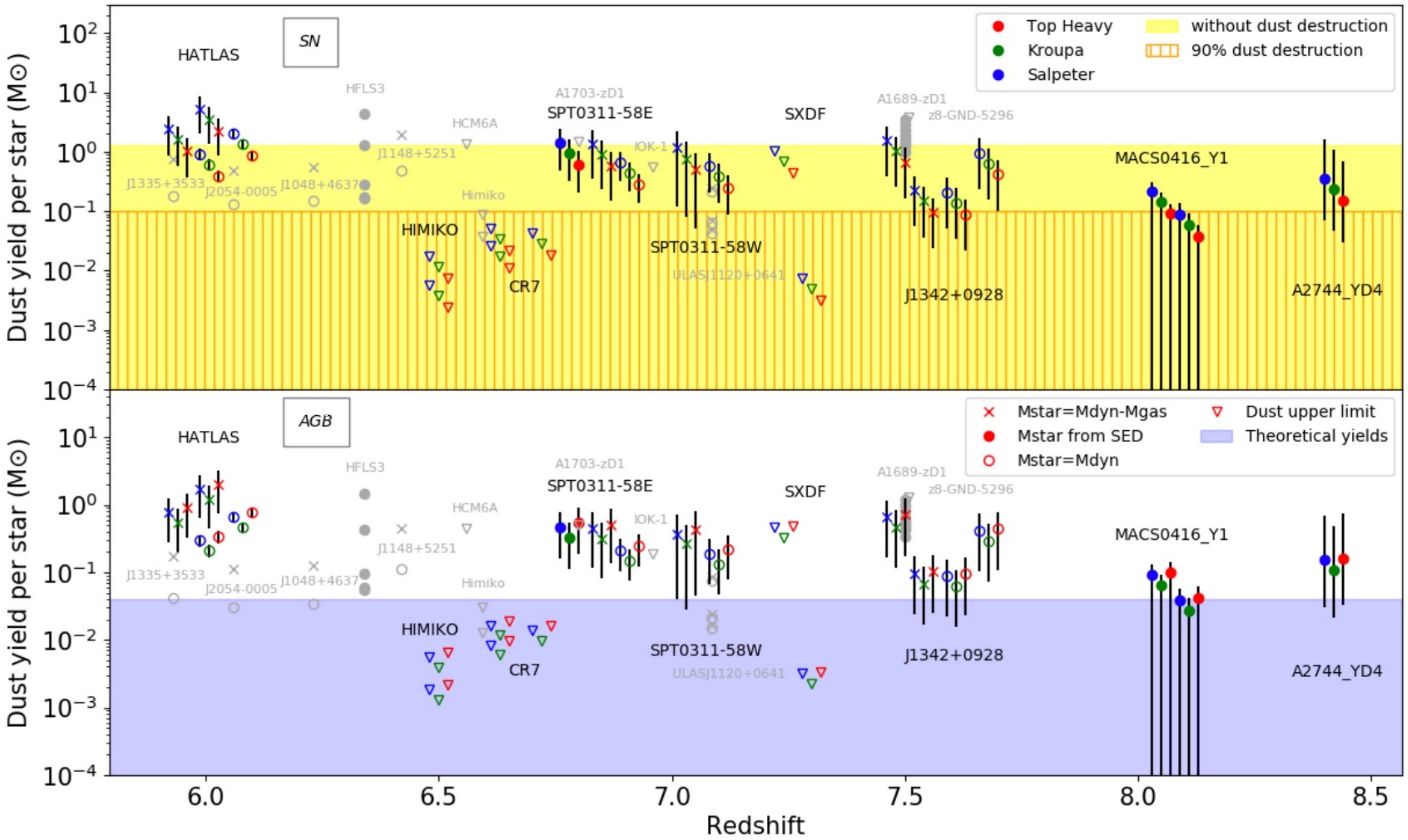

Michałowski et al. 2010; Michałowski 2015; Lesniewska & Michałowski (2019)

“the observed amounts of dust in the galaxies in the early universe were formed either by efficient supernovae or by a non-stellar mechanism, for instance the grain growth in the interstellar medium”

the dust mass in "extreme" galaxies at z ≈ 6: quasar hosts

are stellar sources enough to produce ~ 10^8 M_{sun} of dust in < 1 Gyr?

Valiante et al. 2009, 2011, 2014; Gall et al. 2010, 2011; Dwek & Cherchneff 2011; Mattsson 2011; Pipino et al 2011; Calura et al. 2013

M_{dust} *does not* correlate with M_{star}

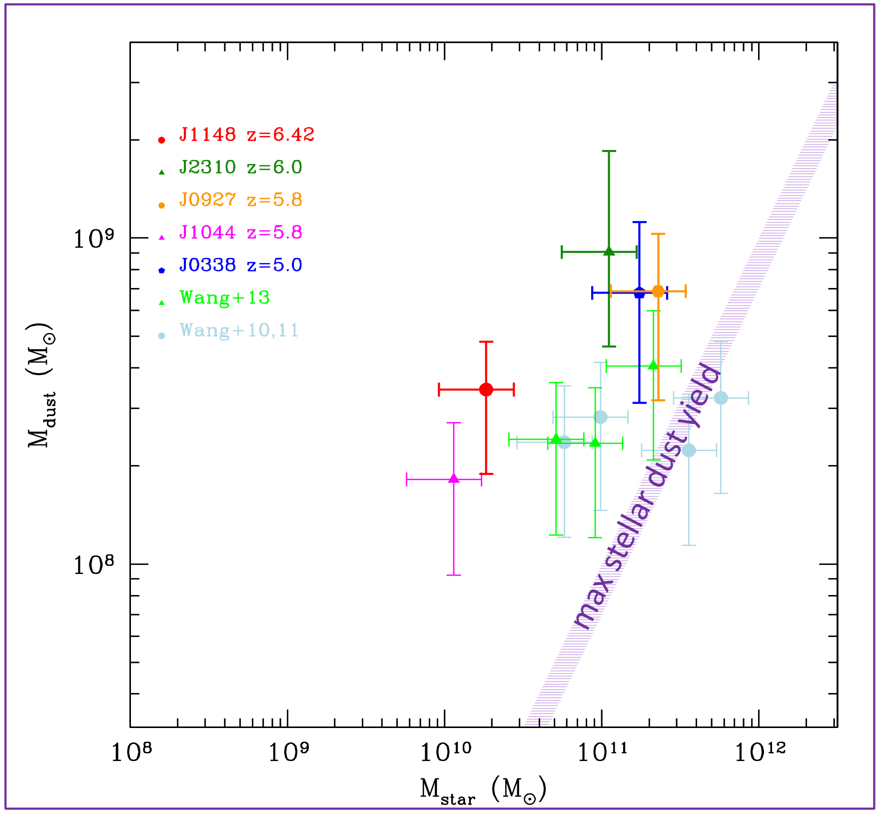

stellar dust is not enough to reproduce the observed M_{dust}

M_{dust} *does* correlate with M_{H2}

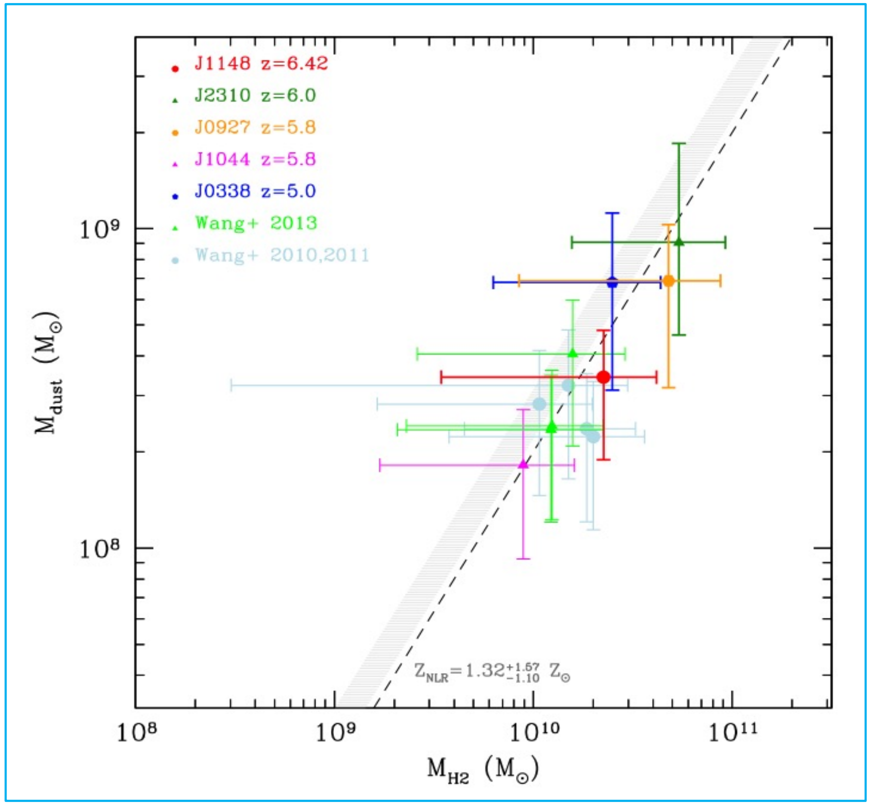

the observed M_{dust} require super-solar metallicities and very efficient grain growth in dense gas

Valiante et al. 2014, 2015

the origin of dust in z ≥ 6 “normal” SF galaxies

semi-numerical approach: SFR, metal and gas masses from a cosmological simulation
dust mass evolution in post-processing

dust vs stellar mass:
simulation results vs observations

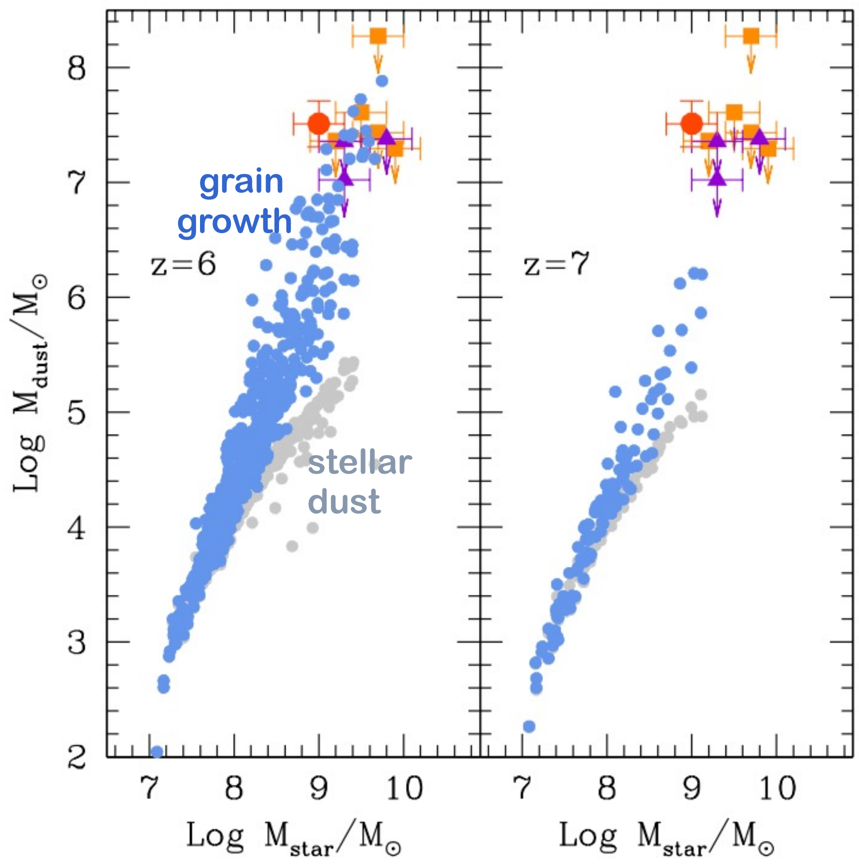

dust evolution of the most massive galaxies

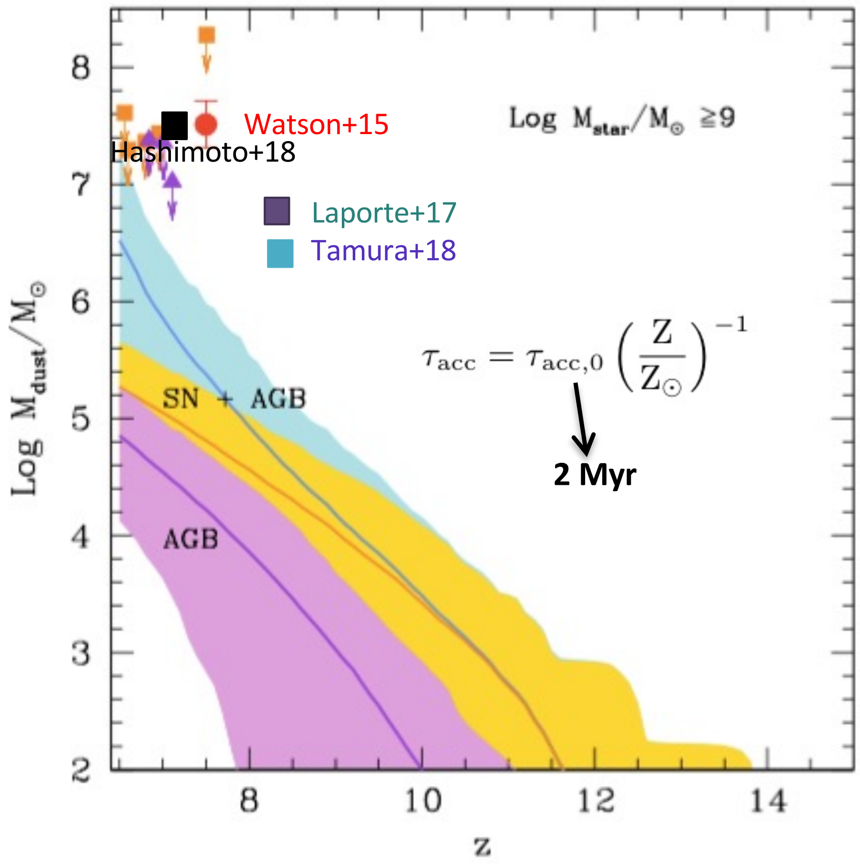

Mancini, RS et al. (2015)

the origin of dust in z ≥ 6 “normal” SF galaxies

semi-numerical approach: SFR, metal and gas masses from a cosmological simulation
dust mass evolution in post-processing

dust vs stellar mass:
simulation results vs observations

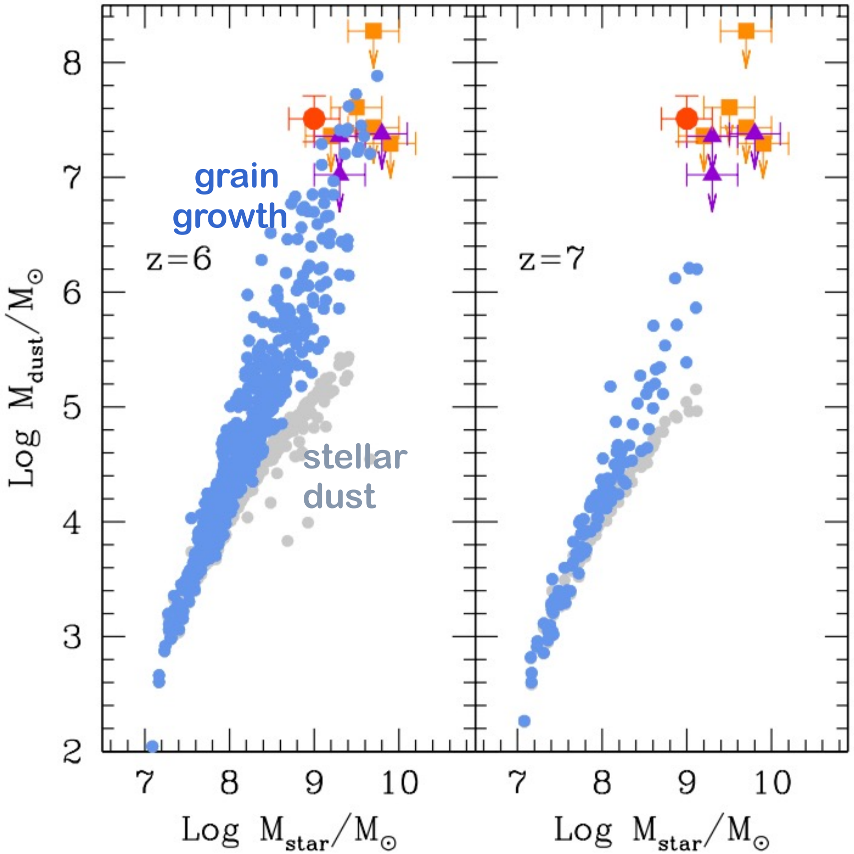

Mancini, RS et al. (2015)

dust evolution of the most massive galaxies

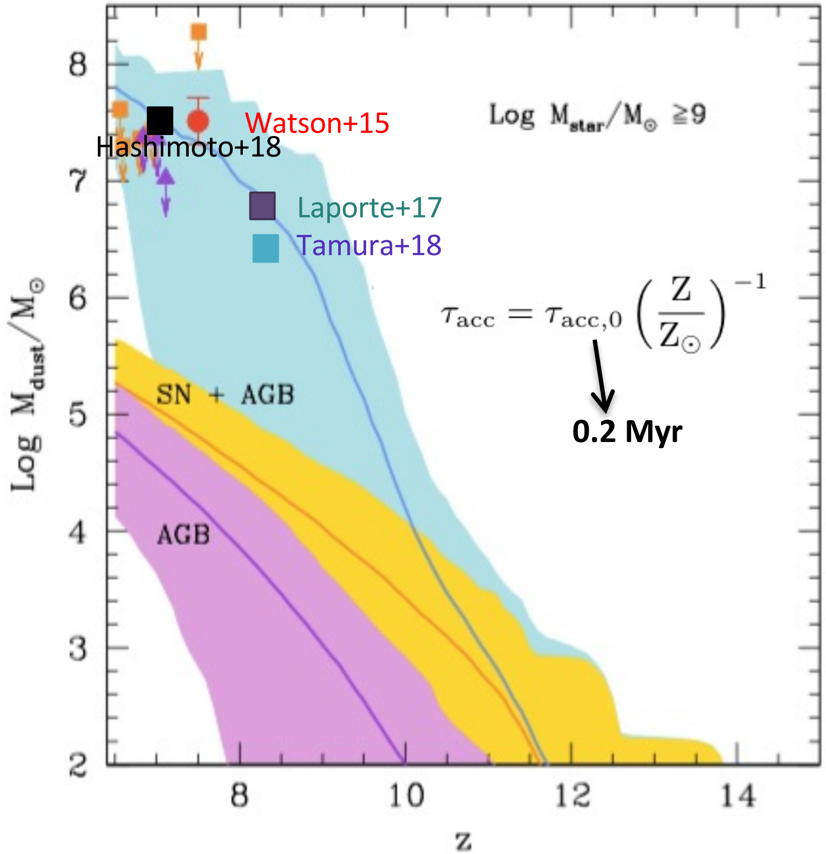

efficient grain growth is required to account for the observed dust masses

implications for the origin of dust

- the dust mass in $M_{star} > 10^8 - 10^9\ M_{sun}$ galaxies is dominated by grain growth in the ISM
- grain growth depends on local conditions: metallicity and density/temperature of dense gas

$$\tau_{acc} \approx 20\,\mathrm{Myr} \times \left(\frac{\bar{a}}{0.1\,\mu\mathrm{m}}\right)\left(\frac{n}{100\,\mathrm{cm}^{-3}}\right)^{-1}\left(\frac{T}{50\,\mathrm{K}}\right)^{-1/2}\left(\frac{Z}{Z_\odot}\right)^{-1} = \tau_{acc,0}\left(\frac{Z}{Z_\odot}\right)^{-1}$$

In the MW galaxy:
Cold Neutral Medium (CNM): $n = 50 - 100\ \mathrm{cm}^{-3}$ and $T = 50 - 100$ K → $\tau_{acc,0} = 20 - 30$ Myr
Molecular gas (MC): $n = 10^2 - 10^4\ \mathrm{cm}^{-3}$ and $T = 10 - 20$ K → $\tau_{acc,0} = 0.4 - 30$ Myr

In QSO host galaxies at $z > 6$:
Molecular gas (MC): $n = 10^{3.6} - 10^{4.3}\ \mathrm{cm}^{-3}$ and $T = 40 - 60$ K → $\tau_{acc,0} = 0.1 - 0.4$ Myr

In normal SF galaxies at $z > 6$?
$\tau_{acc,0} = \tau_{acc,0}^{MW}\,(1+z)^{-7/2} \approx \tau_{acc,0}^{MW}/10^3$ → 0.02 – 0.03 Myr in the CNM!

the dust mass depends on ISM conditions

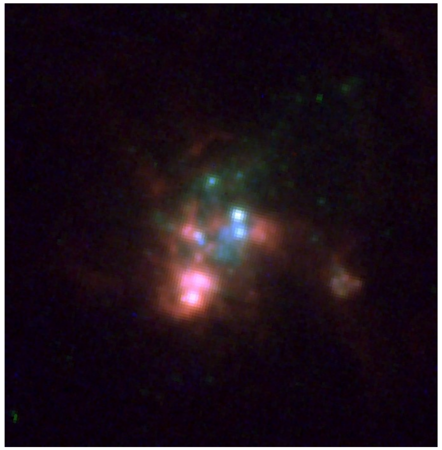

dust-to-gas ratio vs metallicity

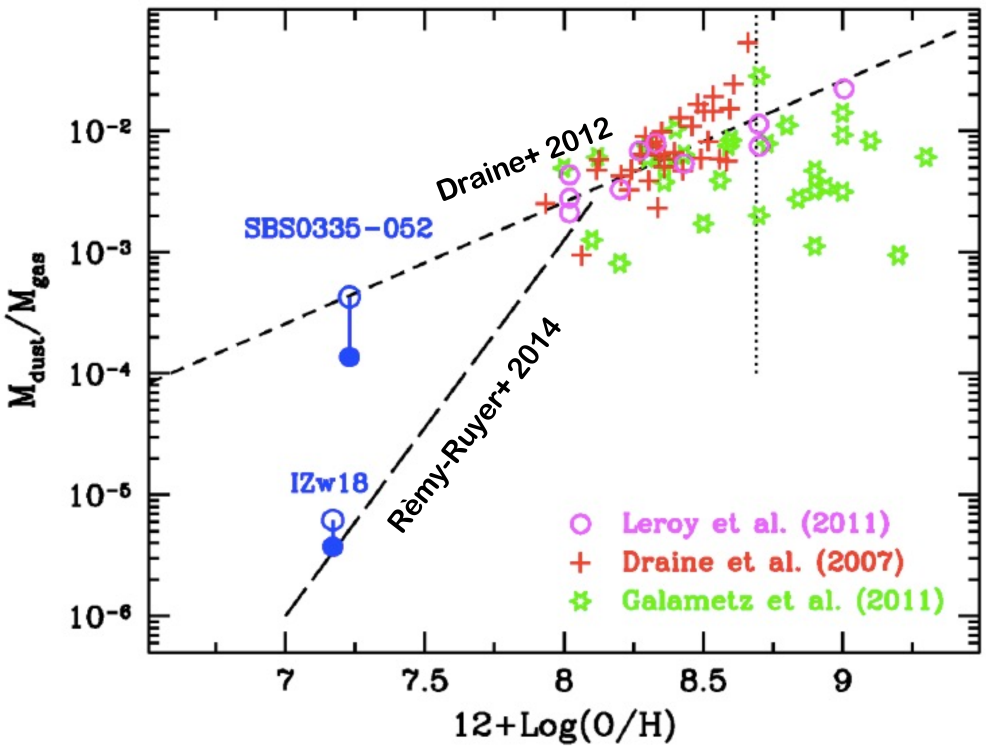

RS, Hunt & Valiante 2016

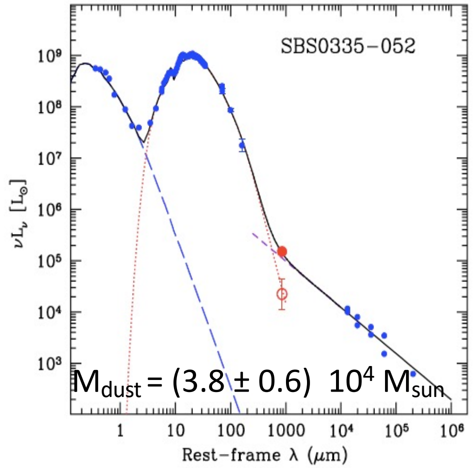

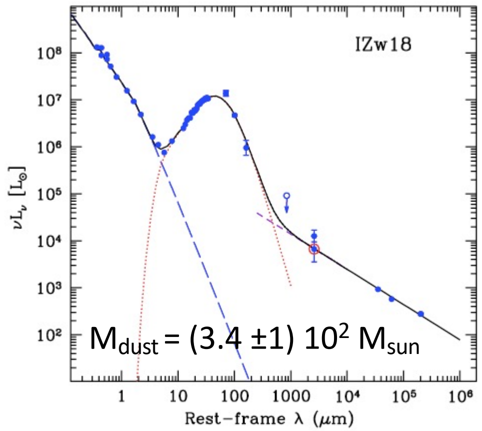

Galaxy	M_{dust}/M_{sun}	Z/Z_{sun}	n/cm^3	T/K
SBS0335-052	**3.8 x 10^4**	0.038	**1500**	80
IZw18	**340**	0.031	**100**	10

the dust mass depends on ISM conditions

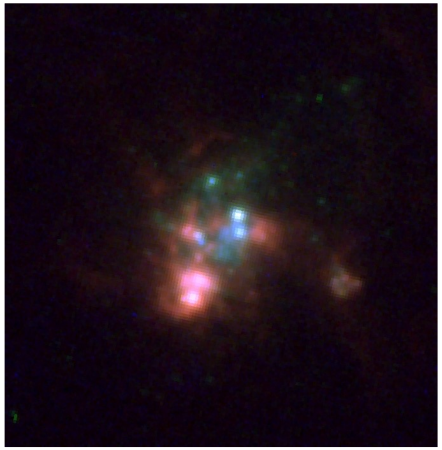

dust-to-gas ratio vs metallicity

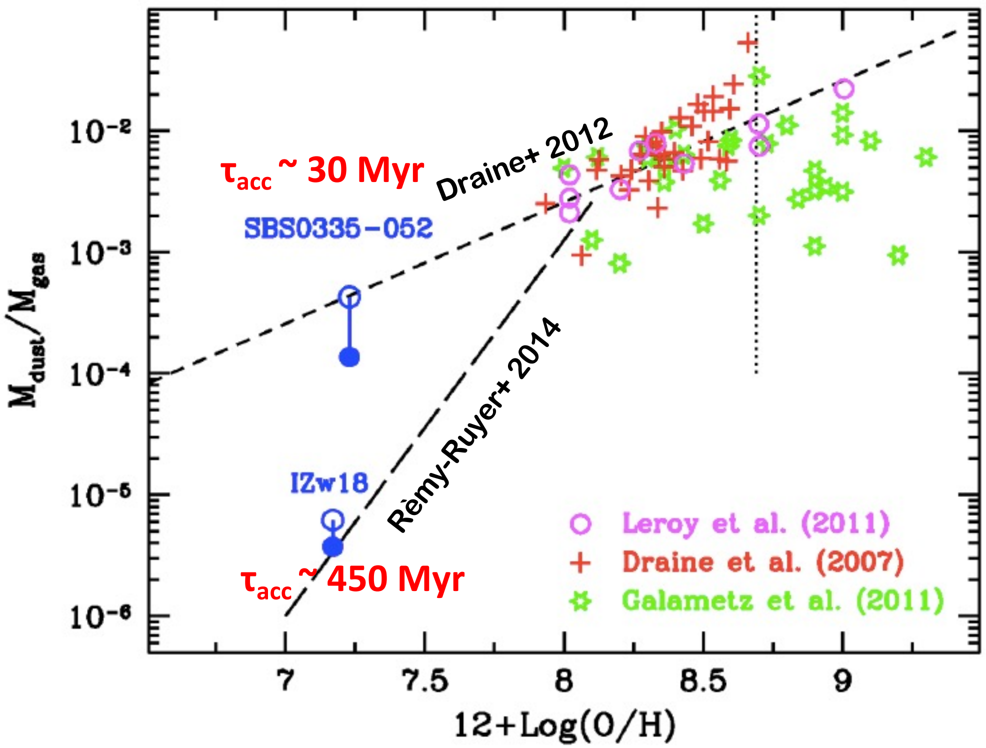

RS, Hunt & Valiante 2016

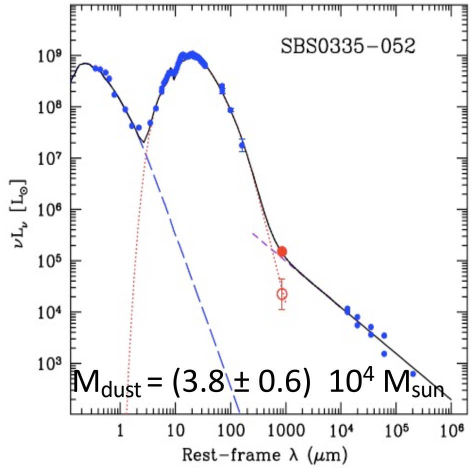

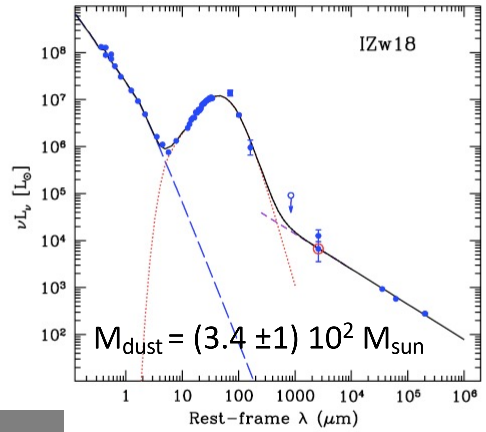

the difference in the observed dust masses could be due to different grain growth times scales

Asano+2013; Hirashita+2014

$$\tau_{acc} = \tau_{acc,0} \left(\frac{Z}{Z_{sun}}\right)^{-1} \qquad \tau_{acc,0} = 2\,\mathrm{Myr} \left(\frac{< a >}{0.1\mu m}\right) \left(\frac{n}{1000\,cm^{-3}}\right)^{-1} \left(\frac{T}{50\,K}\right)^{-1/2}$$

dustyGADGET: a full numerical approach

same simulation adopted in Mancini et al. (2015) but dust evolution is computed self-consistently

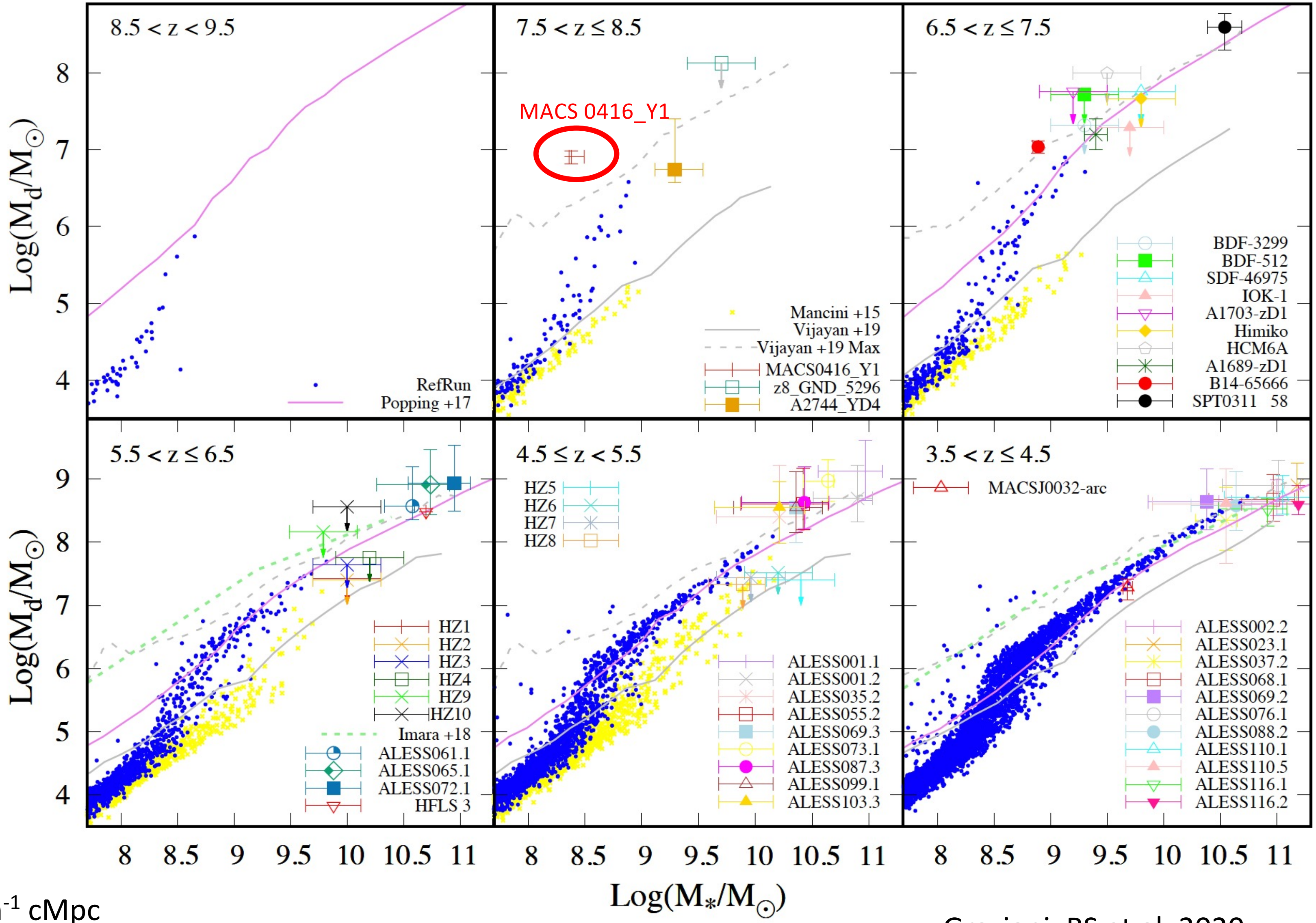

L_{box} = 30 h^{-1} cMpc
320^3 particles
M_{gas} = 9 10^6 h^{-1} M_{sun} and M_{DM}=6 10^7 h^{-1} M_{sun}

Graziani, RS et al. 2020

see also Aoyama+17,18; McKinnon+17; Vogelsberger+18

dustyGADGET: a full numerical approach

Graziani, RS et al. 2020

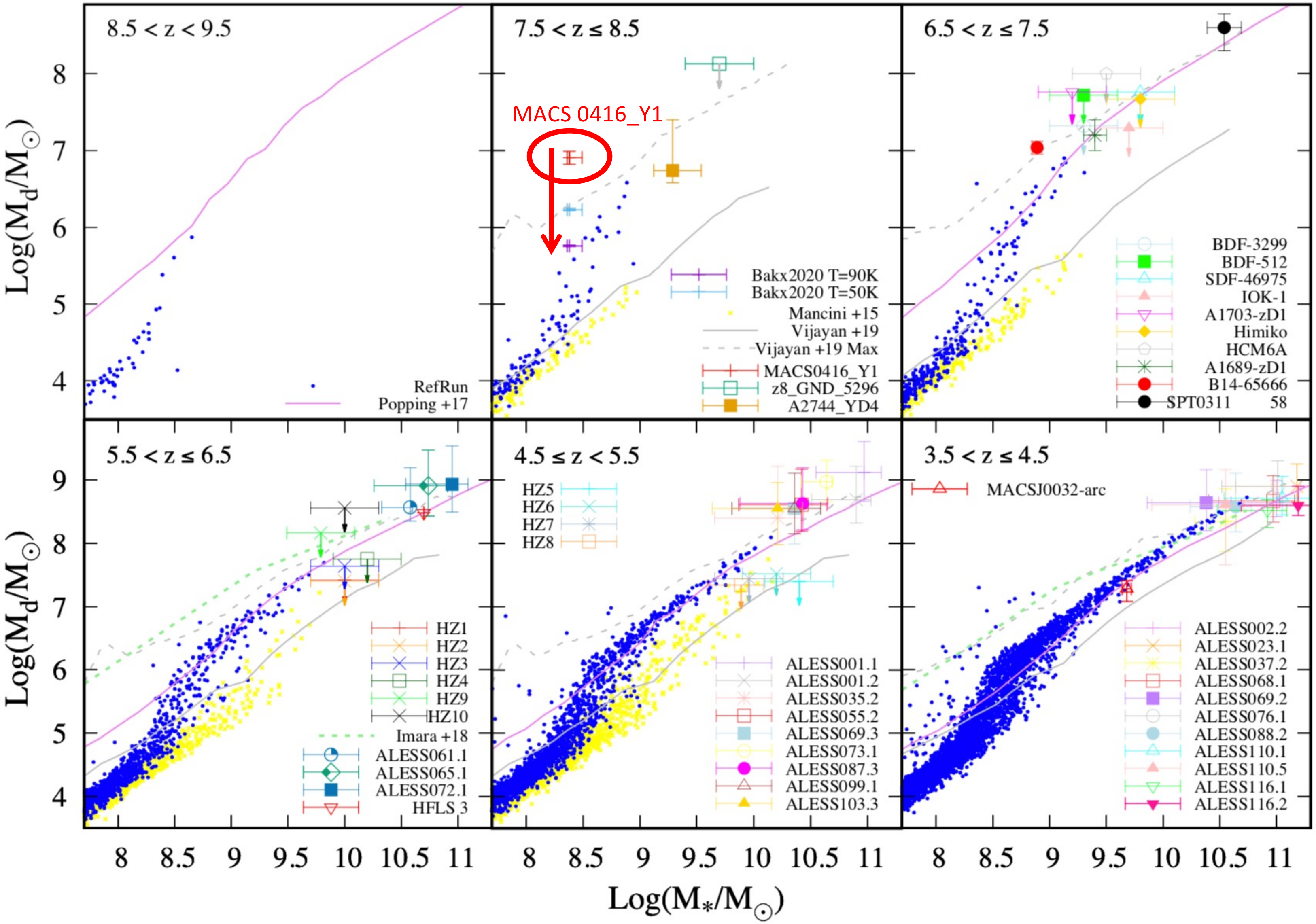

our simulated systems are in good agreement with the variety of high redshift galaxies observed with ALMA

REBELS

Reionization Era Bright Emission Line Search

REIONIZATION ERA BRIGHT EMISSION LINE SURVEY: SELECTION AND CHARACTERIZATION OF LUMINOUS INTERSTELLAR MEDIUM RESERVOIRS IN THE $Z > 6.5$ UNIVERSE

R.J. Bouwens[1], R. Smit[2], S. Schouws[1], M. Stefanon[1], R. Bowler[3], R. Endsley[4], V. Gonzalez[5,6], H. Inami[7], D. Stark[4], P. Oesch[8,9], J. Hodge[1], M. Aravena[10], E. da Cunha[11], P. Dayal[12], I. de Looze[13,14], A. Ferrara[15], Y. Fudamoto[8,16,17], L. Graziani[18,19], C. Li[20,21], T. Nanayakkara[22], A. Pallottini[15], R. Schneider[18,23], L. Sommovigo[15], M. Topping[4], P. van der Werf[1], L. Barrufet[8], A. Hygate[1], I. Labbé[22], D. Riechers[24], J. Witstok[25]

arXiv:2106.13719v1

- Targeted survey of 40 sources
- Photo-z > 6.5
- Massive Lyman-break galaxies
- Spectral scans for [CII] and [OIII]
- In total 60.6 hours observations
- ≈ 85% completed (33 out of 40)

REBELS

Reionization Era Bright Emission Line Search

Dust continuum detections

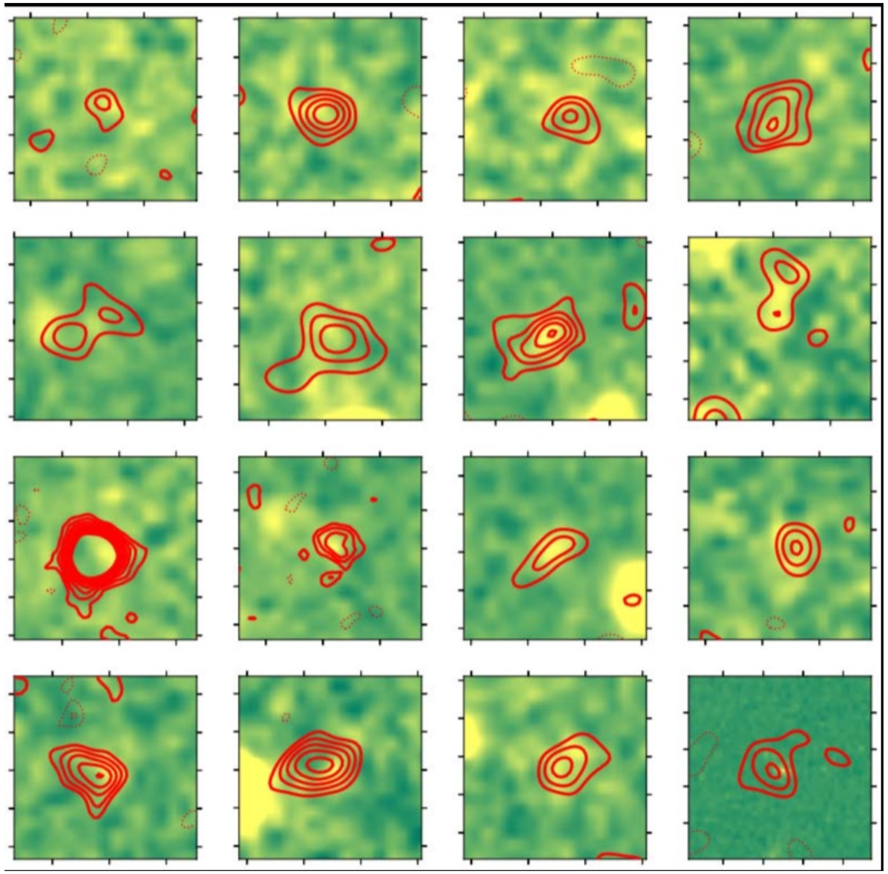

16 with ≧ 3.3σ out of 33 (7 to be observed)

Inami et al. in prep

Summary and take-home messages

- observations at mm wavelengths show that the host galaxies of $z > 6$ SMBHs are highly dust-enriched
- "normal" star forming galaxies at $z > 6$ have a dust-to-stellar mass relation consistent with local galaxies
- stellar dust is dominant at $M_{star} < 10^8\ M_{sun}$ and grain growth is efficient at larger masses
- The vastly different dust content of local metal-poor dwarfs at comparable Z suggests that density plays an important role in the grain growth timescale
- The chemical maturity of $z > 6$ galaxies suggests that early metal and dust enrichment may have been more efficient than previously thought, possibly requiring favorable ISM conditions for SN productions and grain growth

understanding the rapid metal and dust build-up at $z > 6$
will provide important indications on
the star formation history, stellar populations
and interstellar medium properties
in the first galaxies

Bibliography

Introduction to astrophysical dust:
Draine 2003, ARAA, 41, 241
http://adsabs.harvard.edu/abs/2003ARA%26A..41..241D

AGB dust production:
Schneider* et al. 2015, ASPC, 497, 369 and references therein
http://adsabs.harvard.edu/abs/2015ASPC..497..369S
*this is a proceeding where we collect the results published in a series of papers

SN dust production:
Bianchi & Schneider 2007, MNRAS, 378, 973
http://adsabs.harvard.edu/abs/2007MNRAS.378..973B

Marassi, S. 2015, MNRAS, 454, 4250
http://adsabs.harvard.edu/abs/2015MNRAS.454.4250M

Bocchio M. 2016, A&A, 587, A157
https://ui.adsabs.harvard.edu/abs/2016A%26A...587A.157B/abstract

Cosmic dust yield:
Valiante R. et al. 2009, MNRAS, 397, 1661 (first part)
http://adsabs.harvard.edu/abs/2009MNRAS.397.1661V

Lifecycle of dust in the interstellar medium of the MW:
de Bennassuti M. et al. 2014, MNRAS, 445, 3039
http://adsabs.harvard.edu/abs/2014MNRAS.445.3039D

Ginolfi, M. et al. 2018 MNRAS, 473, 4538
https://ui.adsabs.harvard.edu/abs/2018MNRAS.473.4538G/abstract

Dust in the most metal-poor local dwarfs: metallicity is not the only player
Schneider, Hunt, Valiante 2016, MNRAS, 457, 1842
http://adsabs.harvard.edu/abs/2016MNRAS.457.1842S

Bibliography

High-z observations at mm wavelengths:

Casey, Narayanan, Cooray 2014 Physical Reports, 541, 45
http://adsabs.harvard.edu/abs/2014PhR...541...45C

Carilli & Walter 2013, ARAA, 51, 105
http://adsabs.harvard.edu/abs/2013ARA%26A..51..105C

The origin of dust in high-z quasar hosts:

Valiante et al. 2014, MNRAS, 444, 2442
http://adsabs.harvard.edu/abs/2014MNRAS.444.2442V

The origin of dust in high-z "normal" star forming galaxies

Mancini, M. 2015, MNRAS, 451, L70
http://adsabs.harvard.edu/abs/2015MNRAS.451L..70M

Graziani, L. et al. 2020, MNRAS, 494, 1071
https://ui.adsabs.harvard.edu/abs/2020MNRAS.494.1071G/abstract

Star formation at low-metallicity: the role of dust

Schneider et al. 2012a, MNRAS, 419, 1566
http://adsabs.harvard.edu/abs/2012MNRAS.419.1566S

Schneider et al. 2012b, MNRAS, 423, L60
http://adsabs.harvard.edu/abs/2012MNRAS.423L..60S

Marassi et al. 2014, ApJ, 794, 100
http://adsabs.harvard.edu/abs/2014ApJ...794..100M

Chiaki et al. 2020, MNRAS, 497, 3149
https://ui.adsabs.harvard.edu/abs/2020MNRAS.497.3149C/abstract

Chon et al. 2021, MNRAS, submitted
https://ui.adsabs.harvard.edu/abs/2021arXiv210304997C/abstract